Gravitational-Wave Analysis
Lectures 1 & 2

Alessandra Buonanno

Department of Physics, University of Maryland

General Relativity Trimester, Institut Henri Poincaré, Paris

Lectures' content

Lecture 1 (2 and half hours):

- **Basics of data-analysis for compact binaries**
  - Noise spectral density; pattern functions and angular sensitivity
  - Matched filtering; intrinsic and extrinsic parameters; fitting factors

- **Templates in the *adiabatic* approximation for non-spinning and spinning, precessing binaries: low-mass binaries**
  - Stationary phase approximation
  - Features of spinning, precessing dynamics
  - Phenomenological templates
  - Physical templates for single-spin and double-spin binaries

Lectures' content

Lecture 2 (2 and half hours):

- **Templates in the *non-adiabatic* approximation for non-spinning and spinning, precessing binaries: high-mass binaries**
  - **The last cycles problem**
  - **Effective-one-body and Padé resummation**
  - **Transition from inspiral to plunge**
  - **Detection template families**
- **First-order comparisons with numerical relativity**
  - **Features of inspiral-merger(-plunge) and ring-down**
  - **Comparison with adiabatic PN templates**
  - **Comparison with effective-one-body templates**

Basics of data-analysis for compact binaries

The noise spectral density

Output of the detector $o(t) = h(t) + n(t)$

- **Autocorrelation function** $R(\tau) =< n(t+\tau)\, n(t) >$

  $<> \quad \Rightarrow$ **average over different realizations of the noise**

  (one realization is obtained by measuring the noise over an interval T**)**

- **Gaussian, stationary noise is characterized** *only* **by** $R(\tau)$ **and** $< n(t) > \, (= \mathrm{const} = 0)$

- **Generally,** $R(\tau)$ **goes to zero quite fast for** $\tau \to \pm\infty$ **(for white noise** $R(\tau) \sim \delta(\tau)$**)**

  Applying the Fourier transform: $\frac{1}{2} S_n(f) = \int_{-\infty}^{\infty} d\tau\, R(\tau)\, e^{i2\pi f\, \tau}$ **(Wiener-Khintchin rel.)**

- $R(\tau)$ **is real; invariance under time translation** $\Rightarrow S_n(f) = S_n^*(-f) = S_n(-f)$

  $R(\tau) = \frac{1}{2} \int_{-\infty}^{\infty} df\, S_n(f)\, e^{-i2\pi f\, \tau} \qquad R(0) =< n^2(t) >= \int_{-\infty}^{\infty} df\, S_n(f)$

  $\frac{1}{2} S_n(f) =< |\tilde{n}(f)|^2 > \, \Delta f$ with $\Delta f = 1/T \quad \Rightarrow \quad S_n(f) \longrightarrow$ (single-sided) noise spectral density

Pattern functions and angular sensitivity

- **GW propagating along** $\mathbf{N} = (\theta, \phi) : h_{ij}(t) = \sum_{A=+,\times} T^A_{ij}(\mathbf{N}) \int_{-\infty}^{\infty} df\, \tilde{h}_A(f)\, e^{-2\pi\, i\, f\, (t - \mathbf{N}\cdot\mathbf{x}/c)}$

  where $\mathbf{T}_+(\mathbf{N}) \equiv \boldsymbol{e}^R_x \otimes \boldsymbol{e}^R_x - \boldsymbol{e}^R_y \otimes \boldsymbol{e}^R_y$ and $\mathbf{T}_\times(\mathbf{N}) \equiv \boldsymbol{e}^R_x \otimes \boldsymbol{e}^R_y + \boldsymbol{e}^R_y \otimes \boldsymbol{e}^R_x$

- **If** $\mathbf{x}$ **is the detector location and the gravitational wavelength is much larger than its size**

  $$h_{ij}(t) = \sum_{A=+,\times} T^A_{ij}(\mathbf{N}) \int_{-\infty}^{\infty} df\, \tilde{h}_A(f)\, e^{-2\pi\, i\, f\, t} = \sum_{A=+,\times} T^A_{ij}(\mathbf{N})\, h_A(t)$$

- **Scalar output of detector:** $h(t) = \sum_{A=+,\times} \mathcal{D}^{ij}\, T^A_{ij}\, h_A(t)$

  $\mathcal{D}_{ij} = \frac{1}{2} \left[\overline{\boldsymbol{e}}_x \otimes \overline{\boldsymbol{e}}_x - \overline{\boldsymbol{e}}_y \otimes \overline{\boldsymbol{e}}_y\right]^{ij}$ $\quad F_A(\mathbf{N}) \equiv \mathcal{D}^{ij}\, T^A_{ij} \rightarrow$ pattern functions

- **Detector response to a GW:** $h(t) = h_+(t)\, F_+(\theta, \phi) + h_\times(t)\, F_\times(\theta, \phi)$

  If we rotate the axis $\boldsymbol{e}^R_x$ **and** $\boldsymbol{e}^R_y$ **by** ψ

  $F_+(\theta, \phi; \psi) = F_+(\theta, \phi; 0)\, \cos 2\psi - F_\times(\theta, \phi; 0)\, \sin 2\psi$

  $F_\times(\theta, \phi; \psi) = F_+(\theta, \phi; 0)\, \sin 2\psi + F_\times(\theta, \phi; 0)\, \cos 2\psi$

  $h(t)$ **is independent of** ψ

Binary-detector orientation

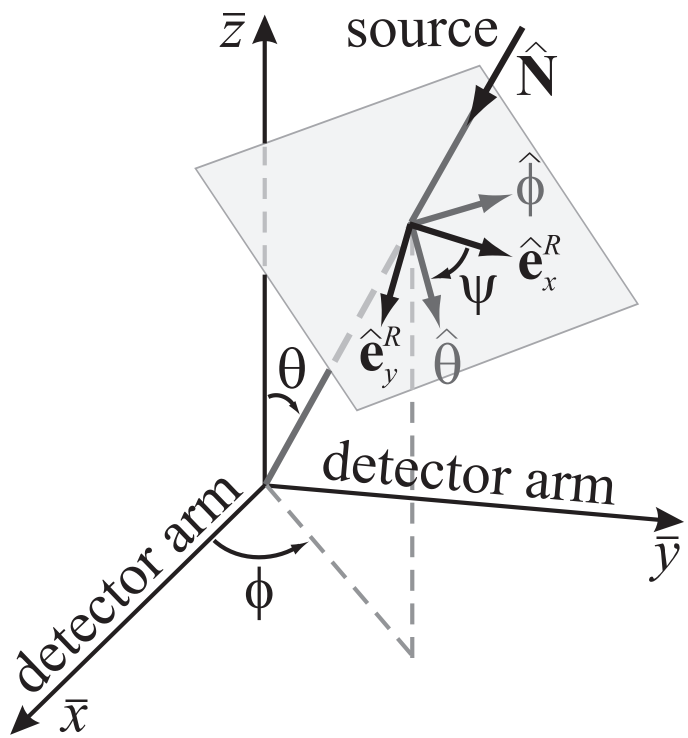

Pattern functions and angular sensitivity (continued)

- **Useful identities independent on $\mathcal{D}_{ij}$**

$$\int \frac{d\Omega}{4\pi} F_+(\mathbf{N})\, F_\times(\mathbf{N}) = 0 \quad \text{where} \quad d\Omega = d\cos\theta\, d\phi$$

$$\int \frac{d\Omega}{4\pi} F_+^2(\mathbf{N}) \neq 0 \qquad \int \frac{d\Omega}{4\pi} F_\times^2(\mathbf{N}) \neq 0$$

$$\int_0^{2\pi} \frac{d\psi}{2\pi} \int \frac{d\Omega}{4\pi} F_+^2(\mathbf{N}) = \int_0^{2\pi} \frac{d\psi}{2\pi} \int \frac{d\Omega}{4\pi} F_\times^2(\mathbf{N}) = F$$

- **Explicit form for ground-based detectors ($F = 2/5$):**

$$F_+ = \frac{1}{2}(1 + \cos^2\theta)\, \cos 2\phi\, \cos 2\psi - \cos\theta\, \sin 2\phi\, \sin 2\psi$$

$$F_\times = \frac{1}{2}(1 + \cos^2\theta)\, \cos 2\phi\, \sin 2\psi + \cos\theta\, \sin 2\phi\, \cos 2\psi$$

How to dig out a weak signal from the noise

- **Output of the detector** $o(t) = h(t) + n(t)$

  How can we extract $h(t)$ **from the noise even when** $|h(t)| \ll n(t)$**?**

- **Example: we (perfectly) know the form of the oscillating signal** $h(t)$

$$\frac{1}{T}\int_0^T dt\, o(t)\, h(t) = \frac{1}{T}\int_0^T dt\, h^2(t) + \frac{1}{T}\int_0^T dt\, h(t)\, n(t)$$

$$\frac{1}{T}\int_0^T dt\, h^2(t) \sim h^2_{\rm ampl} \qquad \frac{1}{T}\int_0^T dt\, h(t)\, n(t) \sim n_{\rm ampl}\, h_{\rm ampl}\, \left(\frac{T_{\rm GW}}{T}\right)^{1/2}$$

- **As long as** $h_{\rm ampl} > n_{\rm ampl} \left(\frac{T_{\rm GW}}{T}\right)^{1/2} \sim n_{\rm ampl}/\mathcal{N}_{\rm GW}^{1/2}$

  we can dig out the signal from the noise, i.e., we don't need $h_{\rm ampl} > n_{\rm ampl}$**.**

Matched filtering

- **We define** $\overline{o} = \int_{-\infty}^{+\infty} dt\, o(t)\, K(t)$ **with** $K(t) \to$ **filter**

  What is the best filter $K(t)$ **that maximizes the signal-to-noise ratio?**

- $\frac{S}{N} = \frac{\text{expected value of } \overline{o}(t) \text{ when signal is present}}{\text{rms of } \overline{o}(t) \text{ when signal is absent}}$

  Since $< n(t) >= 0$**, we have** $S = \int_{-\infty}^{+\infty} dt < \overline{o}(t) >= \int_{-\infty}^{+\infty} df\, \tilde{h}(f)\, \tilde{K}^*(f)$

  While $N^2 = \left[< \overline{o}^2(t) > - < \overline{o}(t) >^2\right]_{h=0}$

  $$= \int_{-\infty}^{+\infty} dt\, dt'\, K(t)\, K(t')\, \int_{-\infty}^{+\infty} df\, df'\, e^{2\pi i f\, t - 2\pi i f'\, t'} < \tilde{n}(f)\, \tilde{n}^*(f) >$$

  Using $< \tilde{n}(f)\, \tilde{n}^*(f) >= \frac{1}{2}\, S_n(f)\, \delta(f - f') \quad \Rightarrow \quad N^2 = \int_{-\infty}^{+\infty} df \frac{1}{2}\, S_n(f)\, |\tilde{K}(f)|^2$

- $$\frac{S}{N} = \frac{\int_{-\infty}^{+\infty} df\, \tilde{h}(f)\, \tilde{K}^*(f)}{\left[\int_{-\infty}^{+\infty} df \frac{1}{2}\, S_n(f)\, |\tilde{K}(f)|^2\right]^{1/2}}$$

Matched filtering: Wiener filter

- **Scalar product between two real functions t and h:**

$$(t,h) = 4\mathrm{Re}\left[\int_0^{+\infty} df\, \frac{\tilde{t}^*(f)\,\tilde{h}(f)}{S_n(f)}\right] \Rightarrow \frac{S}{N} = \frac{(t,h)}{(t,t)^{1/2}} \quad \textbf{where} \quad \tilde{t}(f) = S_n(f)\,\tilde{K}(f)/2$$

$\tilde{t}(f)$ **is a vector in the infinite-dimensional linear-space of functions of frequency**

- **Which is the unit vector $\hat{t} = \tilde{t}(f)/(t,t)^{1/2}$ such that the scalar product with $\tilde{h}(f)$ is maximum?**

Geometric solution: $\hat{t}$ and $\tilde{h}(f)$ have to be parallel

$$\Rightarrow \quad \tilde{K}(f) = \mathrm{const}\,\frac{\tilde{h}(f)}{S_n(f)} \qquad \textbf{Wiener filter}$$

- **Optimal SNR:** $\left(\frac{S}{N}\right)^2 = (h,h) = 4\int_0^{+\infty} df\, \frac{|\tilde{h}(f)|^2}{S_n(f)}$

Matched-filtering statistic, threshold, false alarms

- **Output of the detector** $o(t) = h_\lambda(t) + n(t)$ **where** $\lambda = \{\lambda_1, \ldots \lambda_k\}$ **binary parameters**

- *Detection statistic*: $\rho_{h_\lambda} = \frac{(o, h_\lambda)}{(h_\lambda, h_\lambda)^{1/2}}$

If $o = n$ **and noise is Gaussian,** ρ_{h_λ} **is a normal variable with mean zero and unit variance**

If $o = h_\lambda + n$**,** ρ_{h_λ} **has mean** $(h_\lambda, h_\lambda)^{1/2}$ **and unit variance**

- **We compare the measured output with a bank of templates** $\{h_\lambda\}$ **and find the template that maximizes** ρ_h

- **If** ρ^* **is the** *threshold*, **the** *false-alarm* **probability is**

$$\mathcal{F} = \sqrt{\frac{1}{2\pi}} \int_{\rho^*}^{+\infty} e^{-\rho^2/2}\, d\rho = \frac{1}{2}\,\mathrm{erfc}\left(\frac{\rho_*}{\sqrt{2}}\right)$$

Intrinsic and extrinsic parameters

- *Intrinsic parameters*: **variables on which we lay down templates**

- *Extrinsic parameters*: **variables that can be eliminated from the template space**
  $\Rightarrow$ **we don't need to lay down templates along those directions**

- **Time of arrival t_a: all possible shifts in time can be obtained at once with a single anti-Fourier transform**

$$(o, h(\lambda; t_a)) = 4\mathrm{Re}\left[\int_0^{+\infty} df \, \frac{\tilde{h}^*(f;\lambda)\, \tilde{o}(f)\, e^{2\pi i\, f\, t_a}}{S_n(f)}\right]$$

  We locate the value of t_a for which $(o, h(\lambda; t_a))$ is maximum

- **The overall amplitude is not relevant when searching for the template that maximizes the statistic**

Extrinsic parameters (continued)

- **Maximization over the phase Φ_0 can be done analytically**

$$h(\lambda; \Phi_0) = \mathcal{A}_\lambda(t) \cos\left[\Phi_\lambda(t) + \Phi_0\right]$$

For each $\{\mathcal{A}_\lambda(t), \Phi_\lambda(t)\}$ we need to keep in the template bank only two copies of h

i.e., h_0 and $h_{\pi/2}$ $\Rightarrow (o, h_{\Phi_0}) = \cos\Phi_0\,(o, h_0) + \sin\Phi_0\,(o, h_{\pi/2})$

- **What is $\max_{\Phi_0}(o, h(\Phi_0))$ with $(h, h) = 1$?**

We first orthonormalize h_0 and $h_{\pi/2}$ $\Rightarrow (\hat{h}_0, \hat{h}_0) = (\hat{h}_{\pi/2}, \hat{h}_{\pi/2}) = 1\,,\ (\hat{h}_0, \hat{h}_{\pi/2}) = 0$

$$\Rightarrow \rho_{\Phi_0} \equiv \max_{\Phi_0}(o, h(\Phi_0)) = \sqrt{(o, \hat{h}_0)^2 + (o, \hat{h}_{\pi/2})^2}$$

- **The phase-maximized statistic for the case of Gaussian noise ($o = n$) is the Raleigh distribution** $\mathcal{P}(\rho_{\Phi_0}) = \rho_{\Phi_0}\, e^{-\rho^2_{\Phi_0}/2}$

Extrinsic parameters (continued)

- **More in general if we have α_k parameters such that**

$$(o, h(\lambda; \alpha_k)) = \sum_k \hat{\alpha}_k \, (o, \hat{h}_k) \quad \text{with} \quad \sum_k \hat{\alpha}_k^2 = 1$$

by interpreting it as a scalar product in Euclidean space, the maximum is obtained when the vector $\{\hat{\alpha}_k\}$ is parallel to $(o, \hat{h}_k)/\sqrt{\sum_k (o, \hat{h}_k)^2}$

$$\Rightarrow \quad \hat{\alpha}_k = (o, \hat{h}_k)/\sqrt{\sum_k (o, \hat{h}_k)^2}$$

$$\Rightarrow \quad \rho_{\alpha_k} \equiv \max_{\alpha_k} (o, h(\alpha_k)) = \sqrt{\sum_k (o, \hat{h}_k)^2}$$

- **The maximized statistic for the case of Gaussian noise ($o = n$) is the χ distribution with $2n = k$ degrees of freedom** $\mathcal{P}(\rho_{\alpha_k}) = \rho_{\alpha_k}^{2n-1} \, e^{-\rho_{\alpha_k}^2/2}/(2^{n-1}\,\Gamma(n))$

Reduction in signal-to-noise ratio: Fitting Factor (FF)

True GW signal will be exact solution to Einstein equations

Templates used to search will be, at best, finite order approximation to the exact solution

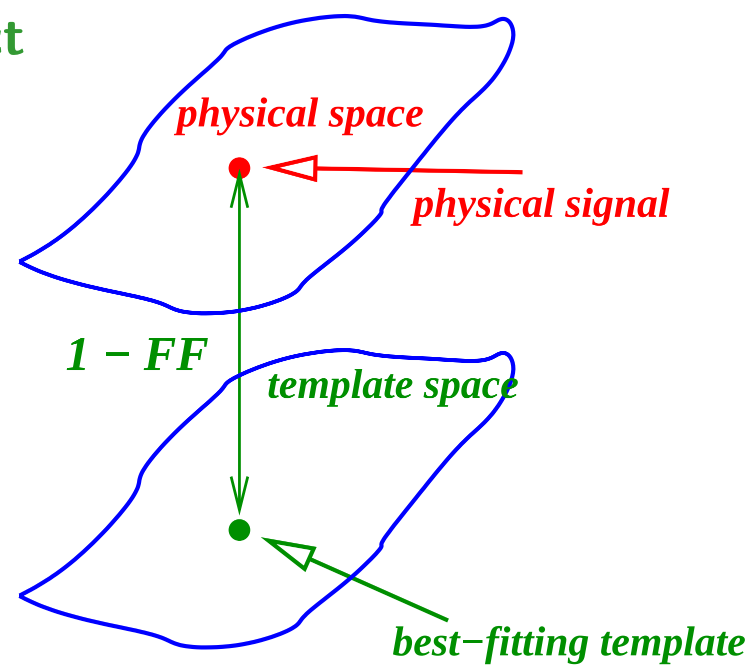

[Apostolatos 96; Chronopoulos & Apostolatos 01]

$$\mathrm{FF} = \max_{\lambda}(\hat{w}, \hat{h}(\lambda))$$

Reduction in signal-to-noise ratio: Minimal Match (MM)

[Balasubramanian, Dhurandhar, Sathyaprakash 91, 94, 96; Owen 96]

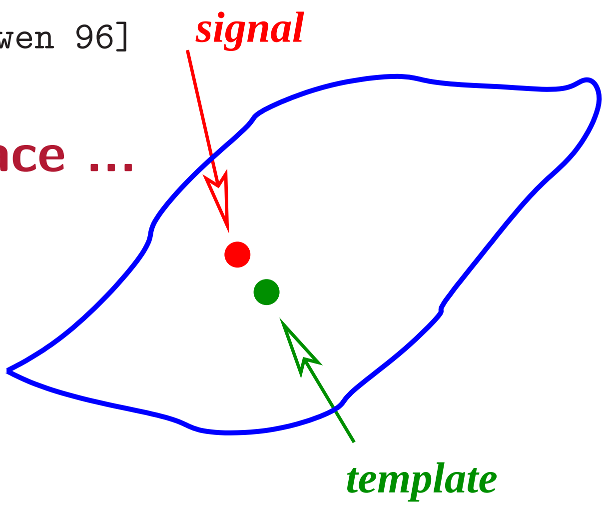

Assuming physical signal lies in template space ...

The parameters (masses, spins, etc.) describing the search templates vary continuously, the set of templates is infinite

Detector output should be correlated with finite subset of templates whose parameter values vary in discrete steps from one template to the other

So, even if GW signal were to lie within template space it would not correspond to any of search templates

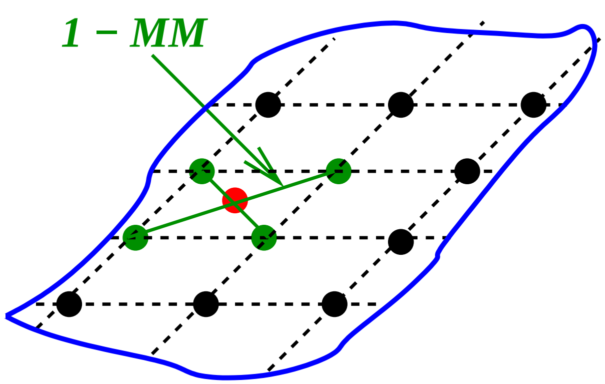

$$\mathrm{MM} = \min_{\lambda'} \max_{\lambda} (\hat{h}(\lambda'), \hat{h}(\lambda))$$

Reduction in event rates due to imperfect matches

$$\tilde{w}(f) = \frac{\mathcal{A}}{R}\,\hat{w}(f) \qquad (\hat{w},\hat{w}) = 1 \qquad (\hat{h},\hat{h}) = 1 \qquad \frac{S}{N} = (w,\hat{h})$$

- If $\hat{h}(f) = \hat{w}(f)$: $\frac{S}{N} = \frac{\mathcal{A}}{R}$ **(optimal match)**

Fixing detection threshold of $\frac{\mathcal{A}}{R} = 8 \rightarrow$

event visible out to $R = \frac{\mathcal{A}}{8}$ **and event rate** $\propto \left(\frac{\mathcal{A}}{8}\right)^3$

- If $\hat{h}(f) \neq \hat{w}(f)$:

If $\frac{S}{N} = \frac{\mathcal{A}}{R}\,(\hat{w},\hat{h})$ **(imperfect match)**

Event rates reduced to (FF+MM-1)$^3 \left(\frac{\mathcal{A}}{8}\right)^3$

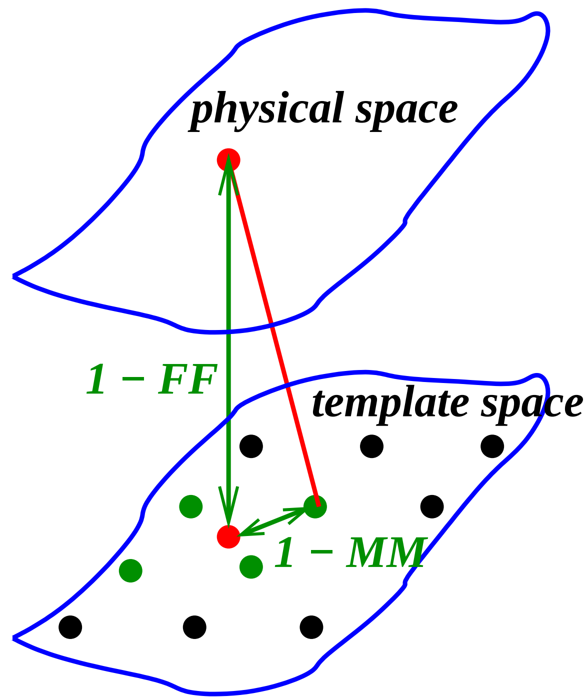

For example, for FF$= 0.98$, MM$= 0.96$ **event rates reduced by** 17%

Typical features of coalescing binaries

• Inspiral: quasi-circular orbits

Throughout the inspiral $T_{\rm RR} \gg T_{\rm orb} \Rightarrow$ **natural** *adiabatic parameter* $\frac{\dot{\omega}}{\omega^2} = \mathcal{O}\left(\frac{v^5}{c^5}\right)$

For compact bodies $\frac{v^2}{c^2} \sim \frac{GM}{c^2 r} \Rightarrow$ **PN approximation: slow motion and weak field**

"Chirping" if $T_{\rm obs} \gtrsim \omega/\dot{\omega}$

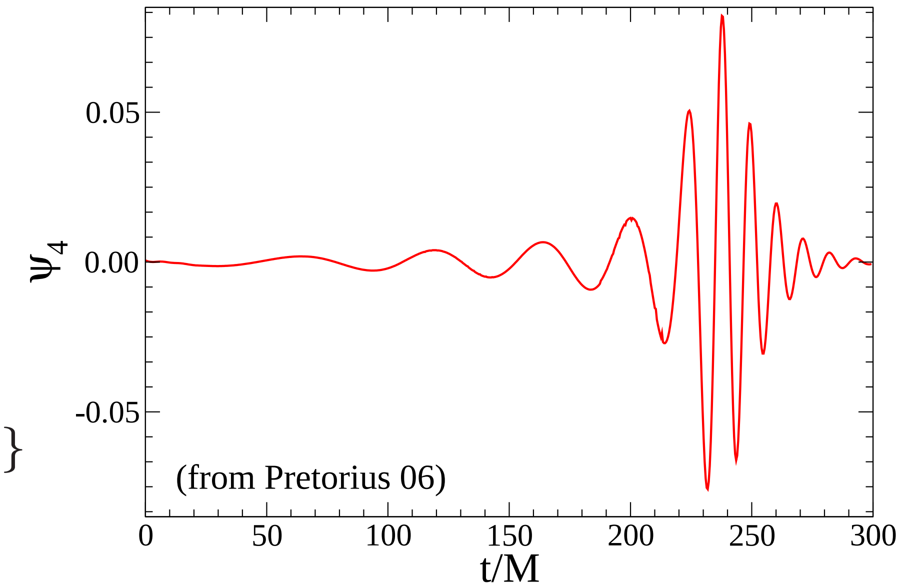

• Inspiral: spin-precessing orbits

$T_{\rm RR} \gg T_{\rm prec} \gg T_{\rm orb}$; $\omega_{\rm GW} = \{\omega_{\rm prec}, 2\omega\}$

• Inspiral: eccentric orbits

$T_{\rm RR} \gg T_{\rm peri\,prec} \gg T_{\rm orb}$; $\omega_{\rm GW} = \{N\,\omega, \cdots\}$

• Last cycles-plunge-merger-ringdown

Numerical relativity; close-limit approx.; PN resummation techniques

First-generation ground-based detectors

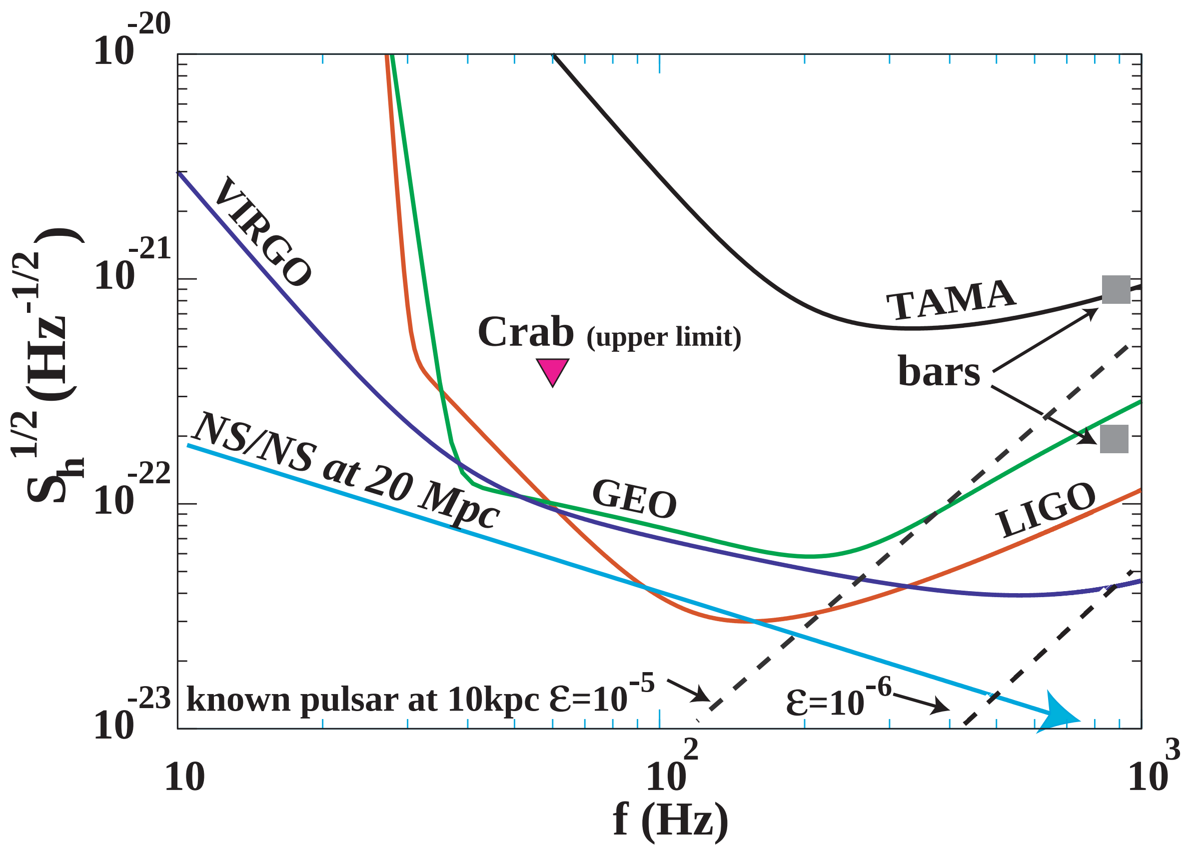

Upper bound for NS-NS (BH-BH) coalescence with LIGO: $\sim 1/3\text{yr}$ **(**$1/\text{yr}$**)**

Second-generation ground-based detectors

Sensitivity improved by a factor $\sim 10 \Rightarrow$ event rates by $\sim 10^3$

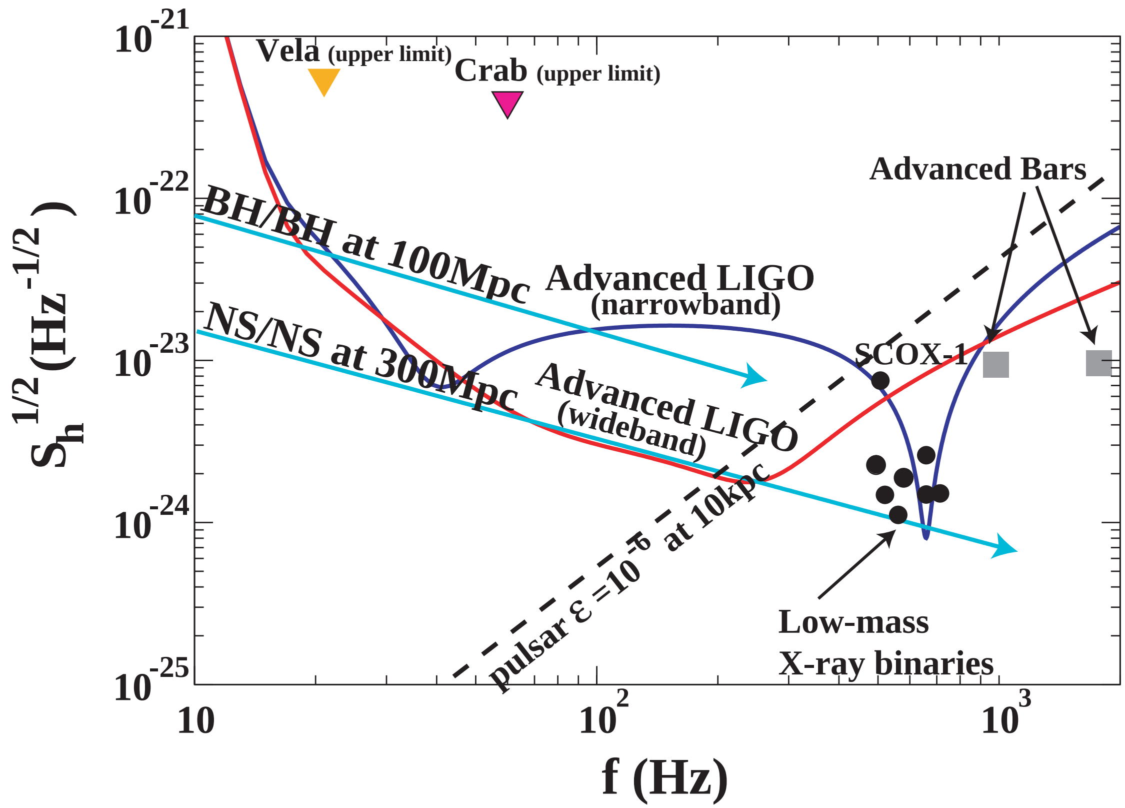

Upper bound for NS-NS binary with Advanced LIGO: a few/month

Massive Binary Black Holes (MBHBs)

– **SMBHB: BH-BH binaries**

$M_{\rm BH} = 10^5\text{–}10^8 M_\odot$

– **IMBH-SMBH binaries**

$M_{\rm IMBH} = 10^2\text{–}10^4 M_\odot$

– **Compact body-IMBH binaries**

– **IMBHB: IMBH-IMBH binaries**

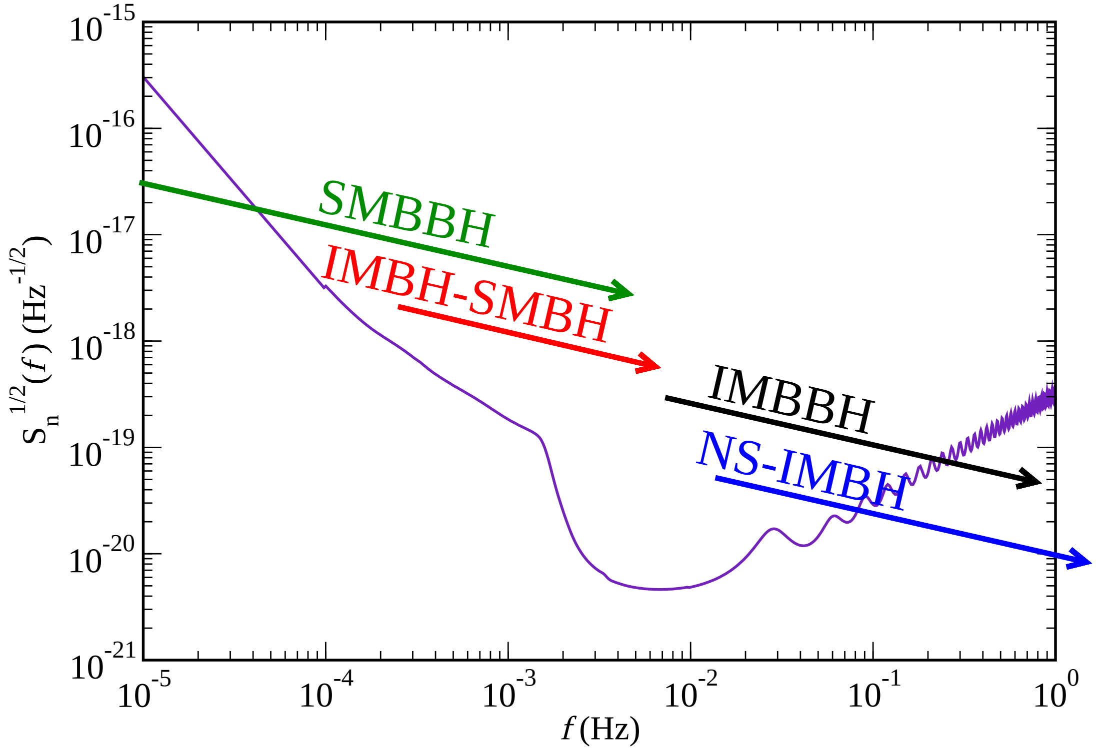

Limiting to quasi-circular orbits

It is generally assumed that gravitational radiation reaction will circularize the orbit by the time the binary is close to the final coalescence [Lincoln & Will 90]

$$e^2 \propto P^{19/9} \quad \text{If } e_i \sim 1, \; P_i > 1\text{h}, \; P_f = 0.2 \text{ sec} \; \Rightarrow \; e_f < 10^{-5}$$

Hulse-Taylor binary has currently an eccentricity of $e_i = 0.617$. In few hundred millions years when the orbital frequency ~ 10 Hz, the eccentricity will be $e_f \sim 10^{-6}$

Binary coalescence time

$$E = \frac{1}{2}\mu\, v^2 - \frac{G\mu\, M}{r} = -\frac{G\mu\, M}{2r} \quad \Rightarrow \quad r = -\frac{G\mu\, M}{2E}$$

$$\dot{r} = \frac{dr}{dE}\,\frac{dE}{dt} = -\frac{64}{5}\frac{G\mu\, M^2}{r^3} \quad \text{integrating} \quad \Rightarrow \quad r(t) = \left(r_0^4 - \frac{256}{5}\,G\mu\, M^2\,\Delta\tau_{\rm coal}\right)^{1/4}$$

If $r(t_f) \ll r_0 \quad \Rightarrow \quad \Delta\tau_{\rm coal} = \frac{5}{256}\frac{r_0^4}{G\mu\, M^2}$

Examples:

- **LIGO/VIRGO/GEO/TAMA source:** $M = (10+10)M_\odot$ **at** $r_0 \sim 500$ **km,**

  $f_{\rm GW} \sim 40$**Hz,** $T_0 \sim 0.05$**sec** $\Rightarrow$ $\Delta\tau_{\rm coal} \sim 1\,\text{sec}$

- **LISA source:** $M = (10^6 + 10^6)M_\odot$ **at** $r_0 \sim 200 \times 10^6\,\text{km}$,

  $f_{\rm GW} \sim 4.5 \times 10^{-5}$ **Hz,** $T_0 \sim 11$ **hours** $\Rightarrow$ $\Delta\tau_{\rm coal} \sim 1\,\text{year}$

Waveforms in the adiabatic approximation

Inspiral and orbital time scales

- **Inspiral time scale**

$$\dot{r} = -\frac{64}{5}\frac{\mu\, M^2}{r^3} \quad \Rightarrow \quad \frac{T_{\rm inspiral}}{M} = \frac{r}{M\,\dot{r}} = \frac{5}{64}\frac{M}{\mu}\left(\frac{r}{M}\right)^4$$

- **Orbital time scale**

$$\omega^2 = \frac{M}{r^3} \quad \Rightarrow \quad \frac{T_{\rm orbital}}{M} = \frac{2\pi}{M\,\omega} = 2\pi\left(\frac{r}{M}\right)^{3/2}$$

$\Rightarrow$ **When bodies are well separated** $\Rightarrow T_{\rm inspiral} \gg T_{\rm orbital}$

What determines the *adiabatic* waveform in PN calculations

- **Inspiral as an adiabatic sequence of circular orbits:**

$$h \propto \omega^{2/3} \cos 2\Phi$$

- **Energy-balance equation:** $\frac{dE(\omega)}{dt} = -F(\omega)$

$E(\omega) \rightarrow$ center-of-mass energy $F(\omega) \rightarrow$ gravitational-wave energy flux

$E(\omega)$ **and** $F(\omega)$ **known as a PN expansion in** $v/c = (GM\omega/c^3)^{1/3}$

$$\Rightarrow \dot{\omega}(t) = -\frac{F(\omega)}{[dE(\omega)/d\omega]} \quad \Rightarrow \quad \Phi_{\rm GW} = 2\Phi = 1/\pi \int \omega \, dt$$

PN circular-orbit energy for equal-mass binary

- **Circular-orbit energy determined at 2PN order in 1995 by** Blanchet, Damour, Iyer Wiseman, Will **and at 3PN order in 2001 by** Damour, Jaranoswki & Schaefer

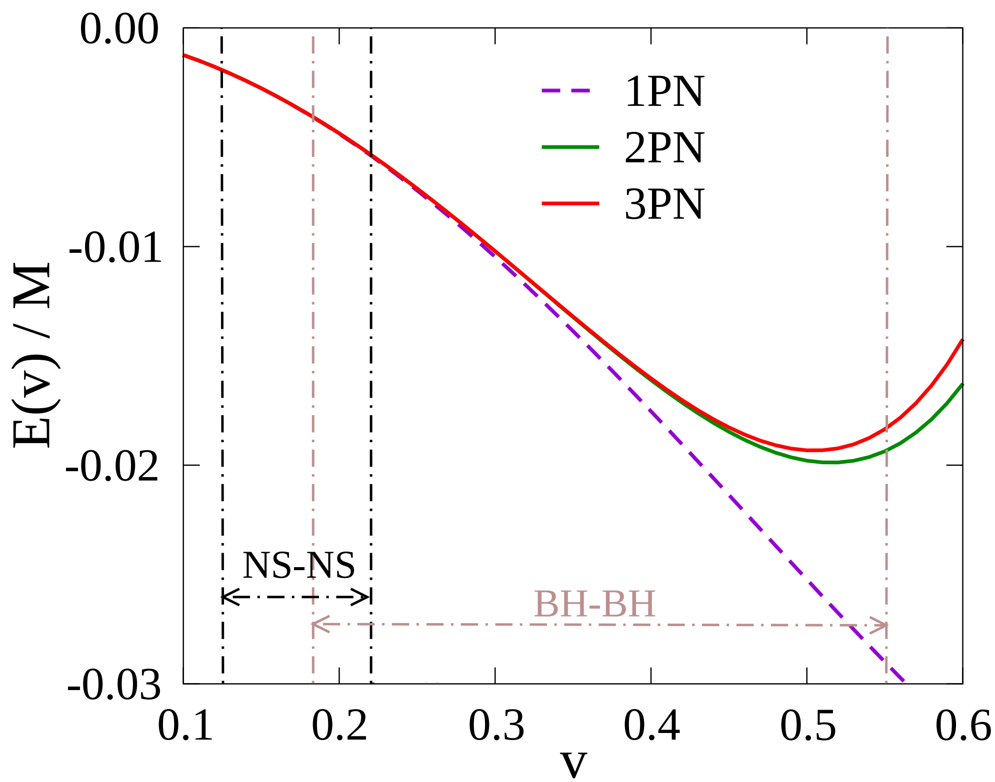

PN GW energy flux for equal-mass binary

- **GW flux determined at 2.5PN order in 1996 by** `Blanchet` **and at 3PN and 3.5PN order in 2004 by** `Blanchet, Damour, Esposito-Farese & Iyer`

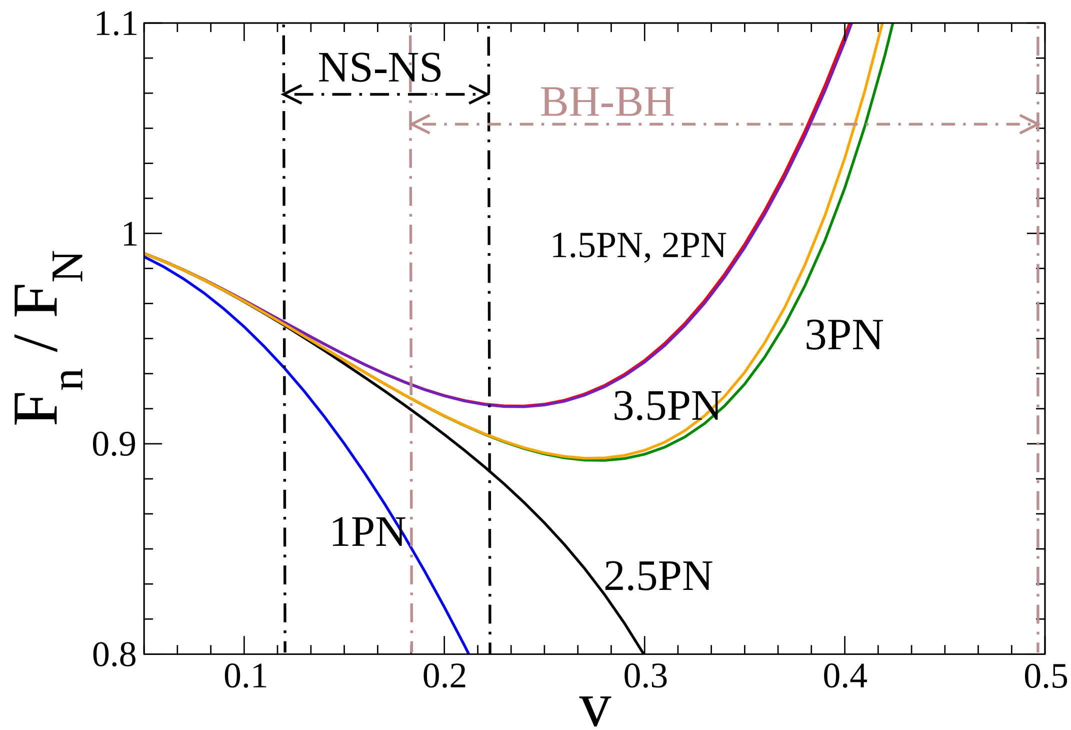

Until when the adiabatic approximation is reliable?

- **Radial potential in black-hole spacetime: Last Stable Orbit or ISCO**

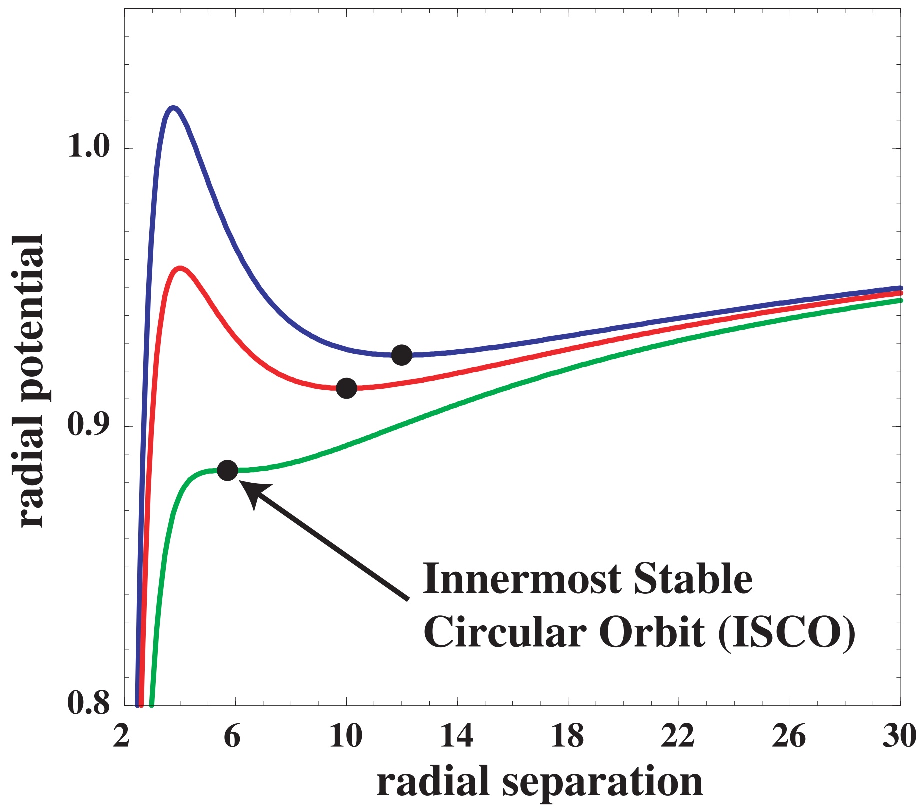

Inspiral: number of GW cycles predicted by standard-PN theory

$M = (1.4 + 1.4) M_\odot$

$f_{\rm in} = 40$ Hz; $f_{\rm fin} = 1570$ Hz

$\chi = |\mathbf{S}|/m^2$

	Number of cycles	**Number of *useful* cycles:**
Newtonian:	16034	247.8
1PN:	$+441$	$+24.0$
1.5PN	-211	-20.0
Spin-orbit:	$+65.7\chi_1 + 65.7\chi_2$	$6.2\chi_1 + 6.2\chi_2$
2PN	$+9.9$	$+1.5$
2.5PN	$-11.7 + 9.2\chi_1 + 9.2\chi_2$	$-2.3 + 0.8\chi_1 + 0.8\chi_2$
3PN:	$+2.6$	$+0.6$
3.5PN:	-0.9	-0.2

Inspiral: number of GW cycles predicted by standard-PN theory

$M = (15 + 15) M_\odot$

$f_{\rm in} = 40$ Hz; $f_{\rm fin} = 147$ Hz

$\chi = |\mathbf{S}|/m^2$

	Number of cycles	**Number of *useful* cycles:**
Newtonian:	302	10.7
1PN:	$+39$	$+4.0$
1.5PN	-37	-6.2
Spin-orbit:	$+11.7\chi_1 + 11.7\chi_2$	$1.9\chi_1 + 1.9\chi_2$
2PN	$+3.3$	$+0.8$
Spin-spin:	$-1.7\chi_1\,\chi_2$	$-0.4\chi_1\,\chi_2$
2.5PN	$-6.2 + 3.6\chi_1 + 3.6\chi_2$	$-2.3\ +0.8\chi_1 + 0.8\chi_2$
3PN:	$+2$	$+1.2$
3.5PN:	-0.8	-0.5

Effect of systematics: number of cycles (SMBHB)

$M = (10^6 + 10^6) M_\odot$ **at** 3 **Gpc**

$f_{\rm in} = 0.045{\rm m}$ Hz; $f_{\rm fin} = 2.2{\rm m}$ Hz (one year observation, SNR ~ 1861)

$\chi = |\mathbf{S}|/m^2$

	Number of cycles	**Number of *useful* cycles:**
Newtonian:	2266	10
1PN:	$+134$	$+4$
1.5PN	-92	-6
Spin-orbit:	$+29\chi_1 + 29\chi_2$	$+2\chi_1 + 2\chi_2$
2PN	$+6$	$+1$
Spin-spin:	$-2\chi_1\,\chi_2$	$0.4\chi_1\,\chi_2$
2.5PN	$-9 + 8\chi_1 + 8\chi_2$	$-2 + 0.8\chi_1 + 0.8\chi_2$
3PN:	$+2$	$+1$
3.5PN:	-1	-0.5

Effect of systematics: number of cycles (IMBHB)

$M = (10^3 + 10^3) M_\odot$ **at** 3 **Gpc**

$f_{\rm in} = 3.3{\rm m}$ Hz; $f_{\rm fin} = 2$ Hz (one year observation) SNR ~ 33

	Number of cycles	**Number of *useful* cycles:**
Newtonian:	170236	74618
1PN:	$+1828$	$+730$
1.5PN	-554	-193
Spin-orbit:	$+173\chi_1 + 173\chi_2$	$+60\chi_1 + 60\chi_2$
2PN	$+17$	$+4$
2.5PN	$-15 + 12\chi_1 + 12\chi_2$	$-2 + 0.8\chi_1 + 0.8\chi_2$
3PN:	$+3$	$+0.1$
3.5PN:	-1	-0.02

Statistical errors versus systematic errors

Monte Carlo with 10^4 sources distributed over sky positions and orientation

$M = (10^6 + 10^6) M_\odot$ **at** 3 **Gpc**

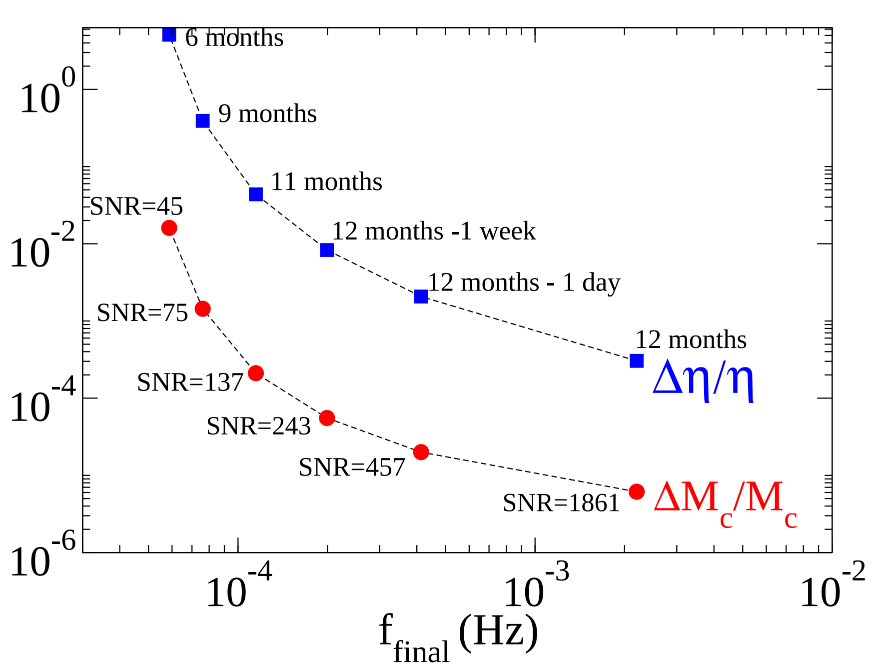

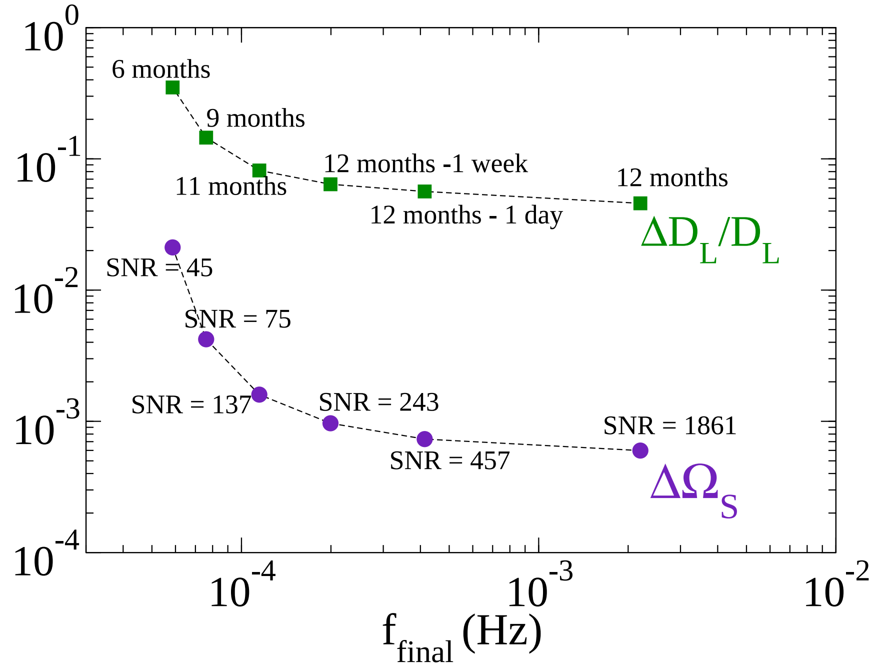

At which time are systematic errors smaller then statistical?

GW signal emitted by a non-spinning binary

$$h_+(t) = \frac{2\mathcal{M}}{R} (\mathcal{M}\,\omega)^{2/3} (1+\cos^2\Theta) \cos(2\Phi + 2\Phi_0) \qquad \mathcal{M} = \mu^{3/5} M^{2/5}$$

$$h_\times(t) = \frac{4\mathcal{M}}{R} (\mathcal{M}\,\omega)^{2/3} \cos\Theta \,\sin(2\Phi + 2\Phi_0)$$

- **Detector response** $h(t) = h_+(t)\,F_+ + h_\times(t)\,F_\times$
- **Defining** $\widetilde{F}_+ = \frac{(1+\cos^2\Theta)\,F_+}{[(1+\cos^2\Theta)^2\,F_+^2 + 4\cos^2\Theta\,F_\times^2]^{1/2}}, \quad \widetilde{F}_\times = \frac{4\cos^2\Theta\,F_\times}{[(1+\cos^2\Theta)^2\,F_+^2 + 4\cos^2\Theta\,F_\times^2]^{1/2}}$

$$\widetilde{F}_+^2 + \widetilde{F}_\times^2 = 1 \quad \Rightarrow \quad \cos\xi \equiv \widetilde{F}_+ \quad \sin\xi \equiv \widetilde{F}_\times$$

- **We introduce** $\mathcal{A}(\theta,\phi,\psi;\Theta) = [(1+\cos^2\Theta)^2\,F_+^2 + 4\cos^2\Theta\,F_\times^2]^{1/2}$

$$\tan\xi(\theta,\phi,\psi;\Theta) = \frac{4\cos^2\Theta\,F_\times}{(1+\cos^2\Theta)\,F_+}$$

GW signal in Fourier domain

$$h(t) = \frac{2\mathcal{M}}{R}\,\mathcal{A}\,(\mathcal{M}\,\omega(t))^{2/3}\cos(2\Phi(t) + 2\Phi_0 - \xi)$$

- **If we are not interested in the "inverse" problem**:
  - ξ **can be re-absorbed in** Φ_0
  - **Averaging over** $(\theta, \phi, \psi, \Theta) \;\Rightarrow\; \overline{\mathcal{A}^2} = \frac{16}{25}$

- **Fourier transform:**

$$\tilde{h}(f) = \int_{-\infty}^{+\infty} e^{2\pi i f t}\,h(t)\,dt = \frac{1}{2}\int_{-\infty}^{+\infty} dt\,A(t)\,\left[e^{2\pi i f t + i\Phi_{\rm GW}(t)} + e^{2\pi i f t - i\Phi_{\rm GW}(t)}\right]$$

where $A(t) = \frac{2\mathcal{M}}{R}\,\mathcal{A}\,(\mathcal{M}\,\omega(t))^{2/3}$ and $\Phi_{\rm GW}(t) = 2\Phi(t) + 2\Phi_0 - \xi$

Stationary phase approximation

$$\tilde{h}(f) = \frac{1}{2}\int_{-\infty}^{+\infty} dt\, A(t)\, \left[e^{2\pi i f t + i\Phi_{\rm GW}(t)} + e^{2\pi i f t - i\Phi_{\rm GW}(t)}\right]$$

- **Dominant contribution from the vicinity of the** *stationary* **points in the phase**

Assuming $f > 0$ **and posing** $\psi(t) \equiv 2\pi\, f\, t - \Phi_{\rm GW}$

Imposing $\left(\frac{d\psi}{dt}\right)_{t_f} = 0 \;\Rightarrow\; \left(\frac{d\Phi_{\rm GW}}{dt}\right)_{t_f} = 2\pi\, f = 2\pi F(t_f)$

Expanding the phase: $\psi(t_f) = 2\pi\, f\, t_f - \Phi_{\rm GW}(t_f) - \pi\, \dot{F}(t_f)\,(t - t_f)^2$

$$\tilde{h}_{\rm SPA}(f) = \frac{1}{2}\frac{A(t_f)}{\sqrt{\dot{F}(t_f)}}\, e^{i(2\pi\, f\, t_f - \Phi_{\rm GW}(t_f)) - i\pi/4}$$

- **How do we compute** $\Phi_{\rm GW}(t_f)$ **and** $\dot{F}(t_f)$**?**

Stationary phase approximation (continued)

- **We need to solve** $v^3 = \dot{\Phi}_{\rm GW}\, M/2$ **and** $\dot{E}(v) = -F(v)$

$$t(v) = t_c + M\ \int_v^{v_c} dv\, \frac{E'(v)}{F(v)}$$

$$\Phi_{\rm GW}(v) = \Phi_c + 2\ \int_v^{v_c} dv\, v^3\, \frac{E'(v)}{F(v)}$$

$$\Rightarrow\ \psi(f) = 2\pi f\, t_c - \Phi_c - \pi/4 + 2\int_v^{v_c} (v_c^3 - v^3)\, \frac{E'(v)}{\mathcal{F}(v)}\, dv$$

$$\Rightarrow\ \dot{F}(t_f) = \frac{\dot{\omega}}{\pi} = \frac{96}{5}\,\frac{1}{\pi}\,\nu\, M^{5/3}\,\omega^{11/3}$$

$$\tilde{h}_{\rm SPA}(f) = \mathcal{A}_{\rm SPA}(f)\, e^{i\psi_{\rm SPA}(f)} \qquad \mathcal{A}_{\rm SPA}(f) = \frac{\mathcal{A}}{R}\,\frac{1}{\pi^{2/3}}\,\left(\frac{5}{96}\right)^{1/2}\,\mathcal{M}^{5/6}\, f^{-7/6}$$

- $\psi_{\rm SPA}(f) = 2\pi\, f\, t_c - \Phi_c - \pi/4 + f^{-5/3}\,\left(\psi_0 + \psi_1\, f^{2/3} + \psi_{3/2}\, f + \cdots\right)$

$$\psi_0 = \psi_0(\mathcal{M})\,, \quad \psi_1 = \psi_1(m_1, m_2)\,, \quad \psi_{3/2} = \psi_{3/2}(m_1, m_2, \boldsymbol{S}\cdot\boldsymbol{L})\,, \cdots$$

Optimal signal-to-noise ratio for SPA waveforms

$$h_{\rm SPA}(f) = \mathcal{A}_{\rm SPA}\, f^{-7/6}\, e^{i\Psi_{\rm SPA}(f)}\,, \qquad \mathcal{A}_{\rm SPA} = \frac{1}{\sqrt{30}\pi^{2/3}}\frac{\mathcal{M}^{5/6}}{R}$$

$$\sqrt{\overline{\left(\frac{S}{N}\right)^2}} = \frac{1}{R}\,\frac{1}{\pi^{2/3}}\,\sqrt{\frac{2}{15}}\,\mathcal{M}^{5/6}\,\left[\int_{f_{\rm low}}^{f_{\rm high}} \frac{f^{-7/3}}{S_n(f)}\right]^{1/2}$$

GW templates in Fourier domain through 2PN order

$$\tilde{h}(f) = \mathcal{A}_{\rm SPA}(f)\, e^{i\psi_{\rm SPA}(f)}$$

$$\begin{aligned}
\psi_{\rm SPA}(f) \quad = \quad & 2\pi f t_c - \Phi_c - \pi/4 + \frac{3}{128}\,(\pi\mathcal{M}f)^{-5/3}\,\{1+ \\
& -\frac{5\hat{\alpha}^2}{336\omega_{\rm BD}}\,\nu^{2/5}\,(\pi\mathcal{M}f)^{-2/3} - \frac{128}{3}\frac{\pi^2 D\,\mathcal{M}}{\lambda_g^2\,(1+z)}\,(\pi\mathcal{M}f)^{2/3} \\
+ \quad & \left(\frac{3715}{756} + \frac{55}{9}\nu\right)\,\nu^{-2/5}\,(\pi\mathcal{M}f)^{2/3} - 16\pi\,\nu^{-3/5}\,(\pi\mathcal{M}f) + 4\beta\,\nu^{-3/5}\,(\pi\mathcal{M}f) \\
+ \quad & \left(\frac{15293365}{508032} + \frac{27145}{504}\nu + \frac{3085}{72}\nu^2\right)\,\nu^{-4/5}\,(\pi\mathcal{M}f)^{4/3} - 10\sigma\,\nu^{-4/5}\,(\pi\mathcal{M}f)^{4/3}\Big\}
\end{aligned}$$

$$\beta = \frac{1}{12}\sum_{i=1}^{2}\chi_i\left[113\frac{m_i^2}{M^2} + 75\nu\right]\widehat{\boldsymbol{L}}\cdot\widehat{\boldsymbol{S}}_i\,, \qquad \sigma = \frac{\nu}{48}\chi_1\chi_2\left(-27\widehat{\boldsymbol{S}}_1\cdot\widehat{\boldsymbol{S}}_2 + 721\widehat{\boldsymbol{L}}\cdot\widehat{\boldsymbol{S}}_1\widehat{\boldsymbol{L}}\cdot\widehat{\boldsymbol{S}}_2\right)$$

Upper limit for NS-NS from LIGO science runs

- **373 hours (15 days) of data from the second science run of LIGO**
- **Max distance 1.5 Mpc (Andromeda Galaxy and other galaxies of the Local Group)**

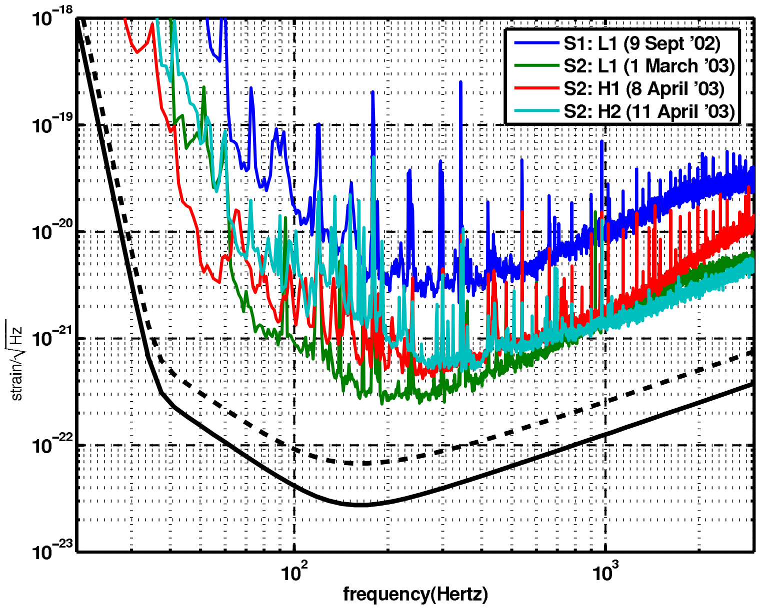

- **Upper limit of less than 47 events per year per Milky Way equivalent galaxy for nonspinning binary neutron stars with $m_{\rm NS} = 1$–$3 M_\odot$**

Precessing versus non-precessing compact binaries

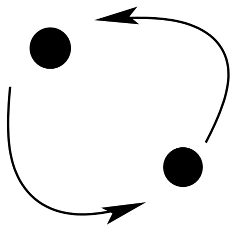

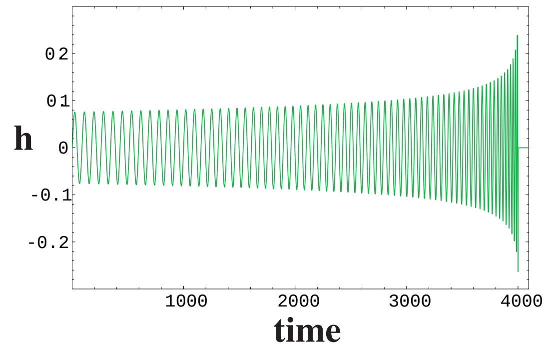

- **Non spinning: Inspiral [$f_{\rm GW} = 2 f_{\rm orb}, f_{\rm end}(m_1, m_2)$], plunge, merger and ring down**

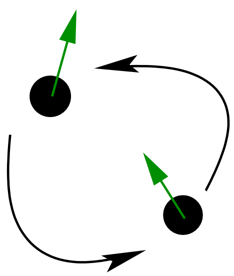

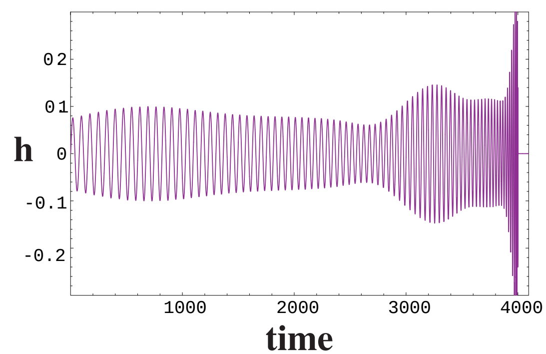

Many more parameters!

- **Precessing: Inspiral [$f_{\rm GW} = (2 f_{\rm orb}, f_{\rm prec}), f_{\rm end}(\boldsymbol{S}, m_1, m_2)$], plunge (?) merger, ring down**

Precession of the orbital plane modulates both amplitude and phase of gravity-wave

Inspiraling spinning binaries

- **Spin effects within the PN framework**

$$S \sim m\, l\, v_{\rm spin}$$

  - **For compact objects:** $l \sim \frac{G\, m}{c^2}$
  - **If maximally rotating:** $v_{\rm spin} \sim c$

$$\Rightarrow S \sim \frac{G\, m^2}{c} \chi \qquad \chi \lesssim 1$$

- **Spin effects:**
  - **Spin-orbit coupling (SO) at 1.5PN order**
  - **Spin-spin coupling (SS) at 2PN order**
  - **1PN corrections to SO coupling at 2.5PN order**

Detectability of inspiraling spinning binaries

Spin-orbit coupling makes two-body gravitational interaction more (less) repulsive when spins are aligned (anti-aligned)

$$V(r) = -\frac{mM}{r} + \frac{L^2}{2mr^2} - \frac{L^4}{m^3r^4} + \cdots + \frac{2}{r^3}\boldsymbol{L}\cdot\boldsymbol{S} + \cdots$$

Duration of inspiral (and signal-to-noise ratio) modified by spin effects

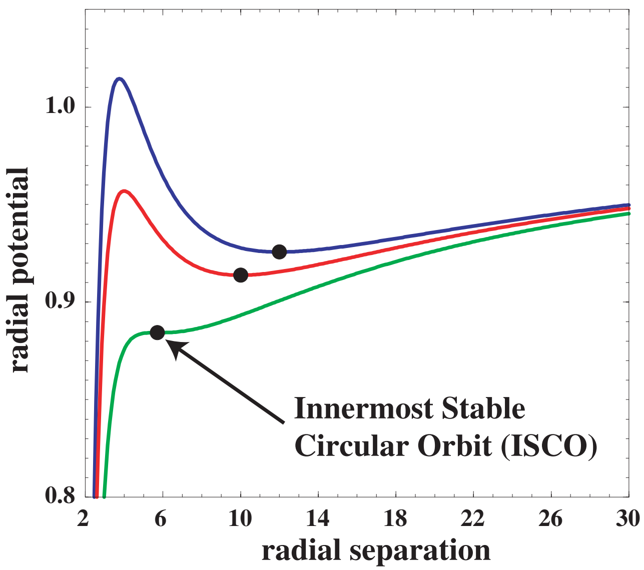

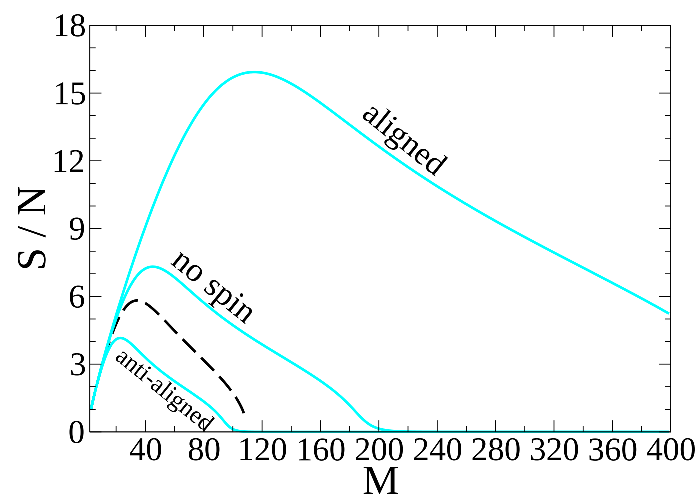

Equal-mass binaries at 100 Mpc

Predictions for spin misalignement and spin magnitude

- **Simulations considering NS-BH and BH-BH in Galactic field**

  [misalignement due to "kick" (recoil velocity) imparted to NSs at birth]

  [Kalogera 00; Grandéclement et al. 04]

– $50\% - 80\%$ **of NS-BH have tilt angle smaller than** 40^o **and** $10 - 20\%$ **between** 40^o **and** 50^o

– **more than** 90% **of BH-BH binaries have tilt angle smaller than** 30^o

- **Spin properties of NS-BH and BH-BH in centers of globular clusters may be very different**

- **No constraints on the orientation and magnitude of spins in massive and supermassive black-hole binaries**

- $S_{\rm BH}/m_{\rm BH}^2 \sim 0 - 1$ **and** $S_{\rm NS}/m_{\rm NS}^2 \sim 0.005 - 0.01$

Time scales characterizing spinning dynamics

- **Inspiral time scale:**

$$E = -\frac{\mu M}{2r} \qquad -\frac{dE}{dt} = \frac{32}{5}\frac{\nu^2 M^5}{r^5} \qquad \Rightarrow \qquad \frac{T_{\rm insp}}{M} \propto \frac{1}{\nu}\left(\frac{r}{M}\right)^4$$

- **Orbital time scale:**

$$\omega^2 = \frac{M}{r^3} \qquad \Rightarrow \qquad \frac{T_{\rm orb}}{M} = \frac{2\pi}{M\omega} \propto \left(\frac{r}{M}\right)^{3/2}$$

- **Precession time scale (spin-orbit coupling):** $\dot{\boldsymbol{S}} \propto \overbrace{\frac{1}{r^3}}^{\Omega^L_{\rm prec}}\boldsymbol{L}\times\boldsymbol{S}\,, \qquad \dot{\widehat{\boldsymbol{L}}} \propto \overbrace{\frac{1}{r^3}}^{\Omega^S_{\rm prec}}\boldsymbol{S}\times\widehat{\boldsymbol{L}}$

$$\frac{T^L_{\rm prec}}{M} = \frac{2\pi}{M\Omega^L_{\rm prec}} \propto \frac{1}{\nu}\left(\frac{r}{M}\right)^{5/2}\,, \qquad \frac{T^S_{\rm prec}}{M} = \frac{2\pi}{M\Omega^S_{\rm prec}} \propto \left(\frac{r}{M}\right)^{3}$$

$$T_{\rm orb} \ll T^L_{\rm prec}, T^S_{\rm prec} \ll T_{\rm insp}$$

Inspiraling dynamics averaging over orbital period: adiabatic limit

[Barker & O'Connell 75; Damour 82; Thorne & Hartle 85; Kidder 95; Kidder, Wiseman & Will 96]
[Tagoshi et al. 01; Owen et al. 98; Faye, Blanchet & AB 06; Blanchet, AB & Faye 06]

$$\dot{\omega} = -F(\omega)/[dE(\omega)/d\omega]$$

$$\frac{\dot{\omega}}{\omega^2} = \frac{96}{5}\,\nu\,(M\omega)^{5/3}\,\Big[1 + c_{1\mathrm{PN}}(m_1,m_2)\,(M\omega)^{2/3} + c_{1.5\mathrm{PN}}(SO,m_1,m_2)\,(M\omega)$$
$$+ c_{2\mathrm{PN}}(SS,m_1,m_2)\,(M\omega)^{4/3} + c_{2.5\mathrm{PN}}(SO,m_1,m_2)\,(M\omega)^{5/3} + c_{3\mathrm{PN}}(m_1,m_2)\,(M\omega)^2$$
$$+ c_{3.5\mathrm{PN}}(m_1,m_2)\,(M\omega)^{7/3}\Big]$$

$$\dot{\boldsymbol{S}}_1 = \frac{(M\omega)^2}{2M}\left\{\left(4+3\frac{m_2}{m_1}\right)\boldsymbol{L} + \frac{1}{M^2}\left[\boldsymbol{S}_2 - 3(\boldsymbol{S}_2\cdot\hat{\boldsymbol{L}})\hat{\boldsymbol{L}}\right] + \cdots\right\}\times\boldsymbol{S}_1$$
$$\dot{\boldsymbol{S}}_2 = \frac{(M\omega)^2}{2M}\left\{\left(4+3\frac{m_1}{m_2}\right)\boldsymbol{L} + \frac{1}{M^2}\left[\boldsymbol{S}_1 - 3(\boldsymbol{S}_1\cdot\hat{\boldsymbol{L}})\hat{\boldsymbol{L}}\right] + \cdots\right\}\times\boldsymbol{S}_2\,,$$
$$\dot{\hat{\boldsymbol{L}}} = -\frac{(M\,\omega^{1/3})}{\nu\,M^2}\,\dot{\boldsymbol{S}} \qquad \boldsymbol{S} = \boldsymbol{S}_1 + \boldsymbol{S}_2$$

Two classes of binaries: single spin

- **Equal-mass binary and SS couplings neglected:**

$$\Rightarrow \boldsymbol{S} = \boldsymbol{S}_{\rm tot} = \boldsymbol{S}_1 + \boldsymbol{S}_2 \quad \text{and} \quad d(\boldsymbol{S}_1 \cdot \boldsymbol{S}_2)/dt = 0$$

- **Small mass-ratio binary:**

$$\Rightarrow m_2 \ll m_1 \quad \Rightarrow \quad |\boldsymbol{S}_2| = m_2^2\,\chi_2 \ll |\boldsymbol{S}_1| = m_1^2\,\chi_1 \quad \Rightarrow \quad \boldsymbol{S} = \boldsymbol{S}_1$$

$$\dot{\boldsymbol{S}} = \frac{\nu (M\omega)^{5/3}}{2M}\left(4 + \frac{3m_2}{m_1}\right) \hat{\boldsymbol{L}} \times \boldsymbol{S} \qquad \dot{\hat{\boldsymbol{L}}} = \frac{\omega^2}{2M}\left(4 + \frac{3m_2}{m_1}\right) \boldsymbol{S} \times \hat{\boldsymbol{L}}$$

$$\dot{\omega} = \dot{\omega}(\omega, \boldsymbol{S} \cdot \boldsymbol{L}, m_1, m_2)$$

$\alpha^J_{\rm prec} = \mathcal{B}\,\omega^{-1}$ if $L \sim \nu M^{5/3} \omega^{-1/3} \gg S$ [large separations, comparable masses]

$\alpha^J_{\rm prec} = \mathcal{B}\,\omega^{-2/3}$ if $S \gg L \sim \nu M^{5/3} \omega^{-1/3}$ [small mass ratio, last stages of inspiral]

$d\alpha^J_{\rm prec}/dt = \Omega^J_{\rm prec}$ [Apostolatos, Cutler, Sussman and Thorne 95]

Precession around the direction of the total angular momentum $\hat{\boldsymbol{J}}$

- **Single spin binary (simple precession)**

$$\dot{\boldsymbol{S}} \propto \frac{J}{r^3}\hat{\boldsymbol{J}} \times \boldsymbol{S}$$

$$\dot{\hat{\boldsymbol{L}}} \propto \frac{J}{r^3}\hat{\boldsymbol{J}} \times \hat{\boldsymbol{L}}$$

$$\Omega^{J}_{\rm prec} \propto \frac{J}{r^3}$$

$$\hat{\boldsymbol{L}} \cdot \hat{\boldsymbol{S}} = \mathrm{const}$$

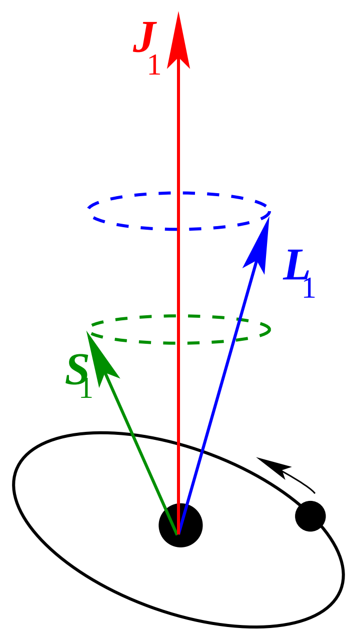

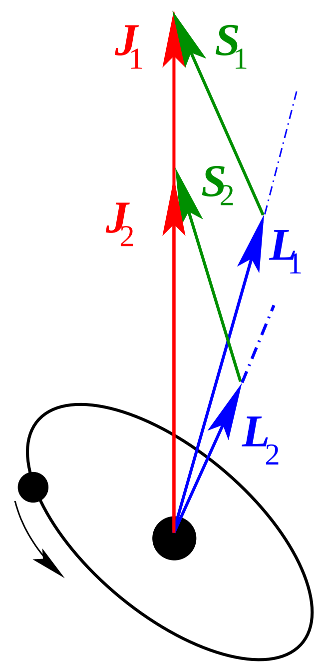

- **Transitional precession** ($\boldsymbol{L} \simeq -\boldsymbol{S}$ the binary tumbles in space)

Example of transitional precession

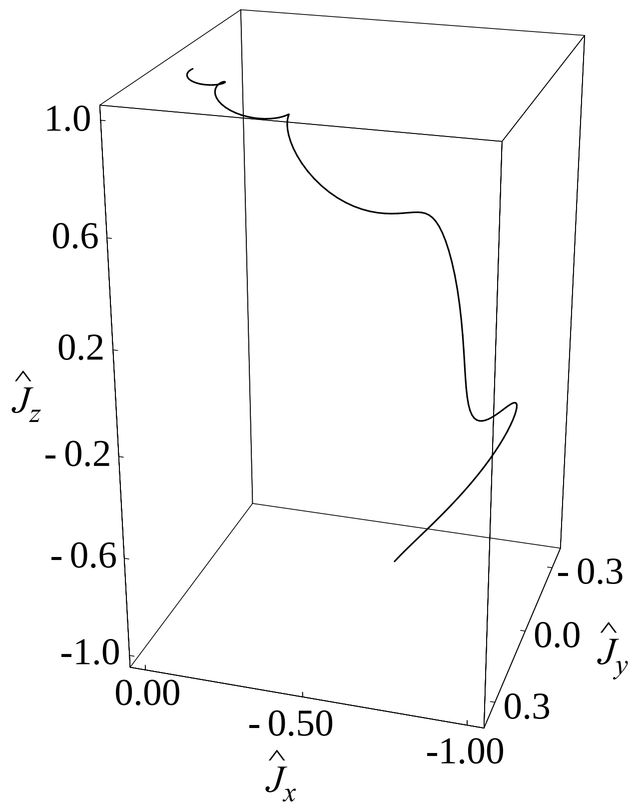

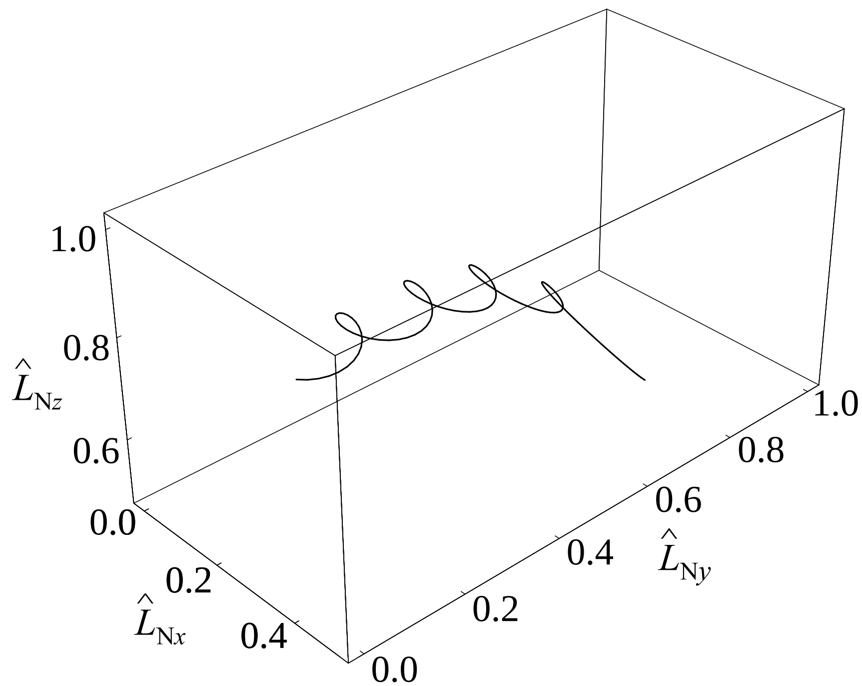

- $(20 + 5) M_\odot$ **with initial angles** $\theta_{S_1} = 175.4^\circ$, $\theta_{S_2} = 105.4^\circ$, $\phi_{S_1} - \phi_{S_2} = 92.0^\circ$

Number of precessing cycles

small mass ratio binary

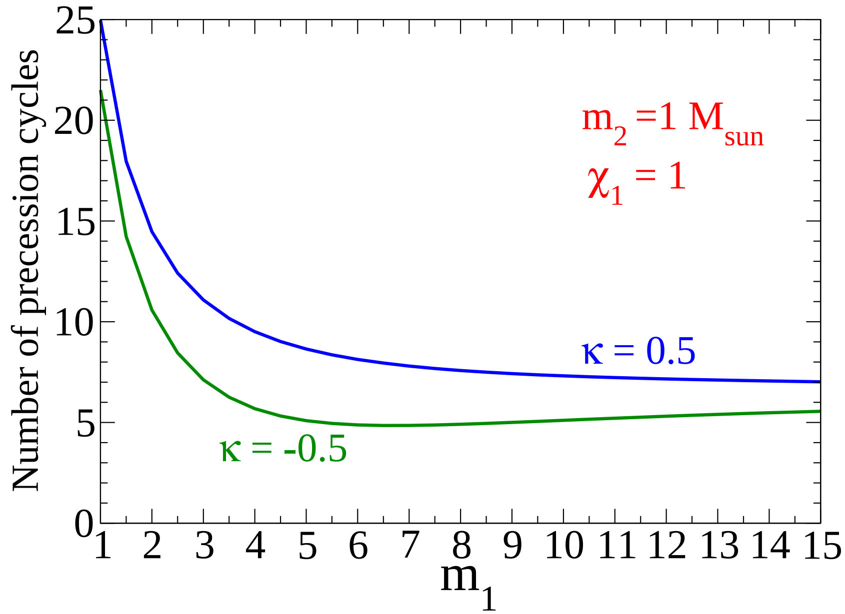

equal-mass binary

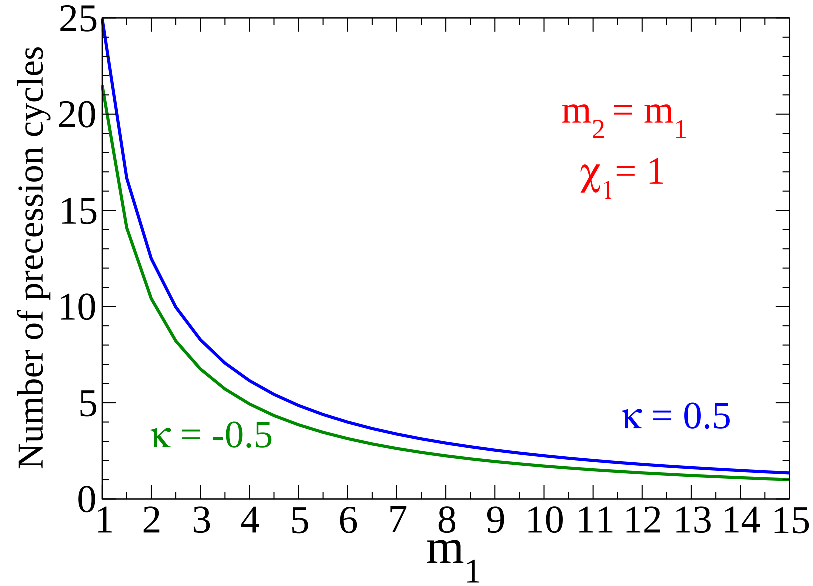

Gravity-wave in the Finn-Chernoff convention

- **Assuming circular orbits, the leading order quadrupole formula reads**

$$h^{ij} = \frac{2\mu}{R}\left(\frac{M}{r}\right) Q_c^{ij} \quad \text{with} \quad Q_c^{ij} = 2\left(\lambda^i \lambda^j - n^i n^j\right)$$

$\widehat{\boldsymbol{n}} \longrightarrow$ **unit vector along binary separation vector** $\mathbf{r}$

$\widehat{\boldsymbol{\lambda}} \longrightarrow$ **unit vector along binary relative velocity** $\mathbf{v}$

$$\widehat{\boldsymbol{n}}(t) = \boldsymbol{e}_1(t)\,\cos\Phi(t) + \boldsymbol{e}_2(t)\,\sin\Phi(t) \qquad \widehat{\boldsymbol{\lambda}}(t) = -\boldsymbol{e}_1(t)\,\sin\Phi(t) + \boldsymbol{e}_2(t)\,\cos\Phi(t)$$

- **Finn-Chernoff convention:**

  – $\boldsymbol{e}_1(t) \equiv \frac{\boldsymbol{e}_z^{\rm S} \times \widehat{\boldsymbol{L}}_{\rm N}}{\sin\iota}$ and $\boldsymbol{e}_2(t) \equiv \frac{\boldsymbol{e}_z^{\rm S} - \widehat{\boldsymbol{L}}_{\rm N}\cos\iota}{\sin\iota}$

  – **the vector $\boldsymbol{e}_1$ points in the direction of the ascending node**

  – Φ **is the orbital phase with respect to the ascending node**

  – $\dot{\Phi} = \omega - \dot{\alpha}\,\cos\iota$ **with** $\dot{\hat{\boldsymbol{n}}} = \omega\,\widehat{\boldsymbol{\lambda}}$

Spinning binary parameters

	,Binary		GW propagation	Detector orientation
M, ν, S_1, S_2	θ_{S_1}, θ_{S_2},$\phi_{S_1} - \phi_{S_2}$	$\theta_{\mathrm{L_N}} \equiv \iota$, $\phi_{\mathrm{L_N}} \equiv \alpha$, $\phi_{S_1} + \phi_{S_2}$	Θ, φ	θ,ϕ, ψ
Basic	Local	Directional		

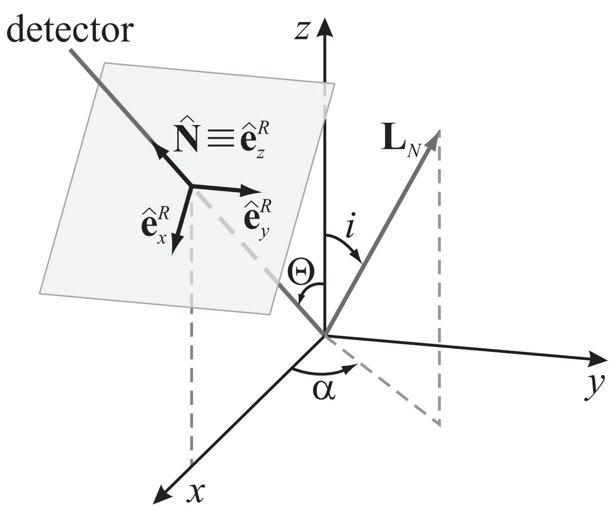

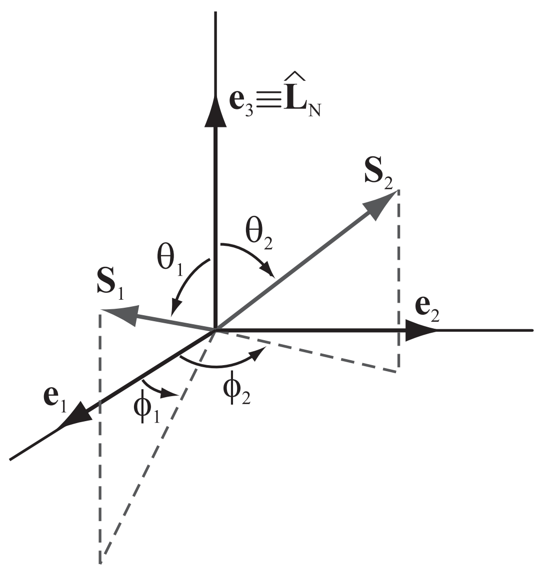

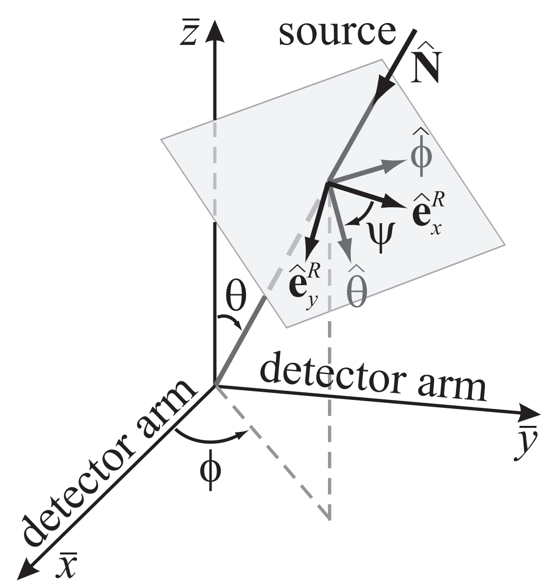

Gravity-wave in the Finn-Chernoff convention (continued)

$$Q_c^{ij} = -2\left(\left[\boldsymbol{e}_+^{ij}(t)\,\cos 2(\Phi(t)+\Phi_0) + \boldsymbol{e}_\times^{ij}(t)\,\sin 2(\Phi(t)+\Phi_0)\right]\right)$$

where $\boldsymbol{e}_+ \equiv \boldsymbol{e}_1 \otimes \boldsymbol{e}_1 - \boldsymbol{e}_2 \otimes \boldsymbol{e}_2$ **and** $\boldsymbol{e}_\times \equiv \boldsymbol{e}_1 \otimes \boldsymbol{e}_2 + \boldsymbol{e}_2 \otimes \boldsymbol{e}_1$

$\mathbf{T}_+ \equiv \boldsymbol{e}_x^R \otimes \boldsymbol{e}_x^R - \boldsymbol{e}_y^R \otimes \boldsymbol{e}_y^R$ **and** $\mathbf{T}_\times \equiv \boldsymbol{e}_x^R \otimes \boldsymbol{e}_y^R + \boldsymbol{e}_y^R \otimes \boldsymbol{e}_x^R$

$$\mathbf{e}_x^R = -\boldsymbol{e}_x^S\,\sin\varphi + \boldsymbol{e}_y^S\,\cos\varphi$$
$$\mathbf{e}_y^R = -\boldsymbol{e}_x^S\,\cos\Theta\,\cos\varphi - \boldsymbol{e}_y^S\,\cos\Theta\,\sin\varphi + \boldsymbol{e}_z^S\,\sin\Theta$$
$$\mathbf{e}_z^R = +\boldsymbol{e}_x^S\,\sin\Theta\,\cos\varphi + \boldsymbol{e}_y^S\,\sin\Theta\,\sin\varphi + \boldsymbol{e}_z^S\,\cos\Theta = \mathbf{N}$$

$$h = h_+\,F_+ + h_\times\,F_\times = \frac{2\mu}{R}\,\frac{M}{r}\,Q_c^{ij}\,([\mathbf{T}_+]_{ij}\,F_+ + [\mathbf{T}_+]_{ij}\,F_+)$$

Phenomenological templates in adiabatic limit: Apostolatos ansatz

Phenomenological waveforms: introducing few *new* parameters and having reasonably good matches with the signal

Apostolatos' ansatz: add modulations to SPA phase [Apostolatos 96]

$$\psi_{\rm SPA}(f) = f^{-5/3}\,\left(\psi_0 + \psi_1\, f^{2/3} + \psi_{3/2}\, f + \cdots\right) + \mathcal{C}\,\cos(\delta + \alpha^J_{\rm prec})$$

$$\alpha^J_{\rm prec} = \mathcal{B} f^{-2/3} \quad \text{or} \quad \mathcal{B} f^{-1} \qquad \text{where} \qquad d\alpha^J_{\rm prec}/dt = \Omega^J_{\rm prec}$$

– **Not very satisfactory performances (why?)** [Grandéclement, Kalogera & Vecchio 96]

– **three** *new* **intrinsic parameters** $(m_1, m_2, \mathcal{C}, \delta, \mathcal{B})$

– **high computational cost**

Performances can improve using "spike" waveforms [Grandéclement & Kalogera 03]

Gravity-wave in precessing convention

[AB, Chen & Vallisneri 03]

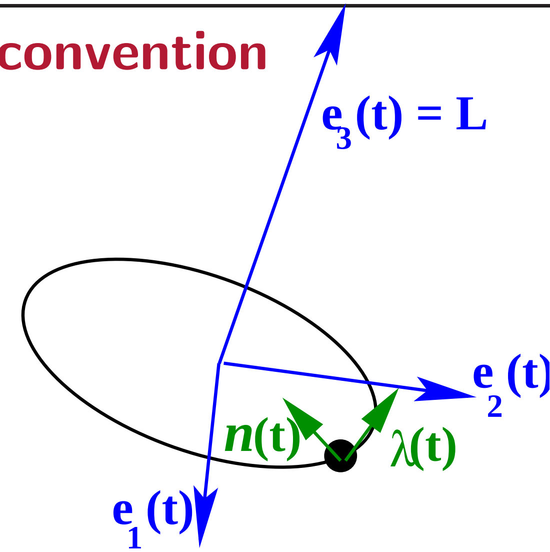

$$h^{ij} \propto \ddot{Q}^{ij}, \qquad \ddot{Q}^{ij} = 2(\lambda^i\lambda^j - n^i n^j)$$

$$\hat{\boldsymbol{n}}(t) = \boldsymbol{e}_1(t)\,\cos\Phi(t) + \boldsymbol{e}_2(t)\,\sin\Phi(t)$$
$$\hat{\boldsymbol{\lambda}}(t) = -\boldsymbol{e}_1(t)\,\sin\Phi(t) + \boldsymbol{e}_2(t)\,\cos\Phi(t)$$

- **adiabatic sequence of spherical orbits** $\Rightarrow \dot{\hat{\boldsymbol{n}}} = \omega\hat{\boldsymbol{\lambda}}$ **but in general** $\dot{\Phi} \neq \omega$
- ω **almost non-modulated**

Precessing convention: $\dot{e}_i(t) = \Omega_e(t) \times e_i(t)$ **such that** $\dot{\Phi} = \omega$ **!**

$$\boldsymbol{\Omega}_e(t) \equiv \boldsymbol{\Omega}_L(t) - [\boldsymbol{\Omega}_L(t)\cdot\hat{\boldsymbol{L}}_N(t)]\,\hat{\boldsymbol{L}}_N(t)\,, \quad \dot{\hat{\boldsymbol{L}}}_N = \boldsymbol{\Omega}_L \times \hat{\boldsymbol{L}}_N(t)\,, \quad \boldsymbol{\Omega}_e\cdot\hat{\boldsymbol{L}}_N = 0$$

Gravity-wave in precessing convention (continued)

[Apostolatos 95; AB, Chen & Vallisneri 03; AB, Chen, Pan & Vallisneri 05]

Clean separation of time-dependent and time-independent parameters in waveforms

$$h(t) = \underbrace{-\frac{2\mu}{R}\,\frac{M}{r(t)}\left[\boldsymbol{e}_{+}^{ij}(t)\,\cos 2(\Phi(t)+\Phi_0) + \boldsymbol{e}_{\times}^{ij}(t)\,\sin 2(\Phi(t)+\Phi_0)\right]}_{\mathrm{Q(t):\,wave\,generation}} \times$$

$$\underbrace{[T_{+\,ij}(\Theta,\varphi)\,F_{+}(\theta,\phi,\psi) + T_{\times\,ij}(\Theta,\varphi)\,F_{\times}(\theta,\phi,\psi)]}_{\mathrm{P:\,detector\,projection}}$$

$P_{ij} \;\Rightarrow\;$ *static* **relative position and orientation of detector and wave with repect to the axes initially defined by the binary**

$$\tilde{h}_{\rm SPA}(f) = -\tilde{h}_{\rm non\,mod}(f)\left([\mathbf{e}_{+}(t_f)]^{jk} + i\,[\mathbf{e}_{\times}(t_f)]^{jk}\right)\,([\mathbf{T}_{+}]_{jk}\,F_{+} + [\mathbf{T}_{\times}]_{jk}\,F_{\times})$$

Initial conditions in precessing convention (single spin)

$$\mathbf{e}_x^S \propto \boldsymbol{S}_1(0) - [\boldsymbol{S}_1(0) \cdot \widehat{\boldsymbol{L}}_\mathrm{N}(0)]\, \widehat{\boldsymbol{L}}_\mathrm{N}(0)\,, \quad \mathbf{e}_y^S = \widehat{\boldsymbol{L}}_\mathrm{N}(0) \times \mathbf{e}_x^S\,, \quad \mathbf{e}_z^S = \widehat{\boldsymbol{L}}_\mathrm{N}(0)$$

$$\mathbf{e}_1(0) = \mathbf{e}_x^S\,, \quad \mathbf{e}_2(0) = \mathbf{e}_y^S\,, \quad \mathbf{e}_3(0) = \mathbf{e}_z^S\,.$$

If $\boldsymbol{S}_1(0)$ and $\widehat{\boldsymbol{L}}_\mathrm{N}(0)$ are parallel, $\mathbf{e}_x^S$ can be chosen to lie in any direction orthogonal to $\widehat{\boldsymbol{L}}_\mathrm{N}(0)$. Φ_0 is defined by

$$\widehat{\boldsymbol{n}}(0) = \mathbf{e}_1(0) \cos\Phi_0 + \mathbf{e}_2(0) \sin\Phi_0\,,$$

$$\widehat{\boldsymbol{L}}_\mathrm{N}(0) = (0, 0, 1) \qquad \hat{\boldsymbol{S}}_1(0) = \left(\sqrt{1-\kappa_1^2}, 0, \kappa_1\right)$$

Comparison between different conventions

Binary				
M, ν, S_1, S_2	θ_{S_1}, θ_{S_2},$\phi_{S_1} - \phi_{S_2}$	$\theta_{\rm L_N} \equiv \iota$, $\phi_{\rm L_N} \equiv \alpha$, $\phi_{S_1} + \phi_{S_2}$	GW propagation Θ, φ	Detector orientation θ,ϕ, ψ
Basic	Local	Directional		

convention	factor P $\mathbf{T}_{+,\times}$ $F_{+,\times}$	factor Q $\Phi(t)$	$\mathbf{e}_{+,\times}(t)$
ACST	function of basic, local, and directional parameters; time dependent	function of basic, local, and directional parameters	function of basic, local, and directional parameters
FC	function of directional parameters; time independent	function of basic, local, and directional parameters	function of basic, local, and directional parameters
precessing	function of directional parameters; time independent	function of basic and local parameters only; coincides with $\Psi(t) = \int \omega \, dt$	function of basic and local parameters only

Templates for spinning, precessing binaries

[Apostolatos 95; AB, Chen & Vallisneri 03; AB, Chen, Pan & Vallisneri 05]

Clean separation of time-dependent and time-independent parameters in waveforms

$$h(t) \propto \underbrace{\frac{1}{r(t)} \left[\boldsymbol{e}_{+}^{ij}(t) \, \cos 2(\Phi(t) + \Phi_0) + \boldsymbol{e}_{\times}^{ij}(t) \, \sin 2(\Phi(t) + \Phi_0) \right]}_{\mathrm{Q(t): wave\ generation}} \times$$

$$\underbrace{[P_{ij}(\Theta, \varphi, \theta, \phi, \psi)]}_{\mathrm{P: detector\ projection}}$$

$$\tilde{h}_{\mathrm{SPA}}(f) = \mathcal{A} \, f^{-7/6} \, e^{i\psi_{\mathrm{SPA}}(f) + i\Phi_0 + 2\pi i f t_0} \times$$

$$\left[1 + \mathcal{C}_{\cos} \, e^{i\phi_{\cos}} \, \cos(\alpha_p(f)) + \mathcal{C}_{\sin} \, e^{i\phi_{\sin}} \, \sin(\alpha_p(f)) \right]$$

$$\psi_{\mathrm{SPA}}(f) \equiv \psi_{\mathrm{SPA}}(f, m_1, m_2, \mathbf{S} \cdot \mathbf{L}, \chi) \qquad \alpha_p(f) \equiv \alpha_p(f, m_1, m_2, \mathbf{S} \cdot \mathbf{L}, \chi)$$

Very fast (analytic) maximization on $\{t_0, \Phi_0, \phi_{\cos}, \phi_{\sin}, \mathcal{C}_{\cos}, \mathcal{C}_{\sin}\}$ **!**

Phenomenological frequency-domain template family

[AB, Chen & Vallisneri 03; AB, Chen, Pan & Vallisneri 05]

$$h(f) = \mathcal{A}(f)\, e^{i\psi(f)}$$

$$\mathcal{A}(f) = f^{-7/6}\, \theta(f_{\rm cut} - f) \times$$

$$[(\mathcal{C}_1 + i\mathcal{C}_2) + (\mathcal{C}_3 + i\mathcal{C}_4)\, \cos\left(\mathcal{B} f^{-p}\right) + (\mathcal{C}_5 + i\mathcal{C}_6)\, \sin\left(\mathcal{B} f^{-p}\right)]$$

$$\psi(f) = f^{-5/3}\, \left(\psi_0 + \psi_{1/2}\, f^{1/3} + \psi_1\, f^{2/3} + \psi_{3/2}\, f + \cdots\right) + 2\pi f\, t_0$$

To get high signal matches, sufficient to set $\psi_0, \psi_{3/2} \neq 0$ and all $\psi_i = 0$

- 3 intrinsic parameters $(\psi_0, \psi_{3/2}, \mathcal{B})$ + $f_{\rm cut}$ and 7 extrinsic parameters $(\mathcal{C}_1, \mathcal{C}_2, \ldots)$
- Fast search on the seven extrinsic parameters ⇒ low computational cost

Phase modulations in target and template: harmonics

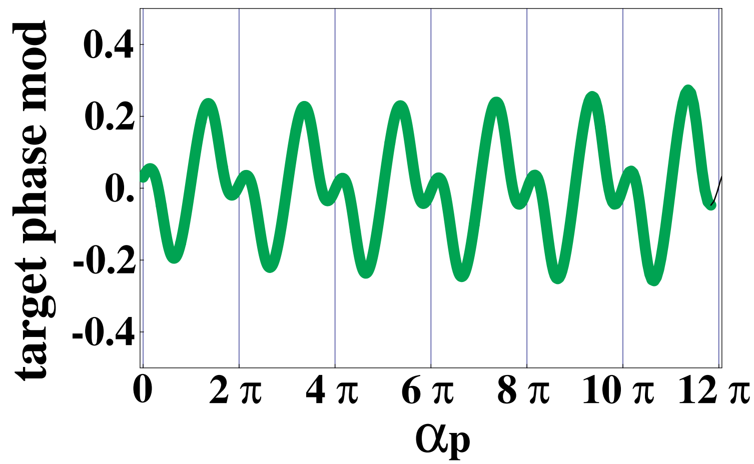

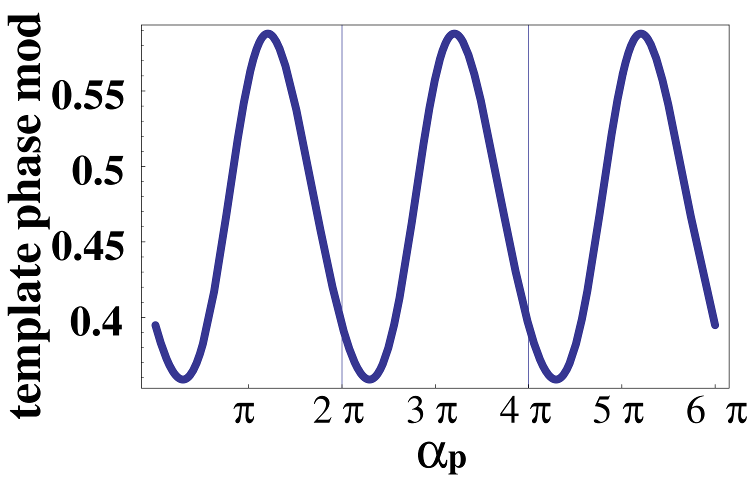

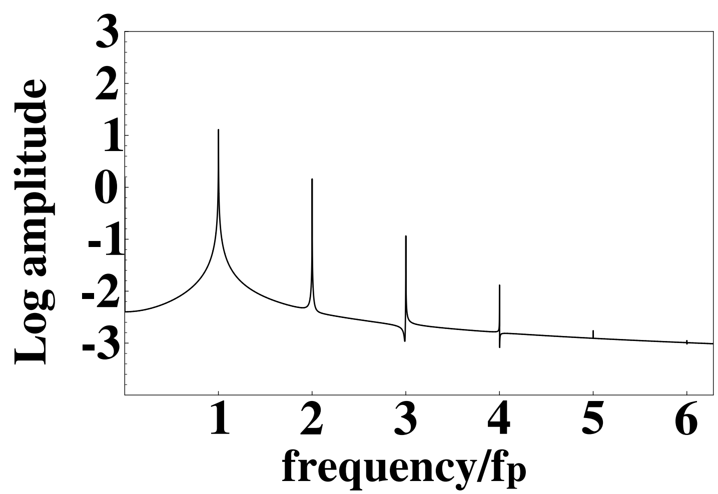

Phase modulations in target and template: harmonics (continued)

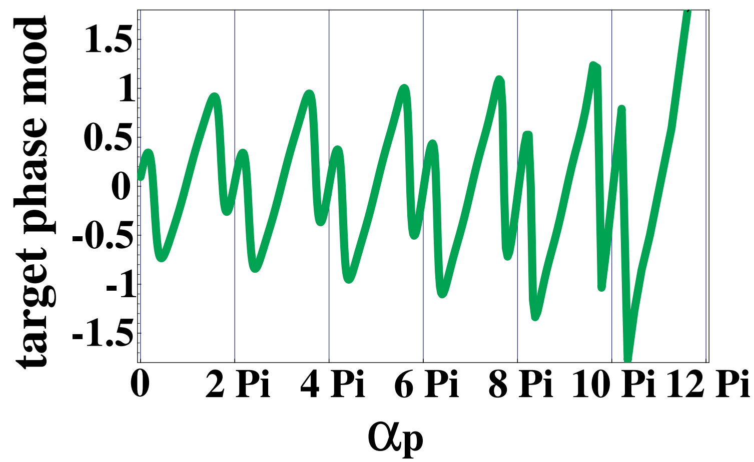

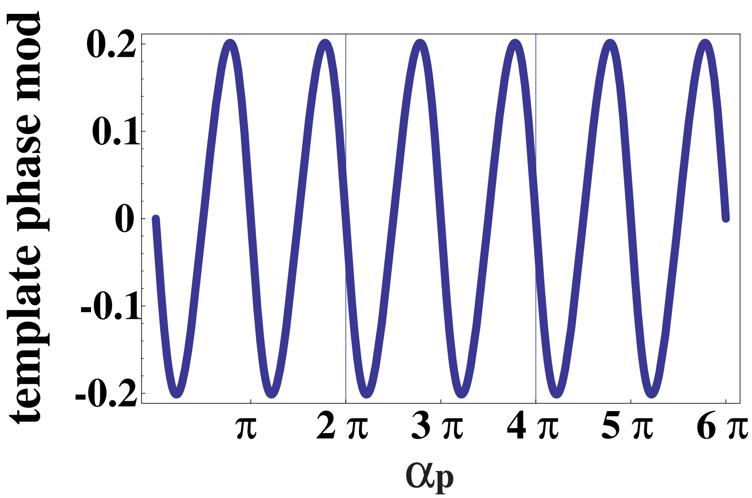

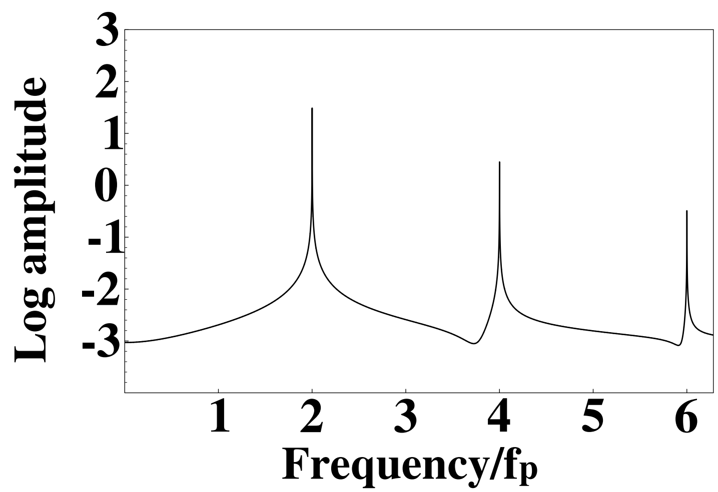

Performances for high mass and small mass-ratio binaries

Averaging over uniform distribution of $S_{1,2}$ and L directions

	High-mass binaries $(7+5)M_\odot$ $\overline{\mathrm{FF}}$	$(10+10)M_\odot$ $\overline{\mathrm{FF}}$	$(15+15)M_\odot$ $\overline{\mathrm{FF}}$	$(20+5)M_\odot$ $\overline{\mathrm{FF}}$	$(20+10)M_\odot$ $\overline{\mathrm{FF}}$
non-mod SPA	0.903	0.894	0.811	0.858	0.826
$(\psi_0\psi_{3/2}\alpha f_{\mathrm{cut}})$	0.929	0.948	0.955	0.899	0.942
$(\psi_0\psi_{3/2}\mathcal{B} f_{\mathrm{cut}})$	0.975	0.986	0.986	0.974	0.984

Increase of overlap can be lower than increase in threshold but templates are closer to signal

	Small mass-ratio and equal–low-mass binaries $(10+1.4)M_\odot$ $\overline{\mathrm{FF}}$	$(12+1)M_\odot$ $\overline{\mathrm{FF}}$	$(12+2)M_\odot$ $\overline{\mathrm{FF}}$	$(6+3)M_\odot$ $\overline{\mathrm{FF}}$	$(6+1)M_\odot$ $\overline{\mathrm{FF}}$	$(2+2)M_\odot$ $\overline{\mathrm{FF}}$
non-mod SPA	0.780	-	-	-	-	-
$(\psi_0\psi_{3/2}\mathcal{B})$	0.933	0.932	0.960	0.975	0.937	0.964

[AB, Chen & Vallisneri 03; AB, Chen, Pan & Vallisneri 05]

Template space

[AB, Chen & Vallisneri 03; AB, Chen, Pan & Vallisneri 05]

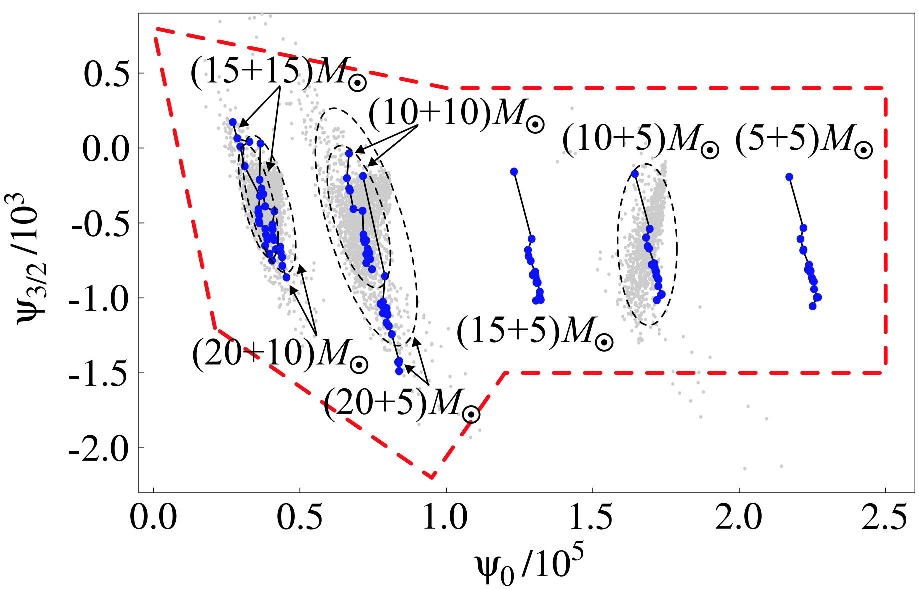

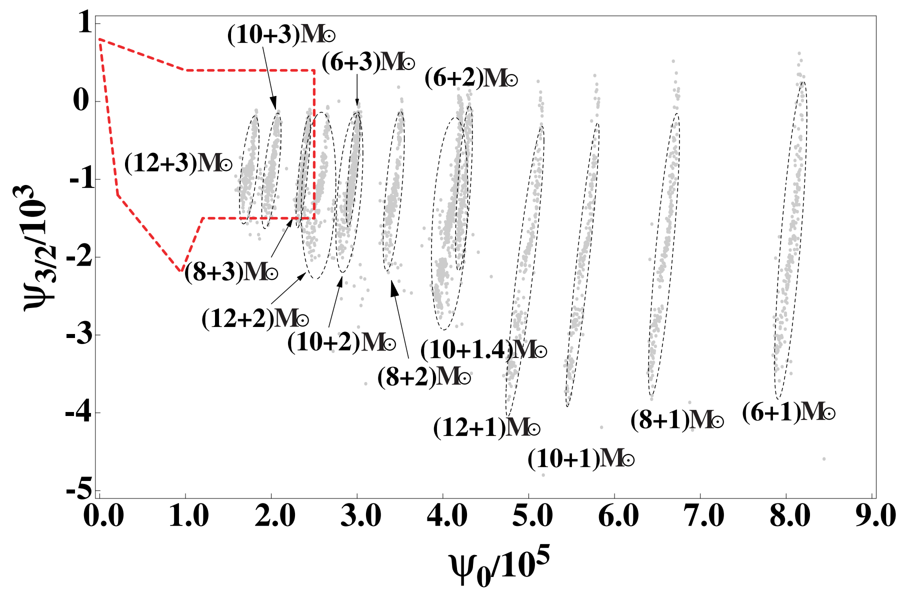

Template space

[AB, Chen & Vallisneri 02; AB, Chen, Pan & Vallisneri 05]

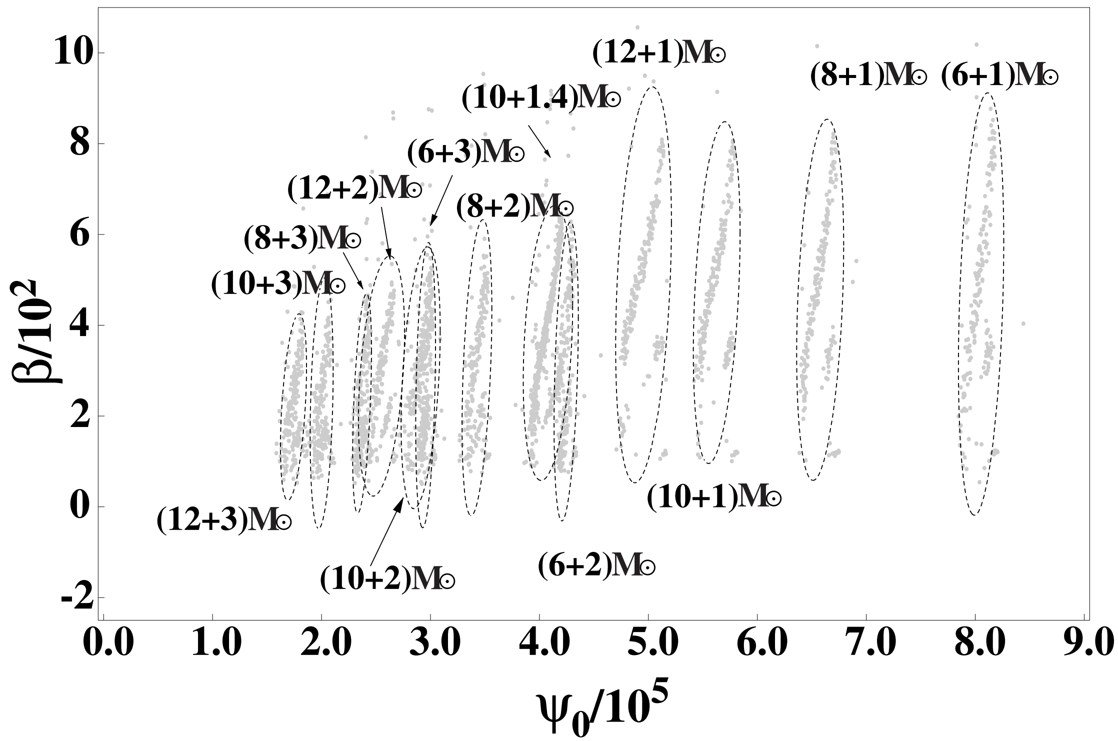

Mismatch template metric and projected metric

[Balasubramanian, Dhurandhar, Sathyaprakash 91, 94, 96; Owen 96]

- $1 - \langle \hat{h}(\lambda^A), \hat{h}(\lambda^A + \Delta\lambda^A)\rangle \equiv \delta[\lambda^A, \lambda^A + \Delta\lambda^A] = g_{BC}\Delta\lambda^B\Delta\lambda^C$

$$g_{BC} = -\frac{1}{2}\frac{\partial^2\left\langle \hat{h}(\lambda^A), \hat{h}(\lambda^A+\Delta\lambda^A)\right\rangle}{\partial(\Delta\lambda^B)\partial(\Delta\lambda^C)}$$

[Pan, AB, Chen & Vallisneri 04; AB, Chen, Pan, Tagoshi & Vallisneri 05]

$X^\alpha \Rightarrow$ **intrinsic parameters** $(\psi_0, \psi_3, \mathcal{B})$, $\Xi^\alpha \Rightarrow$ **extrinsic parameters** $(\mathcal{C}_i, t_0)$

- $\delta(X^i, \Xi^\alpha; X^i + \Delta X^i, \Xi^\alpha + \Delta\Xi^\alpha) = \begin{pmatrix} \Delta X^i & \Delta\Xi^\alpha \end{pmatrix} \begin{pmatrix} G_{ij} & C_{i\beta} \\ C_{\alpha j} & \gamma_{\alpha\beta} \end{pmatrix} \begin{pmatrix} \Delta X^j \\ \Delta\Xi^\beta \end{pmatrix}$

- $\min_{\Delta\Xi^\alpha} \delta(X^i, \Xi^\alpha; X^i + \Delta X^i, \Xi^\alpha + \Delta\Xi^\alpha) = \left[G_{ij} - C_{i\alpha}(\gamma^{-1})^{\alpha\beta}C_{\beta j}\right]\Delta X^i\Delta X^j$

$\equiv g_{ij}^{\text{proj}}\Delta X^i\Delta X^j$ $\qquad g_{ij}^{\text{proj}}$ **depends only on** $\mathcal{B}$ **and** $\mathcal{C}_i$

Projected metric (continued)

[Damour, Iyer and Sathyaprakash 98]

[Pan, AB, Chen & Vallisneri 04; AB, Chen, Pan, Tagoshi & Vallisneri 05]

$$\max_{\Xi^\alpha} \min_{\Delta\Xi^\alpha} \delta(X^i, \Xi^\alpha; X^i + \Delta X^i, \Xi^\alpha + \Delta\Xi^\alpha) \simeq \hat{g}^{\rm proj}_{ij}(\mathcal{B}) \Delta X^i \Delta X^j = 1 - {\rm MM}$$

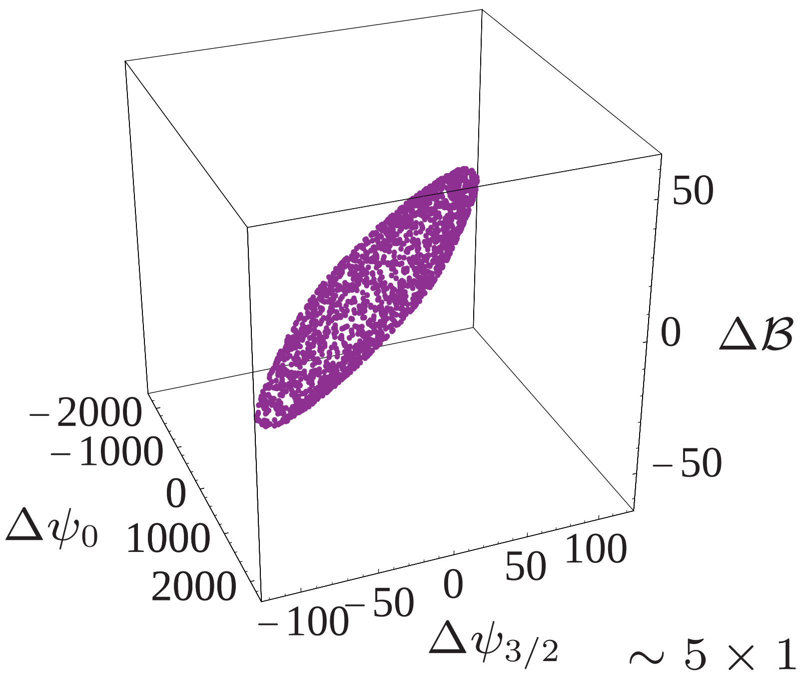

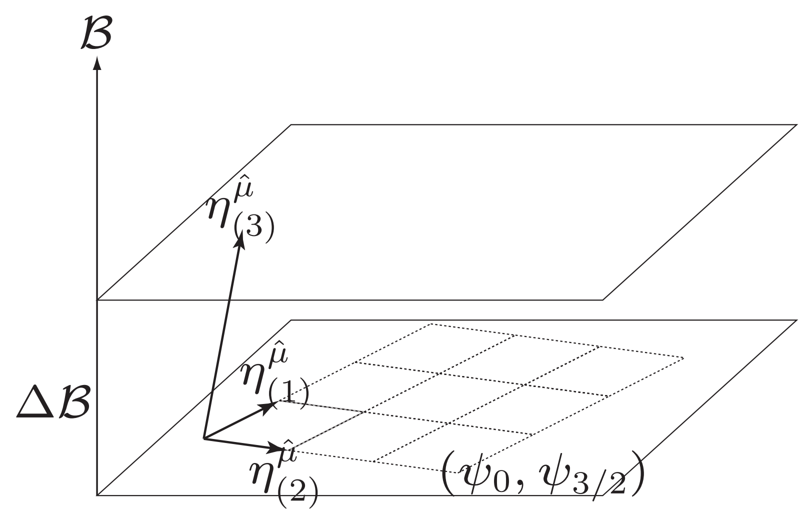

$\sim 5 \times 10^5$ **templates for** $m_1 = 6$–$12 M_\odot$ **and** $m_2 = 1$–$3 M_\odot$

Quasi-physical frequency-domain template family (single spin)

[AB, Chen, Pan & Vallisneri 05]

- The three *phenomenological* parameters $(\psi_0, \psi_{3/2}, \mathcal{B})$ traded with four *physical* parameters (M, ν, κ, χ)
- $\tilde{Q}_c^{ij}(f) \sim \left[\mathcal{C}_0^{ij} + \cos(\delta^{ij} + \alpha^J_{\rm prec}(M,\nu,\kappa,\chi))\,\mathcal{C}_1^{ij}\right] \; f^{-7/6}\, e^{i\psi_{\rm SPA}(M,\nu,\kappa,\chi)}$
- $\alpha^J_{\rm prec}(M,\nu,\kappa,\chi)$ **known analytically !**

  $\alpha^J_{\rm prec} \sim \mathcal{B}\, f^{-p}$

— **The template metric** *is not* **analytical**

— **4D template space**

— **to be used after detection to estimate binary parameters**

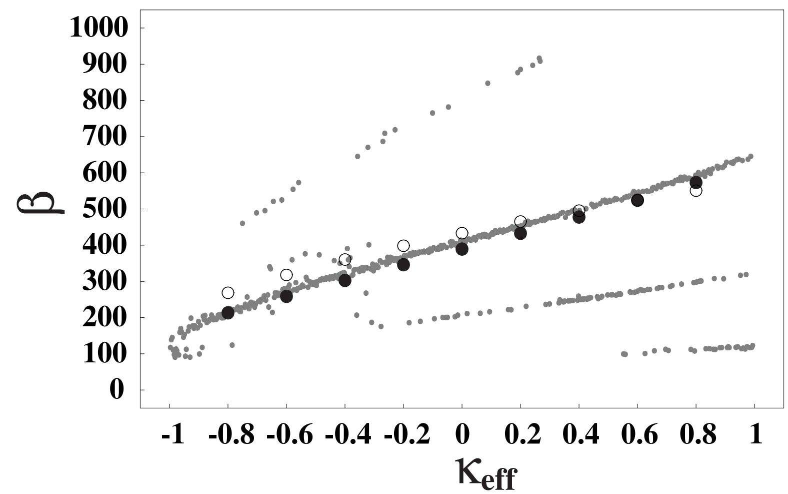

Systematic errors: $\Delta\mathcal{M}/\mathcal{M} \sim 1\%$, $\Delta M/M, \Delta\nu/\nu \sim 10\%$, $\Delta\chi/\chi \sim 20\%$, $\Delta\kappa \sim 2\%$

Quasi-physical frequency-domain template family (single spin) (continued)

$$\Omega_{\rm prec} = \left(2 + \frac{3m_2}{2m_1}\right)\,\sqrt{1 + 2\kappa\gamma + \gamma^2}\,\frac{L}{r^3}\,, \quad \gamma = \frac{S}{L}\,, \quad \kappa = \hat{\boldsymbol{L}}\cdot\hat{\boldsymbol{S}}$$

integrating

$$\begin{aligned}\alpha^{\rm Newt}_{\rm prec}(f) &= \frac{5}{384}\frac{4m_1+3m_2}{m_1} \times \Big\{ -A\,\left[(2-3\kappa^2)\,\chi_M^2 + \kappa\,\chi_M\,v^{-1} + 2\,v^{-2}\right] \\ &+ 3\,\kappa\,(1-\kappa^2)\,\chi_M^3\,\log\left[\pi^{1/3}\eta\left(\kappa\,\chi_M + v^{-1} + A\right)\right]\Big\}\end{aligned}$$

$$v = (\pi M f)^{1/3}\,, \quad \chi_M = \frac{m_1}{m_2}\,\chi\,, \quad A = \sqrt{\chi_M^2 + 2\,\kappa\,\chi_M\,v^{-1} + v^{-2}}$$

Performances for NS/BH binary $(10 + 1.4)M_\odot$

[AB, Chen & Vallisneri 03; AB, Chen, Pan & Vallisneri 05]

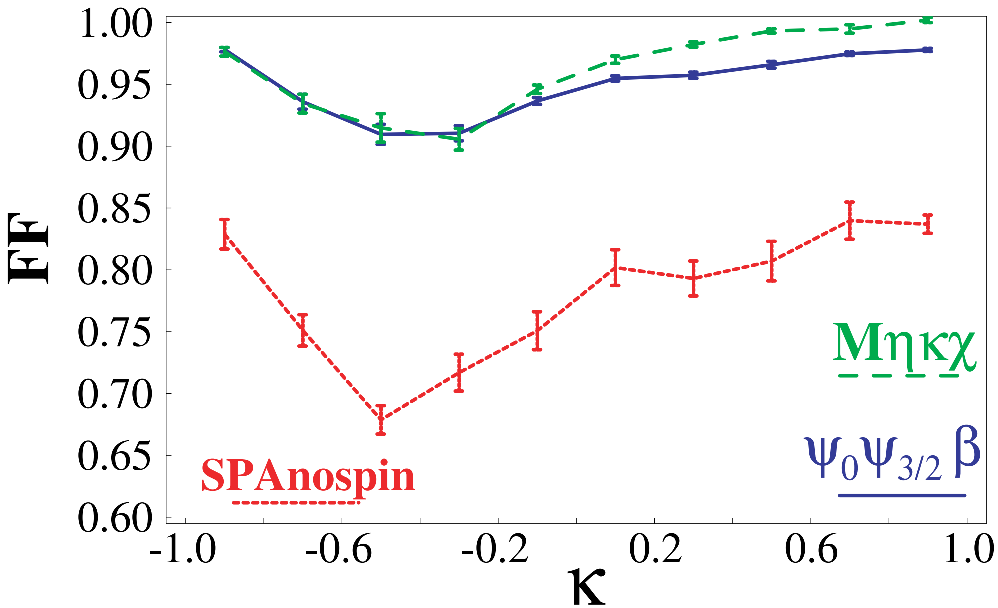

Physical time-domain templates for single-spin precessing binaries

[Pan, AB, Chen & Vallisneri 04]

$$h(t) = -\frac{2\mu}{R}\frac{M}{r}\underbrace{\left[\boldsymbol{e}_{+}^{ij}(t)\,\cos 2(\Phi(t)+\Phi_0)+\boldsymbol{e}_{\times}^{ij}(t)\,\sin 2(\Phi(t)+\Phi_0)\right]}_{\mathrm{Q_{ij}(t):\,wave\,generation}}\times$$

$$\underbrace{\left[T_{+\,ij}(\Theta,\varphi)\,F_{+}(\theta,\phi,\psi)+T_{\times\,ij}(\Theta,\varphi)\,F_{\times}(\theta,\phi,\psi)\right]}_{\mathrm{P_{ij}:\,detector\,projection}}$$

Parameters in $\mathrm{Q}_{ij}(t)$**:** $(m_1, m_2, S_1/m_1^2, \boldsymbol{L}\cdot\boldsymbol{S}_1; t_0, \Phi_0)$ $Q_{ij}, P_{ij} \Rightarrow$ **3D STF tensors**

Parameters in P_{ij}**:** $(\Theta, \varphi, \xi = \arctan(F_+/F_\times))$ $P_I \Rightarrow$ **the 5 components are constrained**

- **Analytic maximization over** Φ_0, ξ **and numerical maximization over** (Θ, φ)
- **Two-stage detection scheme using first the fully algebraic unconstrained statistics**
- **Projected and reduced metric:**
  - **one very small eigenvalue** $\Rightarrow$ **reduction 4D to 3D!**
  - $\sim 2\times 10^5$ **templates for** $m_1 = 7\text{–}12 M_\odot$ **and** $m_2 = 1\text{–}3 M_\odot$

Physical temaples: maximization on extrinsic parameters

[Pan, AB, Chen & Vallisneri 04]

$$\rho_{\Xi^\alpha} \equiv \max_{\Xi^\alpha} (o, \hat{h}(X^i, \Xi^\alpha)) = \max_{t_0,\Phi_0,\Theta,\varphi,\xi} \left[\frac{P_I \left[(o, Q_0^I)_{t_0} \cos 2\Phi_0 + (o, Q_{\pi/2}^I)_{t_0} \sin 2\Phi_0 \right]}{\sqrt{P_I P_J (Q_0^I \cos 2\Phi_0 + Q_{\pi/2}^I \sin 2\Phi_0, Q_0^J \cos 2\Phi_0 + Q_{\pi/2}^J \sin 2\Phi_0)}} \right]$$

Maximizing the detector statistic with respect to Φ_0 and to the five-dimensional vector P_I, *constrained to the three-dimensional physical submanifold* $P_I(\Theta, \varphi, \alpha)$ ($P_I\, P_I = 1, \det P_{ij} = 0$)

Quasi-physical time-domain templates for double-spin precessing binaries

[Apostolatos et al. 94, 96; AB, Chen, Pan & Vallisneri 04]

- **Equal-mass binaries without SS and small mass-ratio binaries described by single spin**
- **What about low total masses and intermediate mass-ratio binaries with SS?**
- **Spin-spin and mass difference modify S and L monotonic evolution by superimposing oscillations**

  $\Rightarrow$ **Single effective-spin description**

$$\dot{\boldsymbol{S}}_{1s} = \frac{\nu_s (M_s \omega)^{5/3}}{2M_s} \left(4 + \frac{3m_{2s}}{m_{1s}}\right) \hat{\boldsymbol{L}} \times \boldsymbol{S}_{1s}$$

$$\dot{\hat{\boldsymbol{L}}} = \frac{\omega^2}{2M_s} \left(4 + \frac{3m_{2s}}{m_{1s}}\right) \boldsymbol{S}_{1s} \times \hat{\boldsymbol{L}}$$

$$\dot{\omega} = \dot{\omega}(\omega, \boldsymbol{S}_{1s} \cdot \boldsymbol{L}, m_{1s}, m_{2s})$$

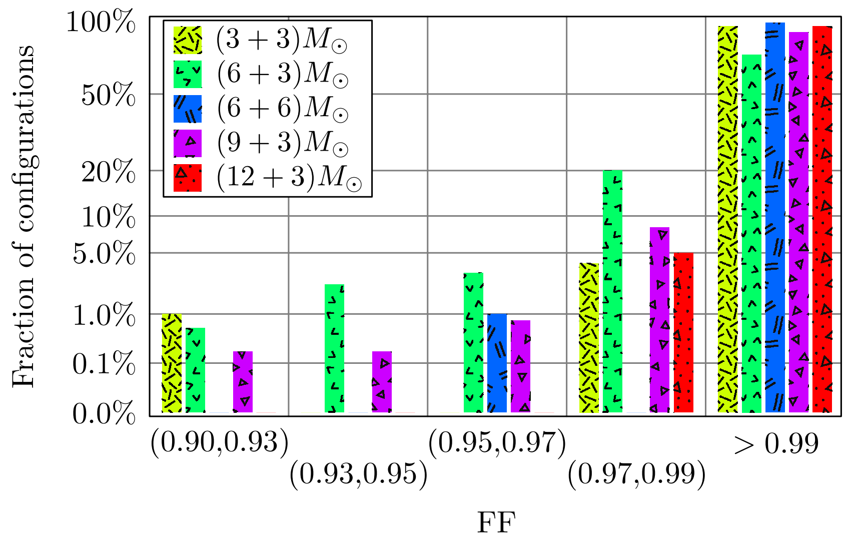

FF for double-spin precessing binaries

templates:	$(3+3)M_\odot$ with spin	$(3+3)M_\odot$ nospin	$(6+3)M_\odot$ with spin	$(6+6)M_\odot$ with spin	$(6+6)M_\odot$ no spin	$(9+3)M_\odot$ with spin	$(12+3)M_\odot$ with spin
FF ≥ 0.99	95%	31%	74%	98%	59%	90%	95%
FF < 0.99	5%	69%	26%	2%	41%	10%	5%
FF < 0.95	0%	38%	3%	0%	25%	1%	0%
lowest FF	0.9085	0.7042	0.9119	0.7250	0.6391	0.8945	0.9734
$\overline{\rm FF}$	≥ 0.989	≥ 0.9376	≥ 0.986	≥ 0.987	≥ 0.9342	≥ 0.989	≥ 0.990

templates:	$(10+10)M_\odot$ with spin	$(10+10)M_\odot$ nospin	$(15+10)M_\odot$ with spin	$(15+10)M_\odot$ no spin	$(15+15)M_\odot$ with spin	$(15+15)M_\odot$ no spin
FF ≥ 0.99	100%	29%	98%	22%	100%	30%
FF < 0.99	0%	71%	2%	78%	0%	70%
FF < 0.95	0%	34%	0%	46%	0%	31%
lowest FF	0.9754	0.7142	0.9691	0.7138	≥ 0.99	0.7546
$\overline{\rm FF}$	≥ 0.990	≥ 0.945	≥ 0.990	≥ 0.936	≥ 0.990	≥ 0.957

Quasi-physical templates for double-spin binaries (continued)

$$(m_1 + m_2) = (6 + 3)M_\odot$$

$$(\theta_S)_{\rm targ} = \arccos(\widehat{\boldsymbol{S}}_{\rm tot} \cdot \widehat{\boldsymbol{J}})$$
$$(\theta_S)_{\rm templ} = \arccos(\widehat{\boldsymbol{S}}_{1s} \cdot \widehat{\boldsymbol{J}})$$
$$\theta_L = \arccos(\widehat{\boldsymbol{L}} \cdot \widehat{\boldsymbol{J}})$$

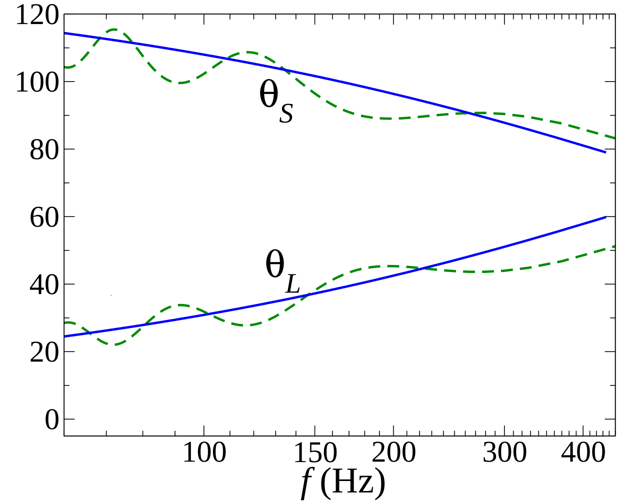

Projected and reduced metric:

$\sim 10^5$ **templates for**

$m_1 = 3$–$15M_\odot$ **and**

$m_2 = 3$–$15M_\odot$

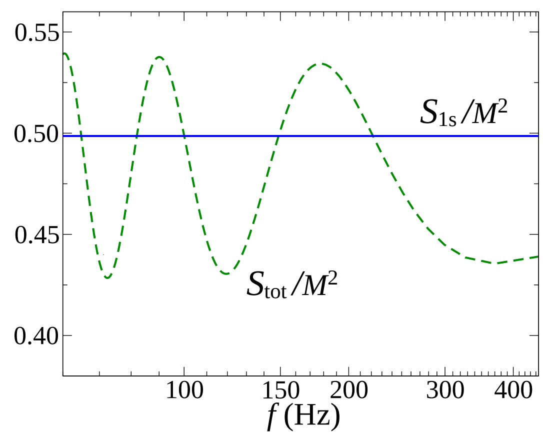

Quasi-physical templates for double-spin binaries (continued)

- **Systematic biased for mass parameters**

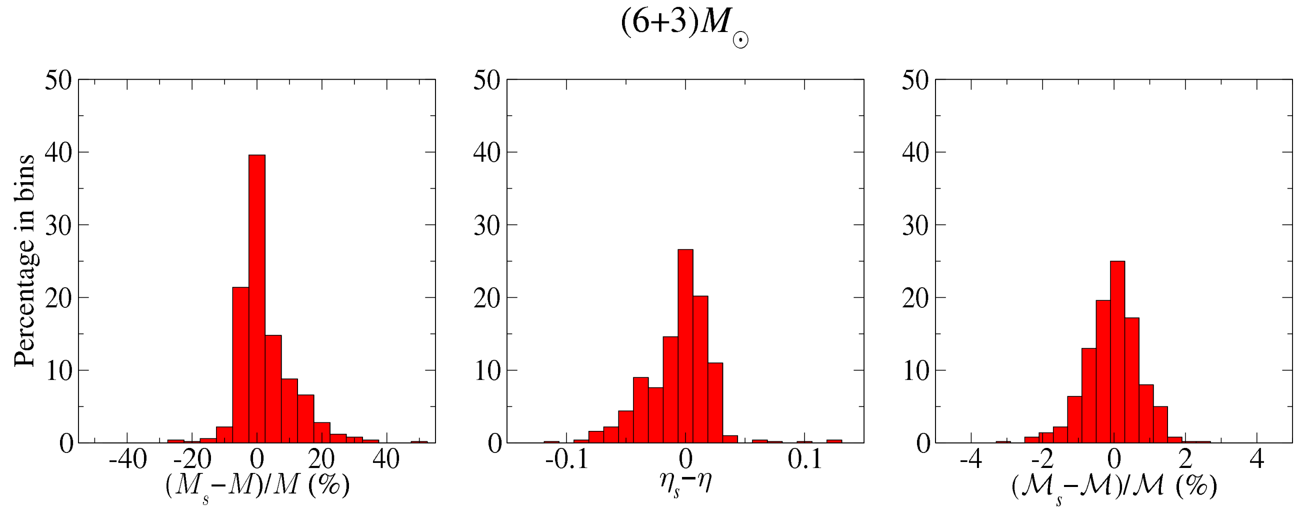

- **Estimation of spin-related parameters**

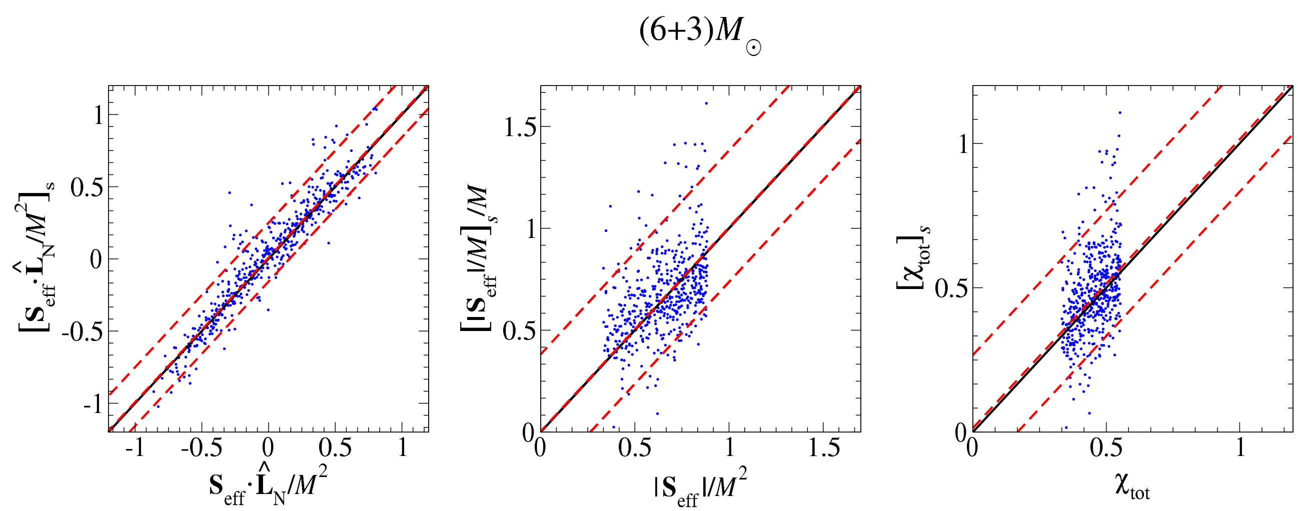

Going beyond the adiabatic approximation

Detecting GWs from comparable-mass BHs: the *last cycles* problem

$M_{\rm BH} = 5$–$20 M_\odot$ **or larger masses if IMBH exists**

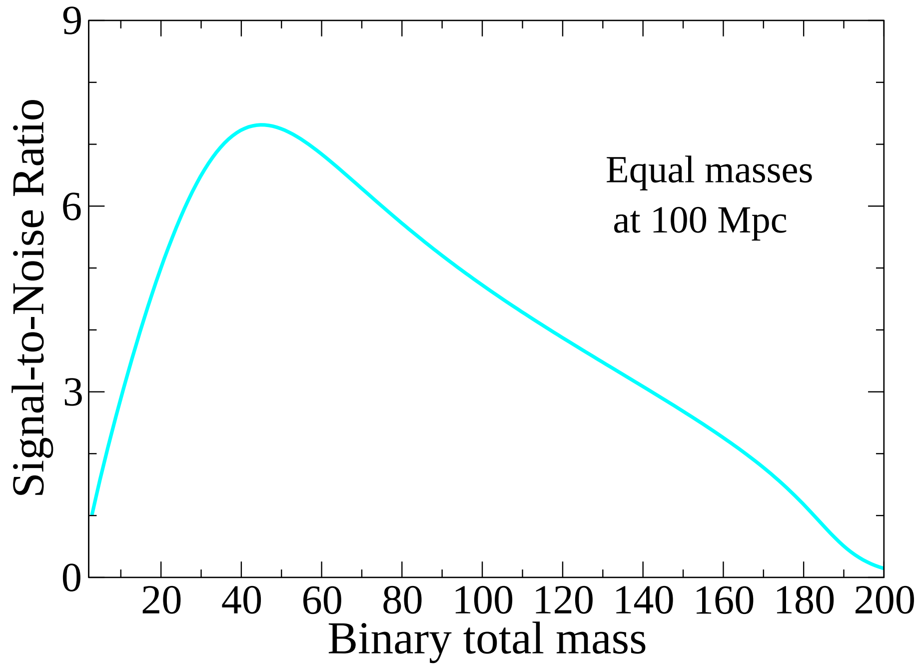

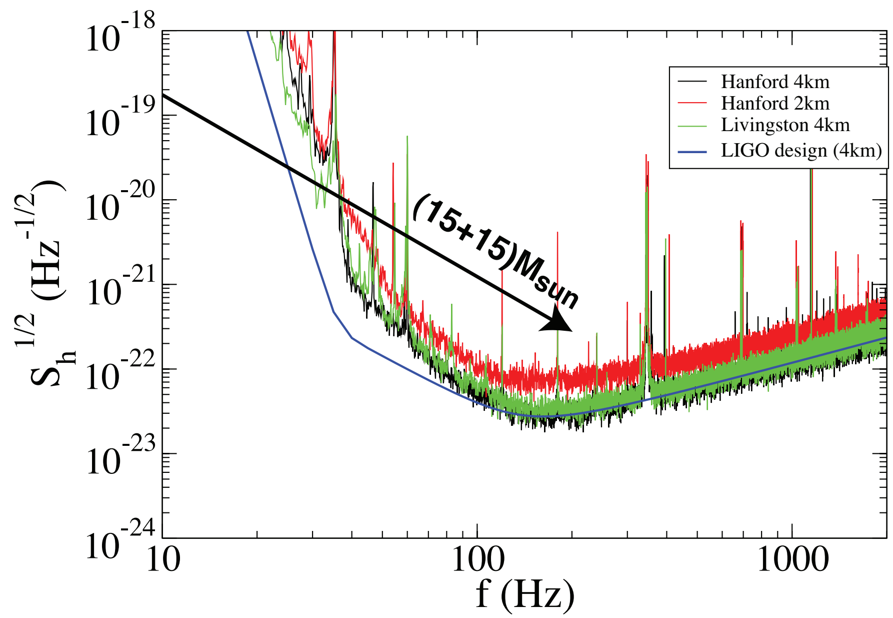

Comparable-mass will merge in band with the highest SNR: which templates do we use?

PN binding energies for equal-mass binaries

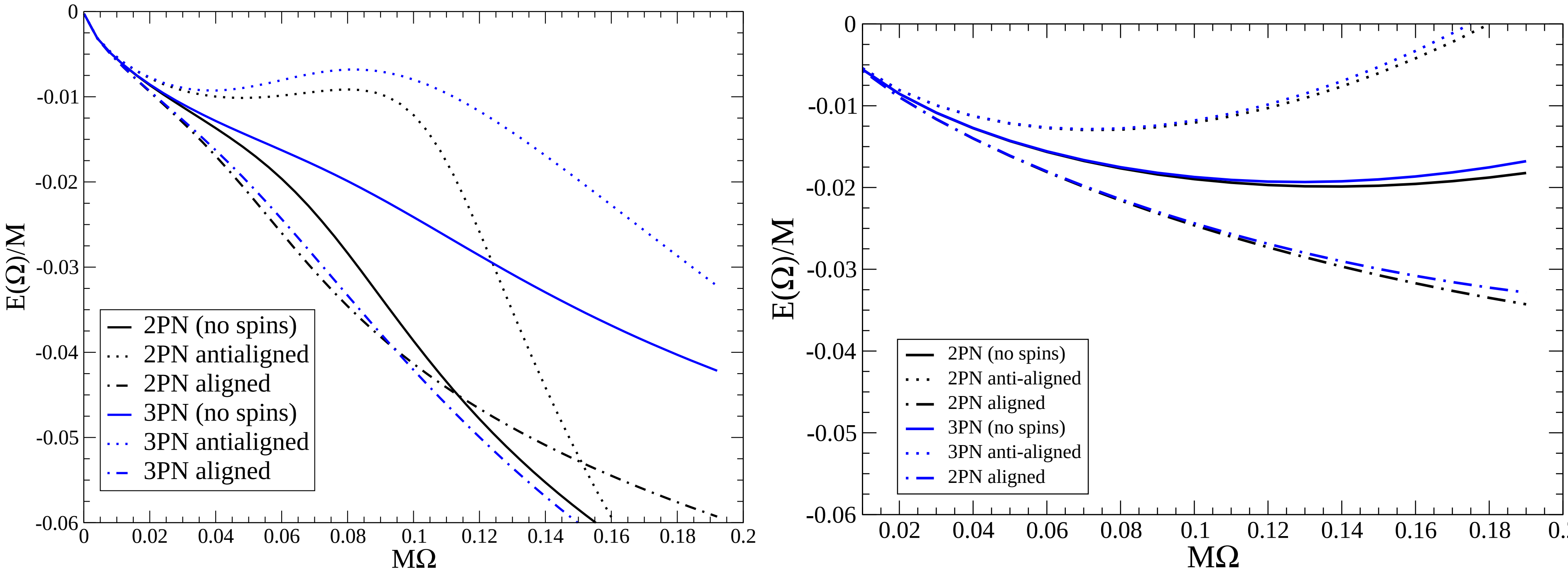

Numerically evaluated: $\Omega = \frac{\partial H(r, p_r{=}0, p_\phi)}{\partial p_\phi}$

$$\frac{\partial H(r, p_r{=}0, p_\phi)}{\partial r} = 0 \quad \Rightarrow \quad p_\phi = p_\phi(r)$$

Analytically evaluated: keeping only terms until nPN order if working at nPN order

Effective-one-body approach

[AB & Damour 99]

$\mu = m_1 \, m_2/M$

$\nu = m_1 \, m_2/M^2$

$0 \leq \nu \leq 1/4$

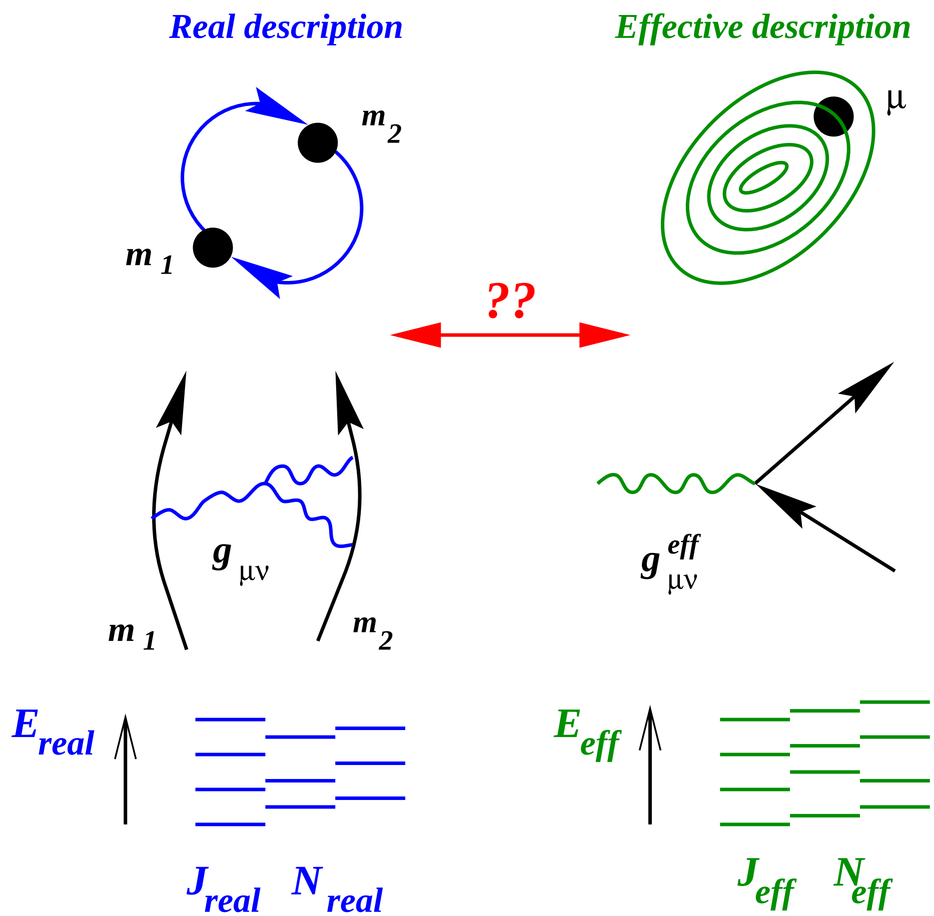

Hamilton-Jacobi formalism: "real" description

The two-body dynamics can be summarized in a coordinate-invariant manner by evaluating the "energy-levels" of the system

$$\mathcal{H}_{\rm real} \sim \mathcal{H}_{\rm New} + \frac{1}{c^2}\mathcal{H}_{\rm 1PN} + \frac{1}{c^4}\mathcal{H}_{\rm 2PN} + \cdots \,, \qquad \mathcal{H}^{\rm NR}_{\rm real} = \mathcal{H}_{\rm real} - M c^2$$

$$S = -E^{\rm NR}_{\rm real}\, t + J_{\rm real}\,\phi + S_R(R, E^{\rm NR}_{\rm real}, J_{\rm real}) \,, \quad \mathcal{H}^{\rm NR}_{\rm real}(\mathbf{P}, \mathbf{Q}) = E^{\rm NR}_{\rm real} \,, \quad \mathbf{P} = \partial S / \partial \mathbf{Q}$$

$$S_R(R, E^{\rm NR}_{\rm real}, J_{\rm real}) = \int dR \sqrt{\mathcal{R}(R, E^{\rm NR}_{\rm real}, J_{\rm real})}$$

radial action variable: $I_R(R, E^{\rm NR}_{\rm real}, J_{\rm real}) = \frac{2}{2\pi} \int_{R_{\rm min}}^{R_{\rm max}} dR \sqrt{\mathcal{R}(R, E^{\rm NR}_{\rm real}, J_{\rm real})}$

$$E_{\rm real}(\mathcal{N}_{\rm real}, J_{\rm real}) = M\, c^2 - \frac{1}{2}\frac{\mu\, \alpha^2}{\mathcal{N}^2_{\rm real}} \left[1 + \mathcal{O}\left(\frac{1}{c^2}\right) \cdots \right]$$

$$\alpha = G\, m_1\, m_2 \qquad \qquad \mathcal{N}_{\rm real} = I_R + J_{\rm real}$$

Hamilton-Jacobi formalism: "effective" description

Effective one-body dynamics in external spacetime

$$\mathcal{S}_{\rm eff} = -\int m_0\, c\, ds_{\rm eff}$$

$$ds^2_{eff} = -A_\nu(r)\, c^2\, dt^2 + \frac{D_\nu(r)}{A_\nu(r)}\, dr^2 + r^2\, d\Omega^2$$

$$A_\nu(r) = \sum_{n=0}^{3} a_n^\nu \left(\frac{GM_0}{c^2 r}\right)^n \qquad D_\nu(r) = \sum_{n=0}^{2} d_n^\nu \left(\frac{GM_0}{c^2 r}\right)^n$$

Hamilton-Jacobi equation: $g^{\mu\nu}_{\rm eff}\, \frac{\partial S}{\partial x^\mu}\, \frac{\partial S}{\partial x^\nu} + m_0^2\, c^2 = 0$

$$S = -E^{\rm NR}_{\rm eff}\, t + J_{\rm eff}\, \phi + S_R(R, E^{\rm NR}_{\rm eff}, J_{\rm eff})$$

$$E_{\rm eff}(\mathcal{N}_{\rm eff}, J_{\rm eff}) = m_0\, c^2 - \frac{1}{2}\frac{m_0\, \alpha^2_{\rm eff}}{\mathcal{N}^2_{\rm eff}} \left[1 + \mathcal{O}\left(\frac{1}{c^2}\right) + \cdots\right]\,,\ \alpha = G\, m_0\, M_0\,,\ \mathcal{N}_{\rm eff} = I_R + J_{\rm eff}$$

Rules to map real to effective problem

Quite natural to impose:

$$m_0 = \mu \qquad M_0 = M$$

$$J_{\rm eff} = J_{\rm real} \quad \& \quad \mathcal{N}_{\rm eff} = \mathcal{N}_{\rm real} \quad \text{with } \mathcal{N} = I + J$$

Allow transformation energy axis: $E_{\rm eff} = f(E_{\rm real})$

$$\frac{E_{\rm eff}^{\rm NR}}{m_0\, c^2} = \frac{E_{\rm real}^{\rm NR}}{\mu\, c^2}\left[1 + \alpha_1 \frac{E_{\rm real}^{\rm NR}}{\mu\, c^2} + \alpha_2 \left(\frac{E_{\rm real}^{\rm NR}}{\mu\, c^2}\right)^2 + \cdots\right]$$

Result from matching the energy

$$\frac{E_{\rm eff}^{\rm NR}}{m_0\, c^2} = \frac{E_{\rm real}^{\rm NR}}{\mu\, c^2}\left(1 + \frac{\nu}{2}\,\frac{E_{\rm real}^{\rm NR}}{\mu\, c^2}\right)$$

Classical gravity (up to 3PN order)

$$E_{\rm real}^2 = m_1^2 + m_2^2 + 2 m_1\, m_2 \left(\frac{E_{\rm eff}}{\mu}\right)$$

Quantum electrodynamics (eikonal approximation) [Brézin, Itzykson & Zinn-Justin 70]

$$E_{\rm real}^2 = m_1^2 + m_2^2 + 2 m_1\, m_2 \,\frac{1}{\sqrt{1 + Z^2\alpha^2/(n-\epsilon_j)^2}}$$

“Canonical transformation”

Relation between the ADM variables $(\mathbf{Q}, \mathbf{P})$ of relative motion to the coordinate and momenta of effective description $(\mathbf{Q}, \mathbf{P})$

$$\mathbf{q} = \mathbf{Q} + \frac{\partial G(\mathbf{Q},\mathbf{p})}{\partial \mathbf{p}} \qquad \mathbf{P} = \mathbf{p} - \frac{\partial G(\mathbf{Q},\mathbf{p})}{\partial \mathbf{Q}} \qquad G \rightarrow \text{generating function}$$

$$1 + \frac{\mathcal{H}^{\rm NR}_{\rm real}(\mathbf{Q},\mathbf{P})}{c^2}\left(1 + \frac{\nu}{2}\frac{\mathcal{H}^{\rm NR}_{\rm real}(\mathbf{Q},\mathbf{P})}{c^2}\right) = \frac{\mathcal{H}^{\rm NR}_{\rm eff}(\mathbf{q}(\mathbf{Q},\mathbf{P}),\mathbf{p}(\mathbf{Q},\mathbf{P}))}{c^2}$$

$$\Rightarrow G = G_{\rm New} + \frac{1}{c^2}\,G_{\rm 1PN} + \frac{1}{c^4}\,G_{\rm 2PN} + \cdots \Rightarrow \mathbf{q} = \mathcal{Q}(\mathbf{Q},\mathbf{P}) \qquad \mathbf{p} = \mathcal{P}(\mathbf{Q},\mathbf{P})$$

Energy-dependent “canonical” rescaling of the time coordinate:

$$dt_{\rm eff}\,\mathcal{H}_{\rm eff} = dt_{\rm real}\,\mathcal{H}_{\rm real}$$

EOB approach: resummed Hamiltonian (non-spinning black holes)

[AB & Damour 99; Damour, Jaranowski & Schaefer 00]

"Effective" description

"Real" description

$$\mathcal{H}_{\rm real}(\mathbf{Q},\mathbf{P}) \sim M\left\{1+\nu\left[\frac{\mathbf{P}^2}{2}+\frac{M}{Q}\right]+c_4\,\mathbf{P}^4+\cdots\right\}$$

$$\mathcal{H}^{\nu}_{\rm eff}(\mathbf{q},\mathbf{p}) = \sqrt{A_\nu(q)\,\left[1+\mathbf{p}^2+\left(\frac{A_\nu(q)}{D_\nu(q)}-1\right)\,(\mathbf{n}\cdot\mathbf{p})^2+\mathcal{T}_4(\mathbf{p})\right]}$$

$$\boxed{\mathcal{H}^{\rm improved}_{\rm real}(\mathbf{Q},\mathbf{P}) = \sqrt{1+2\nu\,\left(\mathcal{H}^{\nu}_{\rm eff}(\mathbf{q},\mathbf{p})-1\right)}}$$

$$ds^2_{\rm eff} = -A_\nu(q)\,dt^2+\frac{D_\nu(q)}{A_\nu(r)}\,dq^2+q^2\,d\Omega^2$$

- **Canonical transf. (resummed dynamics):** $\mathbf{q}=\mathcal{Q}(\mathbf{Q},\mathbf{P})$, $\mathbf{p}=\mathcal{P}(\mathbf{Q},\mathbf{P})$
- **All dynamics condensed in** $A_\nu(q)$ **and** $D_\nu(q)$**!**

New resummed *orbital energy* **function:** $E^{\rm impr}_{\rm real}(v)$

Effective one-body approach at 3PN

[Damour, Jaranowski & Schafer 00]

At 3PN order: one more equation to satisfy than number of unknowns

Higher order derivatives in the effective description

$$0 = m_0^2 + g_{\rm eff}^{\alpha\beta}\, p_\alpha\, p_\beta + A^{\alpha\beta\gamma\delta}\, p_\alpha\, p_\beta\, p_\gamma\, p_\delta + \cdots$$

Same matching between real and effective energy

$$\mathcal{H}^{\nu}_{\rm eff,3PN}(\mathbf{q},\mathbf{p}) = \sqrt{A_\nu(q)\,\left[\cdots + z_1\,\frac{\mathbf{p}^4}{q^2} + z_2\,\frac{\mathbf{p}^2\,(\mathbf{n}\cdot\mathbf{p})^2}{q^2} + z_3\,\frac{(\mathbf{n}\cdot\mathbf{p})^4}{q^2}\right]}$$

Result for effective metric at 2PN order and beyond it

$$ds^2_{\rm eff} = -A_\nu(q)\, c^2\, dt^2 + \frac{D_\nu(q)}{A_\nu(q)}\, dq^2 + q^2\, d\Omega^2$$

$$A_\nu(q) = 1 - 2\,\frac{GM}{c^2 q} + 2\nu\,\left(\frac{GM}{c^2 q}\right)^3 \qquad D_\nu(q) = 1 - 6\nu\,\left(\frac{GM}{c^2 q}\right)^2$$

Effective potential: $W_j(q) = A_\nu(q)\,[1 + \frac{j^2}{q^2}]$

Location of the ISCO: $\frac{\partial W_j}{\partial q} = 0 = \frac{\partial^2 W_j}{\partial q^2}$

At higher PN orders: $A_\nu(q) = 1 - 2\,\frac{GM}{c^2 q} + 2\nu\,\left(\frac{GM}{c^2 q}\right)^3 + 18.7\nu\,\left(\frac{GM}{c^2 q}\right)^4 + \mathcal{O}\left(\frac{GM}{c^2 q}\right)^5$

Possible resummation of $A_\nu(q)$ to improve its behaviour

e.g., Padé approximants [Damour, Jaranowski & Schaefer 00]

EOB approach with spins

- **Map of the conservative dynamics of two spinning black holes of mass m_1 and m_2 onto the dynamics of a non-spinning particle of mass $\mu = m_1\, m_2/M$ moving in an effective metric** [Damour 01]

- **This metric can be viewed as a $\nu = \mu/M$ deformation of a Kerr metric of mass $M = m_1 + m_2$ and spin $S_{\rm eff}$**

As a simpler alternative, spin effects added to the non-spinning EOB Hamiltonian [AB, Chen & Damour 05]

$$\mathcal{H}^{\rm impr}_{\rm real}(\mathbf{q},\mathbf{p},\boldsymbol{S}_1,\boldsymbol{S}_2) = \mathcal{H}^{\rm impr}_{\rm real}(\mathbf{q},\mathbf{p}) + H_{\rm SO}(\mathbf{q},\mathbf{p},\boldsymbol{S}_1,\boldsymbol{S}_2) + \mathcal{H}_{\rm SS}(\mathbf{q},\mathbf{p},\boldsymbol{S}_1,\boldsymbol{S}_2)$$

$$\mathcal{H}_{SO} = \frac{2\boldsymbol{S}_{\rm eff}\cdot\boldsymbol{L}}{q^3}\,, \quad \boldsymbol{S}_{\rm eff} \equiv \left(1+\frac{3}{4}\frac{m_2}{m_1}\right)\boldsymbol{S}_1 + \left(1+\frac{3}{4}\frac{m_1}{m_2}\right)\boldsymbol{S}_2$$

Comparing EOB-resummed and PN-expanded binding energies for equal-mass binaries

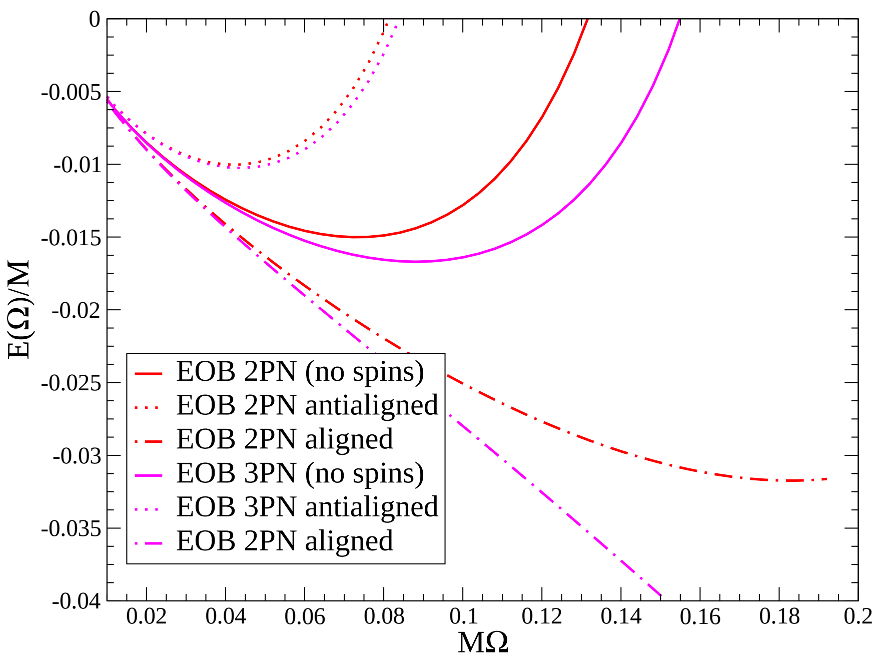

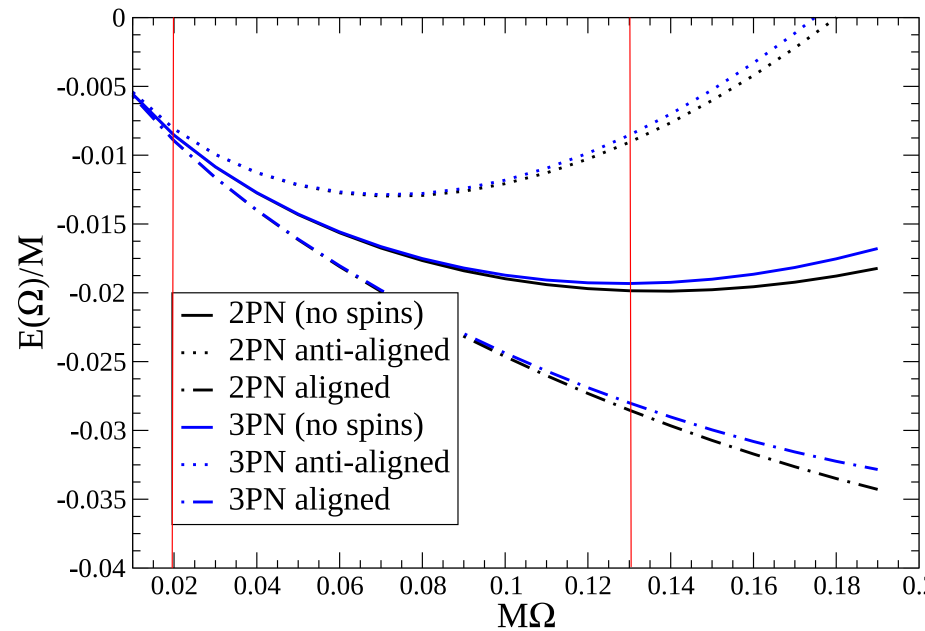

Numerically evaluated: $\Omega = \frac{\partial \mathcal{H}^{\rm impr}(q, p_q{=}0, p_\phi)}{\partial p_\phi}$

$$\frac{\partial \mathcal{H}^{\rm impr}(q, p_q{=}0, p_\phi)}{\partial q} = 0 \quad \Rightarrow \quad p_\phi = p_\phi(q)$$

Analytically evaluated: keeping only terms until nPN order if working at nPN order

Comparing LSSO predictions for energy and frequency

Equal-mass and equal-spin binaries

[AB, Chen & Damour 05]

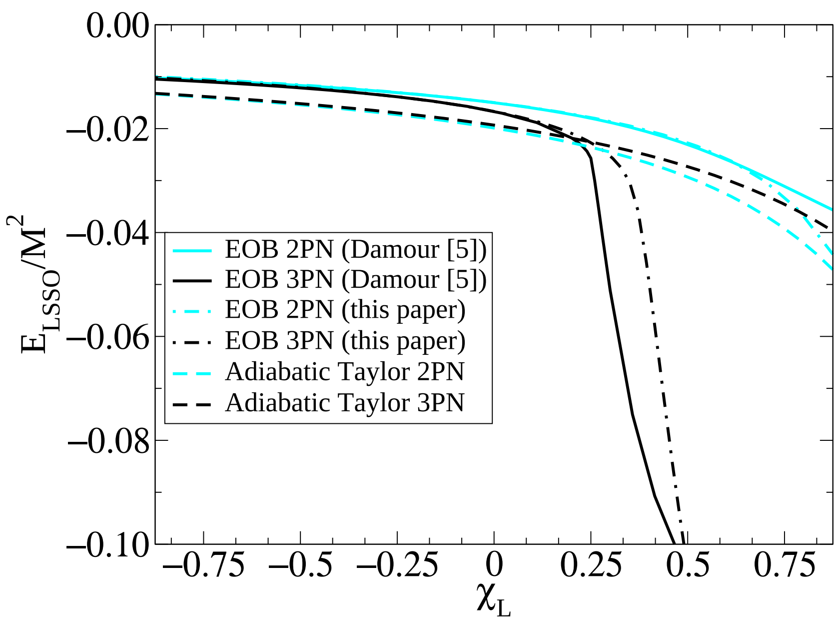

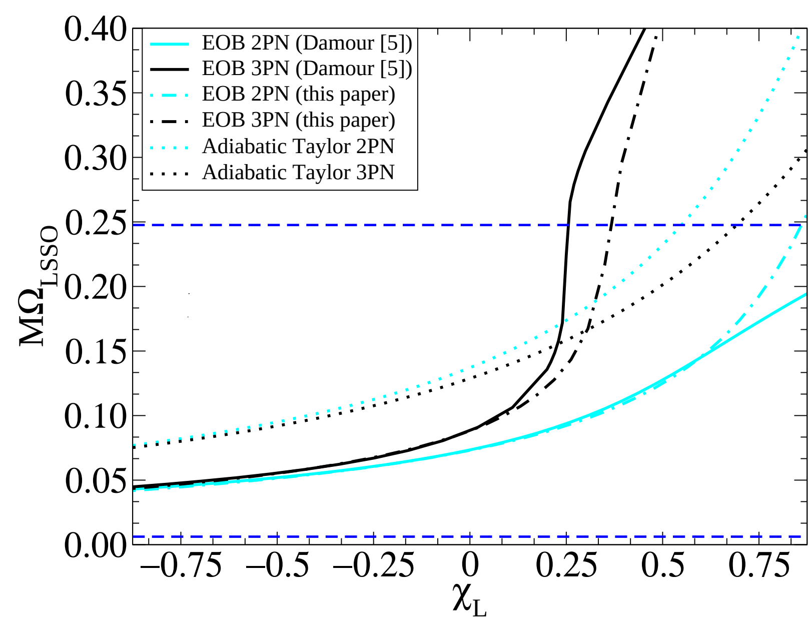

For spins aligned with angular momentum ⇒ non-linear effects dominate ⇒ predictions differ, but for LIGO this would affect *only* **binaries with mass** $\gtrsim 40 M_\odot$

EOB approach: incorporating radiation reaction effects

[AB & Damour 00; AB, Chen & Damour 05]

$$\frac{dq^i}{dt} = \frac{\partial \mathcal{H}^{\rm impr}}{\partial p_i} \qquad \frac{dp_i}{dt} = -\frac{\partial \mathcal{H}^{\rm impr}}{\partial q^i} + \mathcal{F}_i$$

- **Assumptions: quasi-circular orbits and leading spin-dependent terms**

- **Radiation-reaction force matches known rates of energy and angular momentum loss for quasi-adiabatic orbits**

$$\mathcal{F}_i = \frac{1}{\Omega\,|\boldsymbol{L}|}\frac{dE}{dt}\,p_i + \frac{8}{15}\,\nu^2\,\frac{v^8}{\boldsymbol{L}^2{}_q}\left\{\left(61 + 48\,\frac{m_2}{m_1}\right)\mathbf{p}\cdot\boldsymbol{S}_1 + \left(61 + 48\,\frac{m_1}{m_2}\right)\mathbf{p}\cdot\boldsymbol{S}_2\right\}\,L_i$$

- **Padé resummation of the GW flux including spin effects**

[Damour, Sathyaprakash & Iyer 98; Porter & Sathyaprakash 04; AB, Chen & Damour 05]

Padé approximants

Function $e(v)$ known only through its Taylor approximant:

$$E_N(v) = e_0 + e_1\, v + \cdots + e_N\, v^N \equiv T_N[e(v)]$$

Padé summation: replace the power series $E_N(v)$ by the sequence of rational functions:

$$P^M_K[e(v)] = \frac{A_M(v)}{B_K(v)} \equiv \frac{\sum_{j=0}^{M} a_j\, v^j}{\sum_{j=0}^{K} b_j\, v^j}$$

with $M + K = N$ and $T_{M+K}[P^M_K e(v)] = E_N(v)$ $(b_0 = 1)$

$M, K \to +\infty$, $P^M_K[e(v)]$ should converge to $e(v)$ more rapidly than

$T_N[e(v)]$ converges to $e(v)$ for $N \to +\infty$.

Taylor and Padé approximants to the GW energy flux

[Damour, Iyer & Sathyaprakash 98]

test mass limit

PN-expanded flux

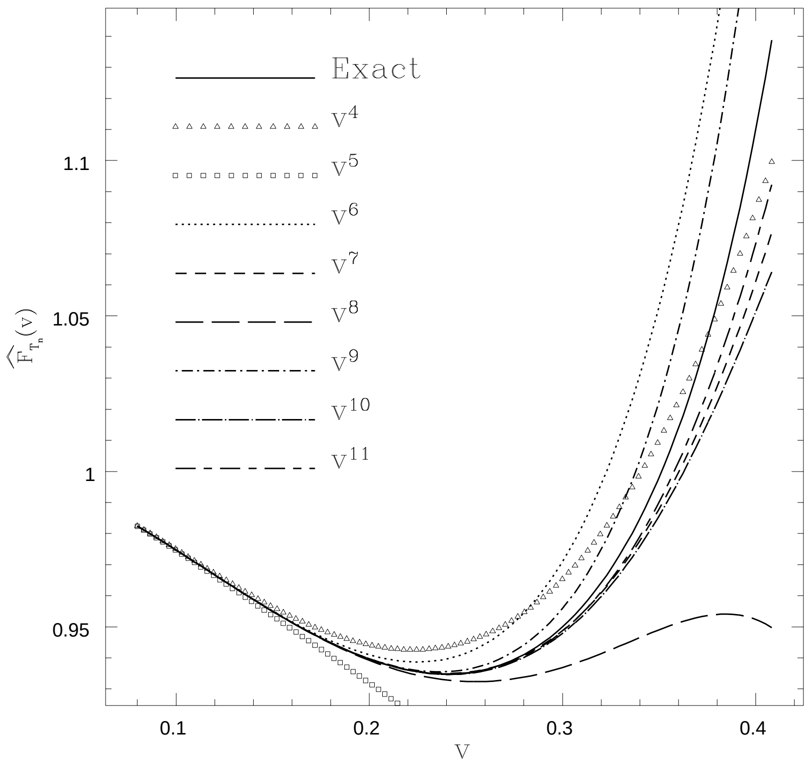

Padé-resummed flux

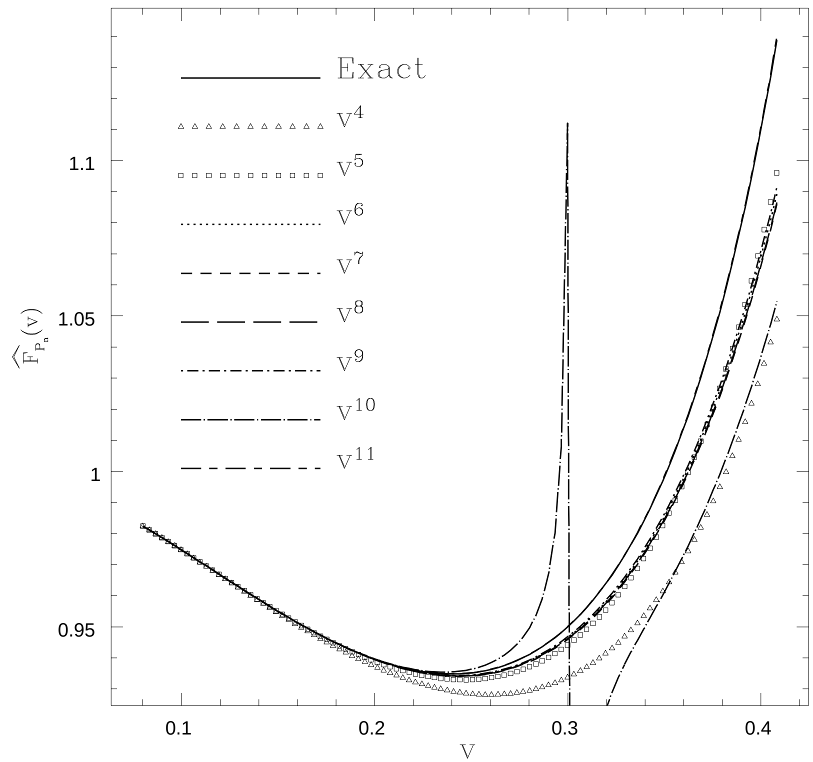

Padé versus Taylor approximants to the GW energy flux

$v = (M\omega)^{1/3}$

equal-mass limit

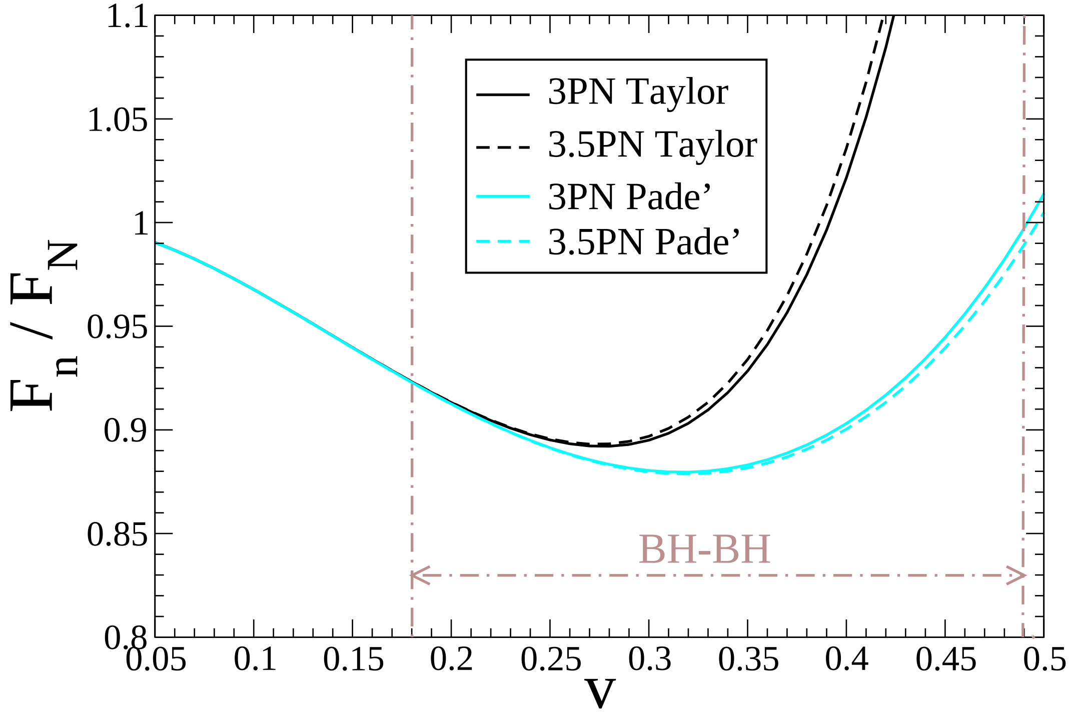

Evaluation of waveform and energy released

Quadrupole approximation: [AB & Damour 00; AB, Chen & Damour 05]

$$h_{ij} = \frac{H_{ij}}{D} \equiv \frac{2\mu}{D}\frac{d^2}{dt^2}(q_i\, q_j), \quad \ddot{q}_k = -M\, q_k/q^3 \Rightarrow H_{ij} = 4\mu\left(V_i\, V_j - M\frac{q_i\, q_j}{q^3}\right)$$

- $\delta\mathcal{H}$

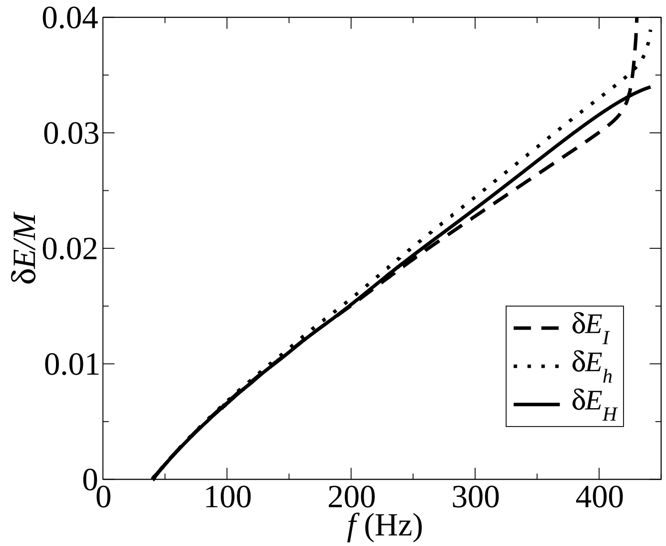

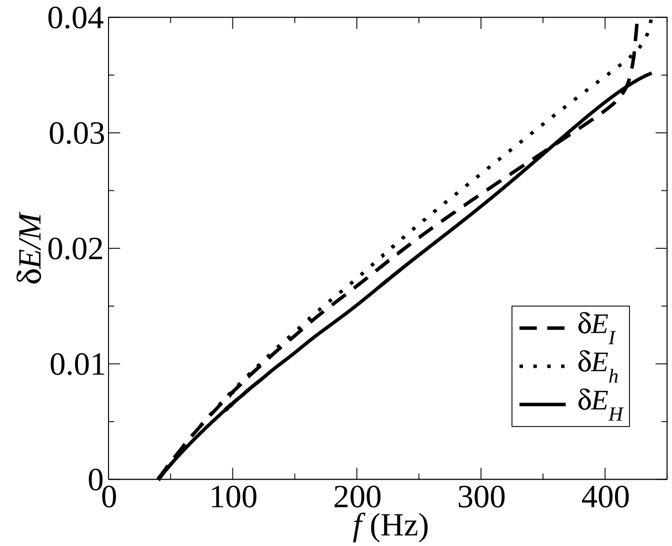

- The time integral of E_h with $\frac{dE_h}{dt} = \frac{1}{20}\int \sum_{ij} \dot{H}_{ij}^{\mathrm{TF}}\, \dot{H}_{ij}^{\mathrm{TF}}$
- The time integral of E_I with $\frac{dE_I}{dt} = \frac{1}{5}\frac{d^3 I_{ij}}{dt^3}\frac{d^3 I_{ij}}{dt^3}$ $I_{ij} = \mu\,\left(q_i\, q_j - \frac{1}{3}\delta_{ij}\, q^k\, q_k\right)$

Energy and angular-momentum released during inspiral and plunge

- **Maximal spins and $(15+15)M_\odot$** [AB, Chen & Damour 05]
- **Energy release before $40\,\mathrm{Hz}$ is $\sim 0.008/M$**

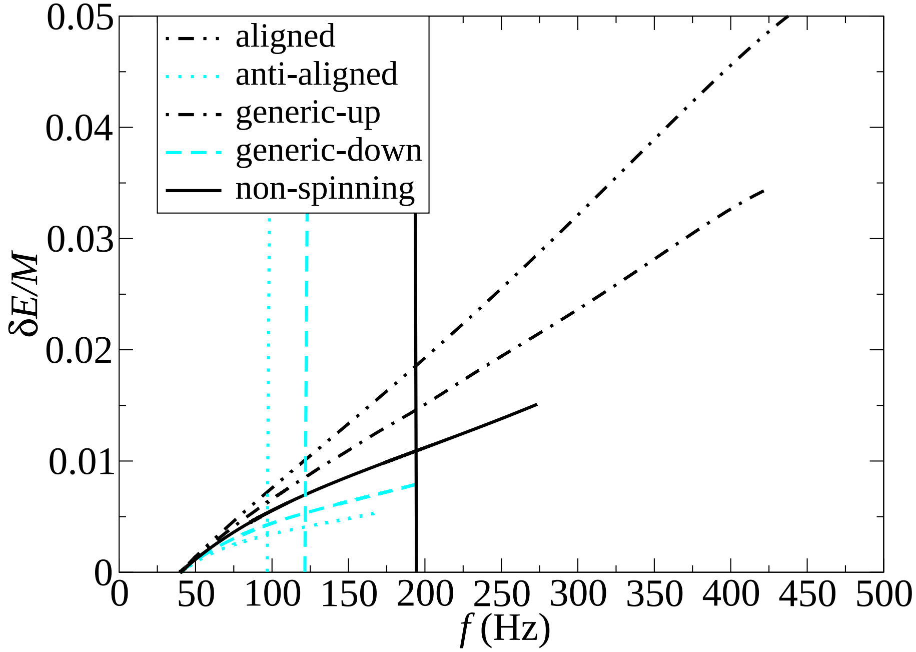

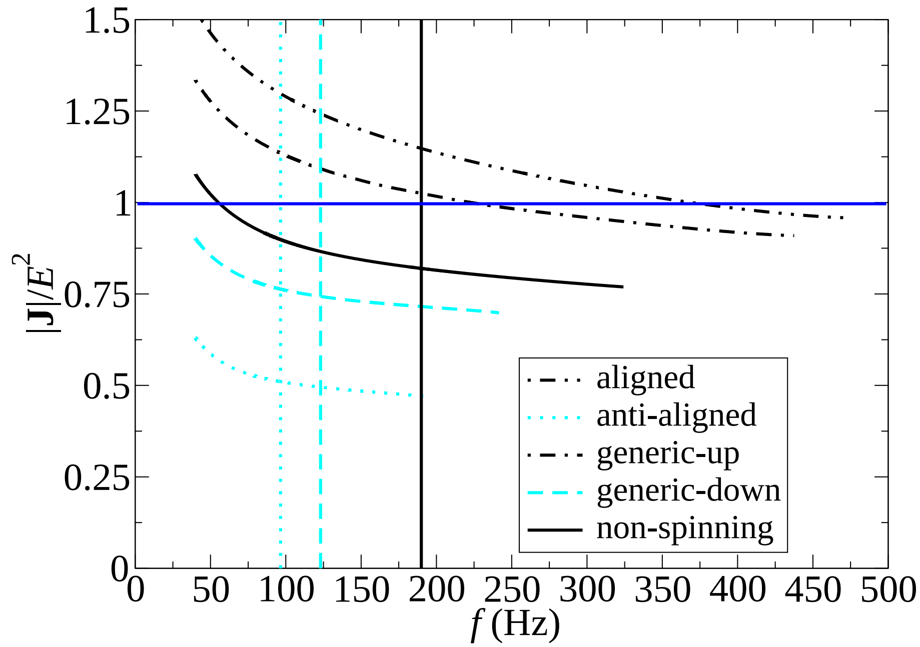

Rotation parameter J/E^2 smaller than one at the end of inspiral

$\Rightarrow$ **Kerr black hole could already form**

EOB merger–ring-down

- **The transition merger–ring-down was assumed** *very short*
- One single **QNM matched using** $M_{\rm BH} = E_{\rm lr} = 0.9761\,M$, $a_{\rm BH} = \boldsymbol{J}_{\rm lr}/E_{\rm lr}^2 = 0.7952$

[Davis et al. 71, 72; Press 71; Price & Pullin 94]

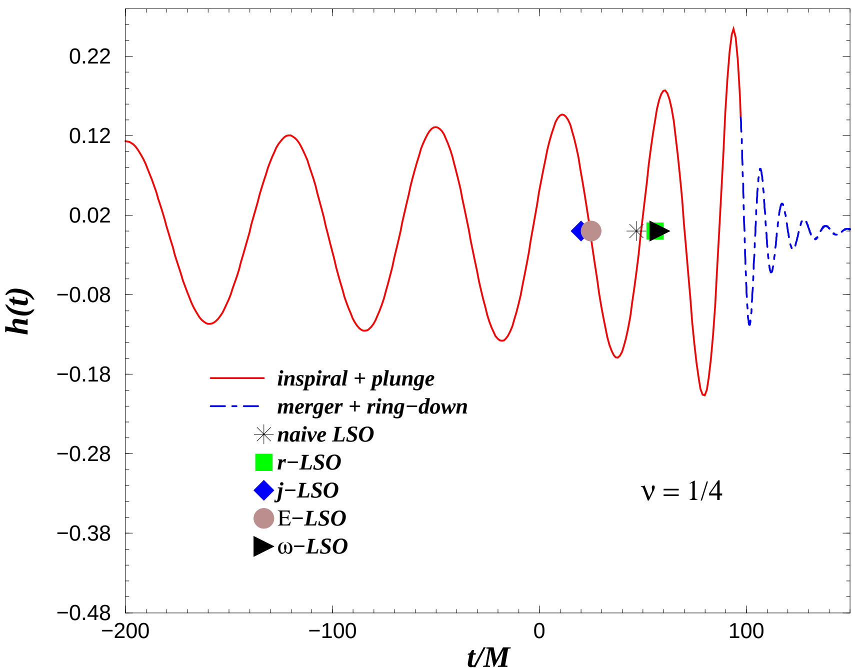

[AB & Damour 99, 01]

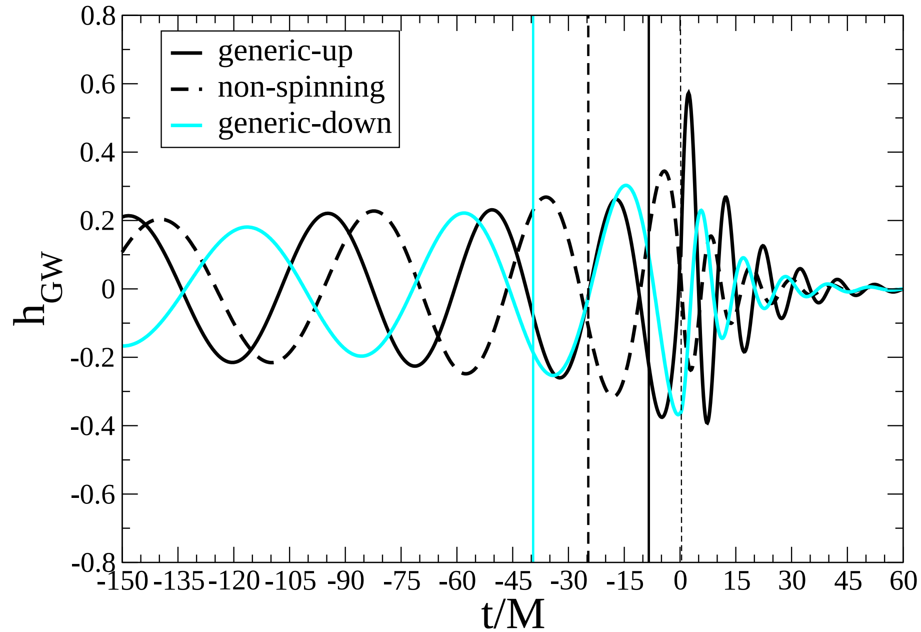

[AB, Chen & Damour 05]

What we learned from the EOB model

- **The plunge (~ 1.5 cycles) is a smooth continuation of the adiabatic inspiral phase**
- **The motion is quasi-circular throughout the evolution**

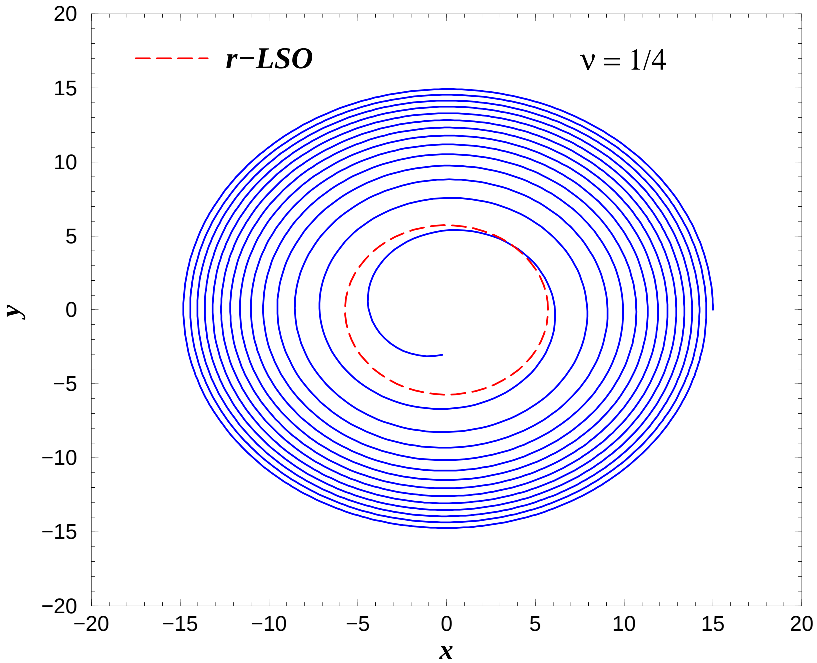

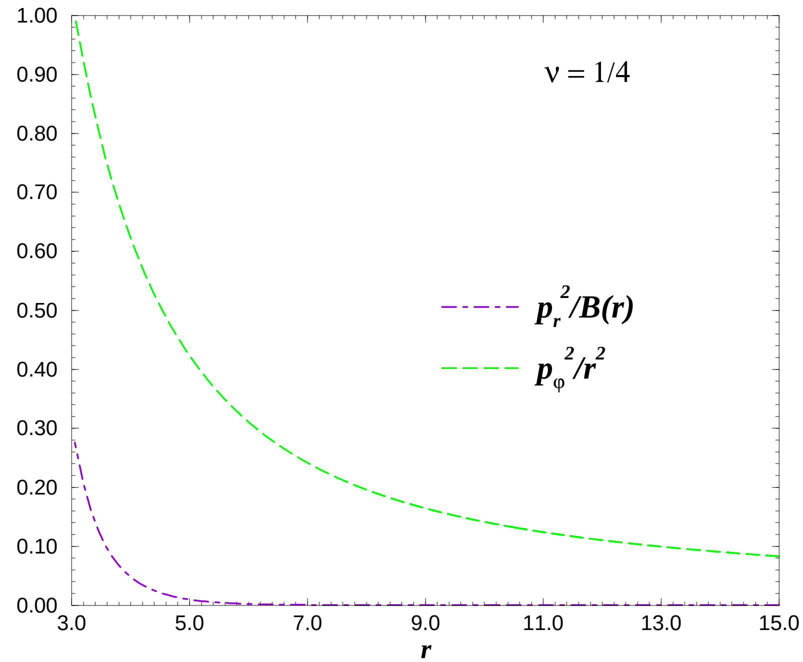

[AB & Damour 99, 01]

Another way of coping with signals emitted by high, comparable mass binaries

Observation:

Worse maximized overlap between different PN models ~ 0.92–0.93, but at the cost of systematic errors in binary parameters

GW detection:

To avoid $\gtrsim 20\%$ of loss in event rates $\Rightarrow$ template families that "cover" the majority of the PN models and even more

[AB, Chen & Vallisneri 03; Damour, Iyer, Jaranowski & Sathyaprakash 03]

- **extend the PN templates in unphysical regions of parameters**
- **allow different values of the GW ending frequencies**
- **including PN corrections to the GW amplitude**
- **drawback: more signal shapes, higher false alarms**

Detection templates for non-spinning and spinning binaries

[AB, Chen, Pan & Vallisneri 03, 04, 05]

- $\tilde{h}_{\rm SPA}^{\rm no\,spin}(f) = \mathcal{A}\, f^{-7/6}\, \left(1 + \alpha\, f^{2/3}\right)\, e^{i\psi_{\rm SPA}(f) + i\Phi_0 + 2\pi i f t_0}$

$$\psi_{\rm SPA}(f) = f^{-5/3}\,\left(\psi_0 + \psi_1\, f^{2/3} + \psi_{3/2}\, f + \cdots\right)$$

$$\psi_i \equiv \psi_i(m_1, m_2) \quad \text{with} \quad i = 0, 1, 3/2, 2, 5/2, \cdots$$

- $\tilde{h}_{\rm SPA}^{\rm spin}(f) = \mathcal{A}\, f^{-7/6}\, e^{i\psi_{\rm SPA}(f) + i\Phi_0 + 2\pi i f t_0} \times$

$$\left[1 + \mathcal{C}_{\cos}\, e^{i\phi_{\cos}}\, \cos(\alpha_p(f)) + \mathcal{C}_{\sin}\, e^{i\phi_{\sin}}\, \sin(\alpha_p(f))\right]$$

$$\psi_i \equiv \psi_i(m_1, m_2, \mathbf{S}\cdot\mathbf{L}, \chi) \qquad \alpha_p(f) \equiv \alpha_p(f, m_1, m_2, \mathbf{S}\cdot\mathbf{L}, \chi)$$

Very fast (analytic) maximization on $\{t_0, \Phi_0, \phi_{\cos}, \phi_{\sin}, \mathcal{C}_{\cos}, \mathcal{C}_{\sin}\}$

BCV Template space

[AB, Chen & Vallisneri 03]

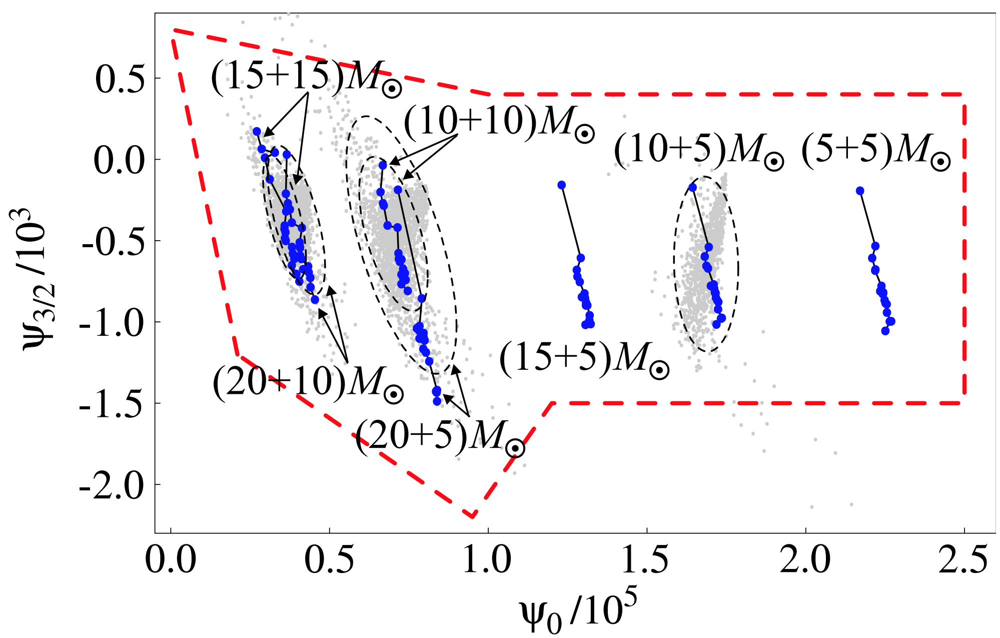

Search of BH-BH from LIGO science runs

- **385.6 hours (15 days) of data from the second science run of LIGO**
- **Max distance 1 Mpc**

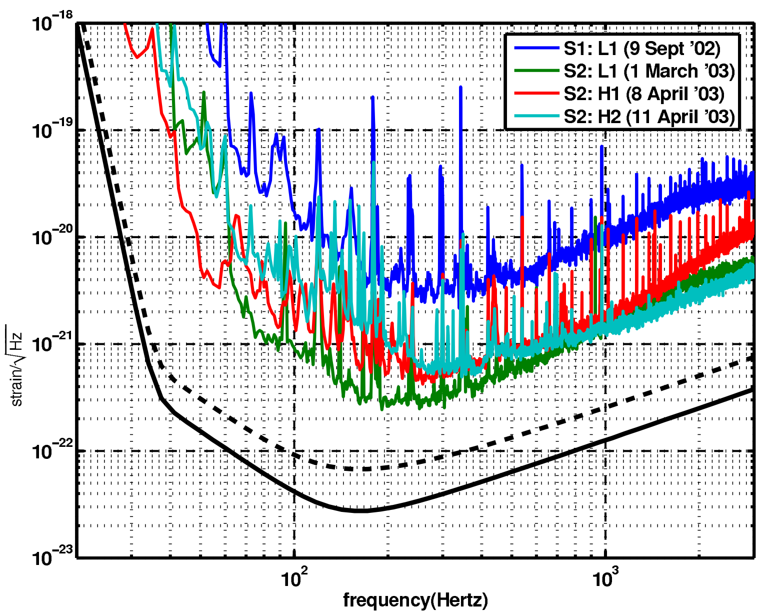

- **No events that could be identified with nonspinning binary BHs with $m_{\rm BH} = 3$–$20 M_\odot$**

First-order comparisons with numerical relativity

Some features of the numerical-relativity runs investigated

- **Code based on generalized harmonic coordinates** (Pretorius)

- **Quasi-equilibrium initial-data sets constructed by** Cook and Pfeiffer 04; Grandéclement et al. 01

Runs at three different resolutions: h, 3/4 h and 1/2 h

	d=16	d=19
M_f/m	0.954 ± 0.005	0.952 ± 0.005
$E_{\rm GW}/m$	0.043 ± 0.004	0.052 ± 0.004
a_f/M_f	0.71 ± 0.02	0.70 ± 0.02
number of orbits	2.47 ± 0.09	4.39 ± 0.18
$t_{\rm CAH}/m$	228 ± 16	529 ± 22
$(t_{\rm peak} - t_{\rm CAH})/m$	≈ 9	≈ 9
$(t_{\rm dec} - t_{\rm CAH})/m$	≈ -11	≈ -9
initial eccentricity e_1	—	0.018 ± 0.003
initial eccentricity e_2	—	$0.012(+0.014, -0.012)$
Max. GW amp. error	9%	8%
(Max. GW phase error)/(2π)	0.7	1
(Max. "shifted" GW phase error)/(2π)	0.06	0.05

Initial data *close* to PN and EOB at 3PN order

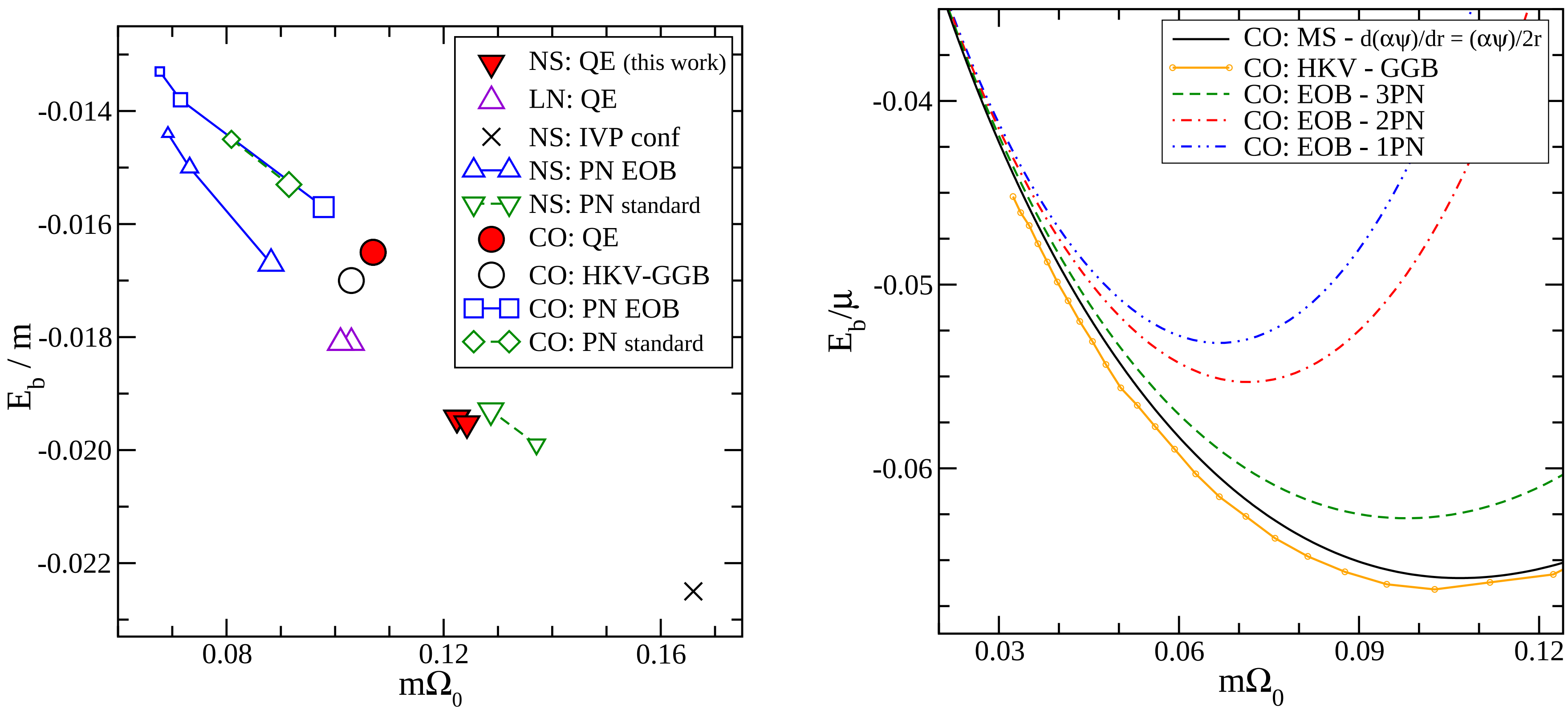

[Grandéclement et al. 01; Damour et al. 02; Blanchet 02; Cook & Pfeiffer 04; Caudill et al. 06]

NR results: very smooth transition inspiral to merger

[AB, Cook & Pretorius 06]

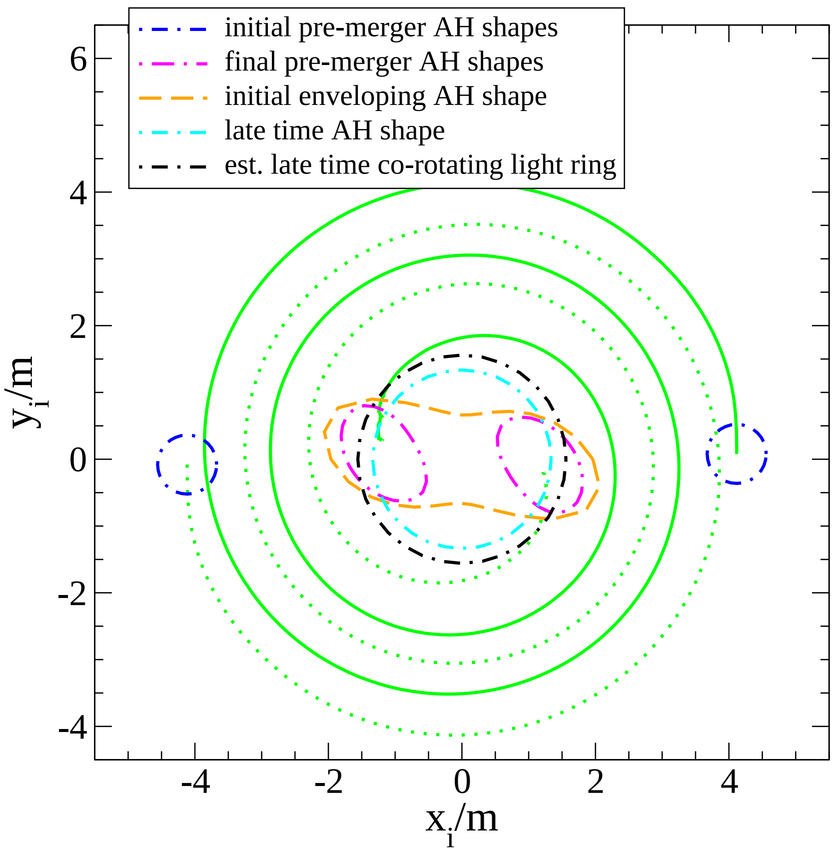

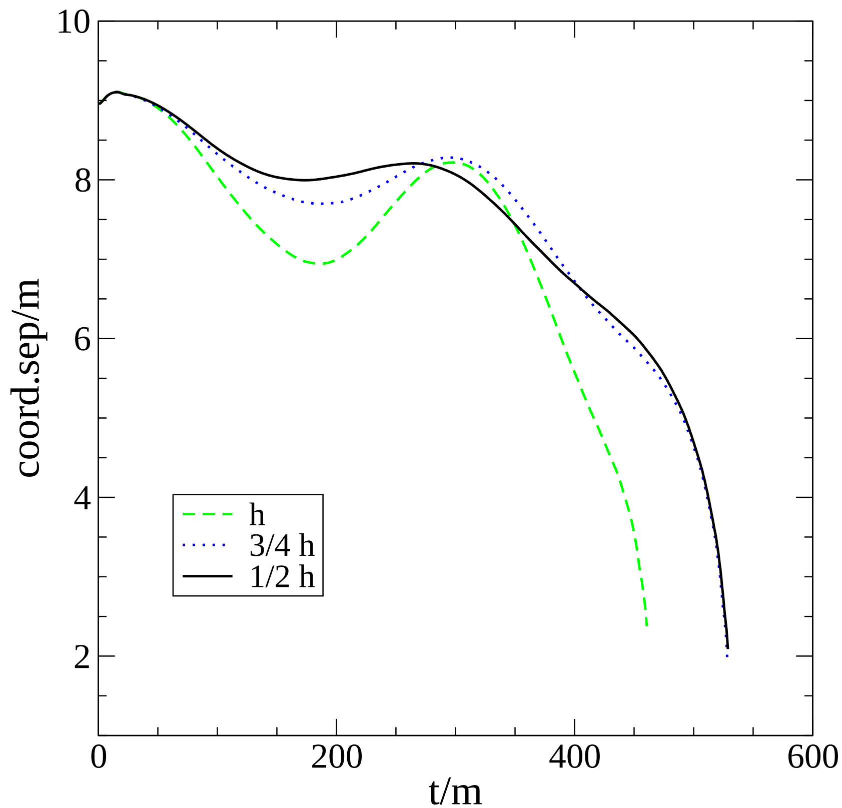

Presence of eccentricity

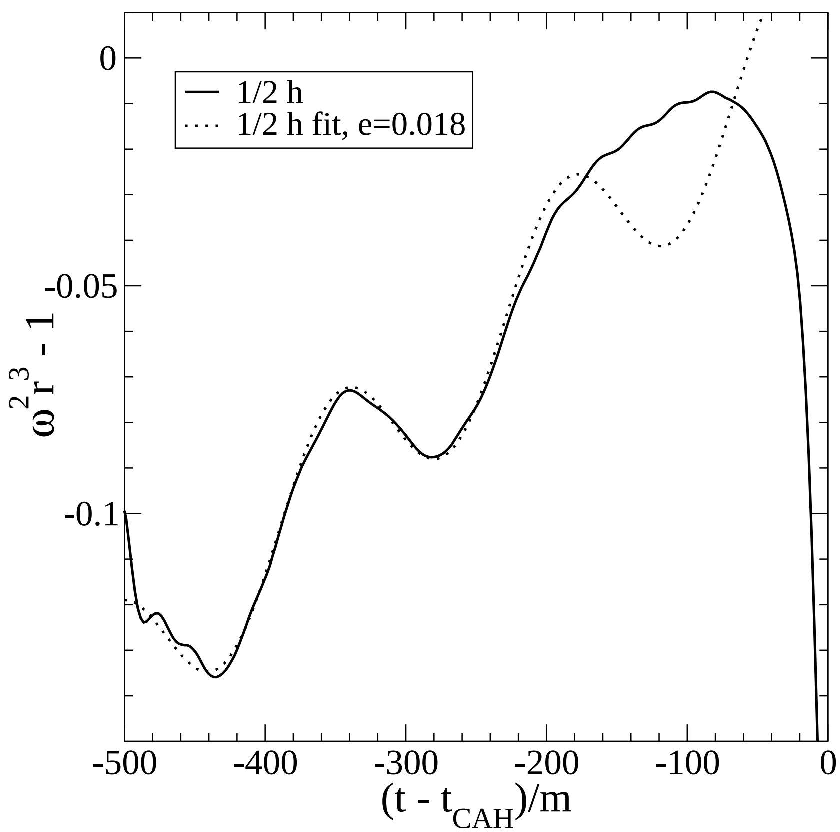

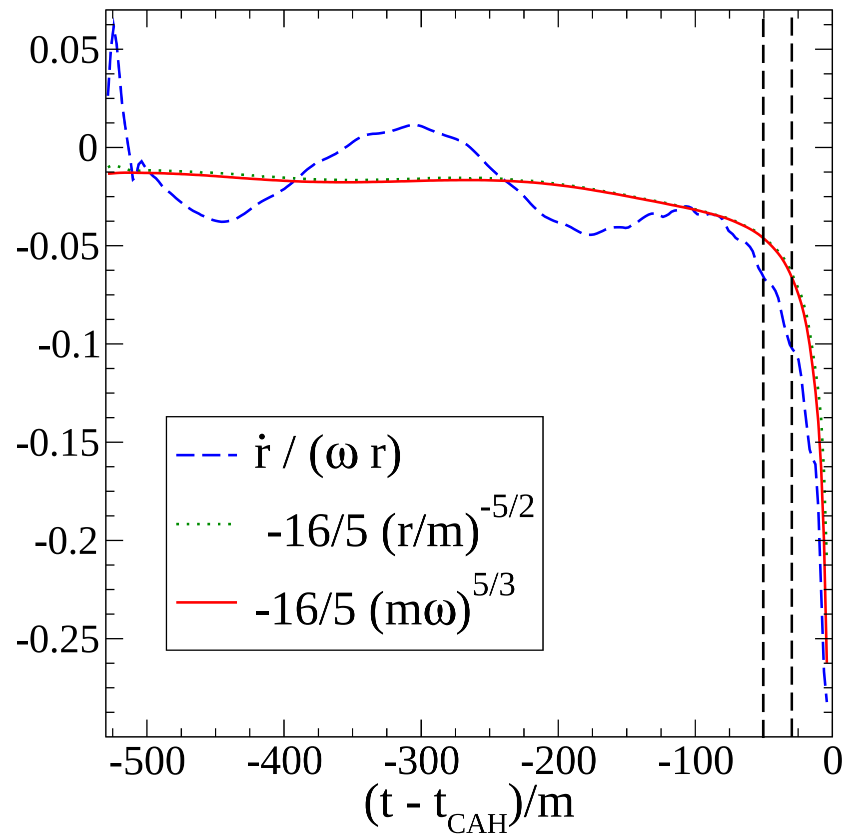

Frequency evolution

$$\omega_{D2} = -1/2 \mathrm{Im}[\dot{C}_{22}/C_{22}] \qquad \omega_{NQC}(t) = [\sqrt{5/\pi}/(32\nu)\,|_{-2}C_{2\pm 2}|(t)]^{3/8}$$

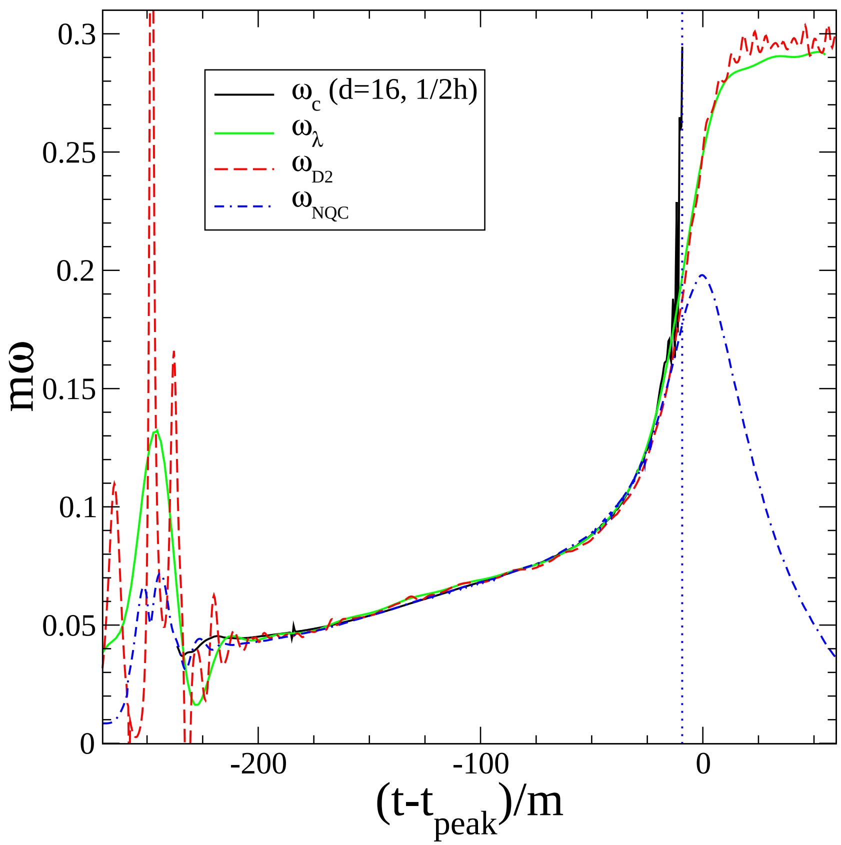

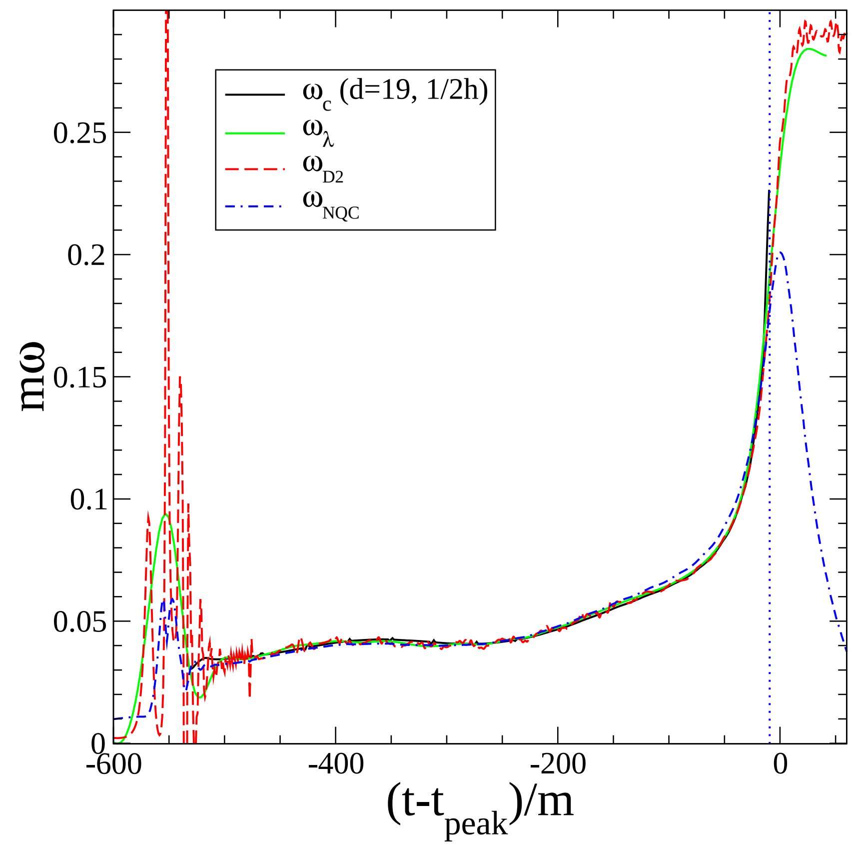

Applying *directly* the quadrupole formula

Computing Ψ_4 by taking directly five derivatives of the binary quadrupole

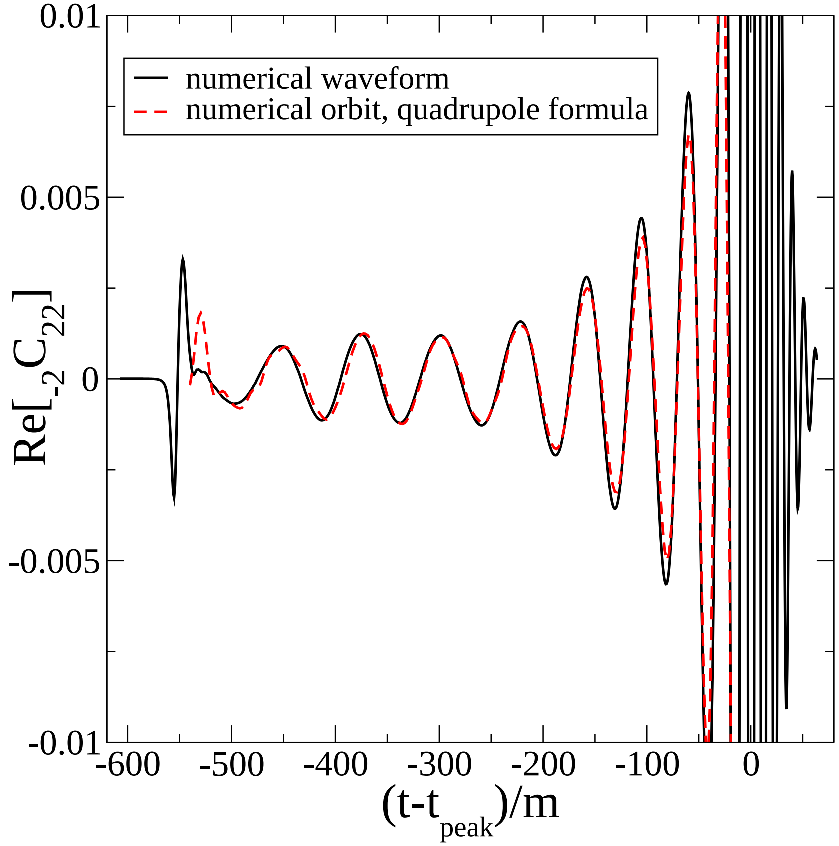

ψ_4 and multipole decomposition

$$\ddot{h}_+ = \frac{1}{2}(\ddot{h}^{TT}_{\hat{\theta}\hat{\theta}} - \ddot{h}^{TT}_{\hat{\phi}\hat{\phi}}) \qquad \ddot{h}_\times = \ddot{h}^{TT}_{\hat{\theta}\hat{\phi}} \qquad \Psi_4 = \ddot{h}_+ - i\ddot{h}_\times$$

$${}_sY_{\ell m}(\theta,\phi) \equiv (-1)^s \sqrt{\frac{2\ell+1}{4\pi}}\, d^\ell_{m(-s)}(\theta)\, e^{im\phi}$$

$$d^\ell_{ms}(\theta) \equiv \sum_{t=C_1}^{C_2} \frac{(-1)^t \sqrt{(\ell+m)!(\ell-m)!(\ell+s)!(\ell-s)!}}{(\ell+m-t)!(\ell-s-t)!t!(t+s-m)!} (\cos\theta/2)^{2\ell+m-s-2t} (\sin\theta/2)^{2t+s-m}$$

$$\Psi_4(t,\vec{r}) = \sum_{\ell m} {}_{-2}C_{\ell m}(t,r)\, {}_{-2}Y_{\ell m}(\theta,\phi)$$

Comparison NR and PN-adiabatic model (shorter run)

- The initial frequency $\omega_{\rm NR} \sim 0.0416/M$ **(e.g., for a** $(15+15)M_\odot$**,** $f_{\rm GW} \sim 89$ **Hz)**
- **The binary evolves for 2.5 orbits before a common apparent horizon forms**

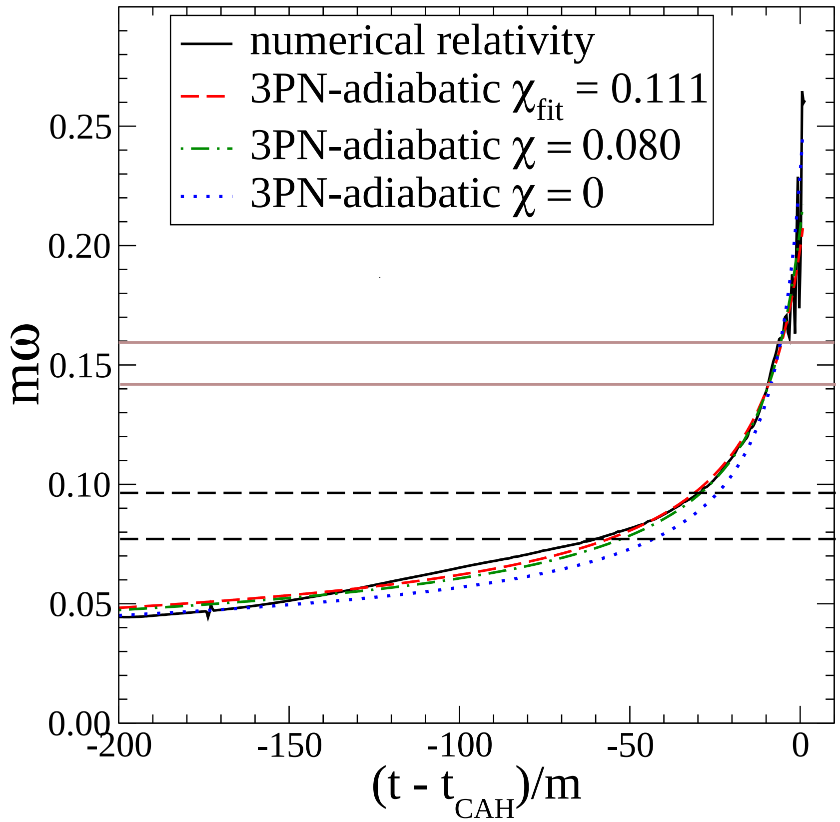

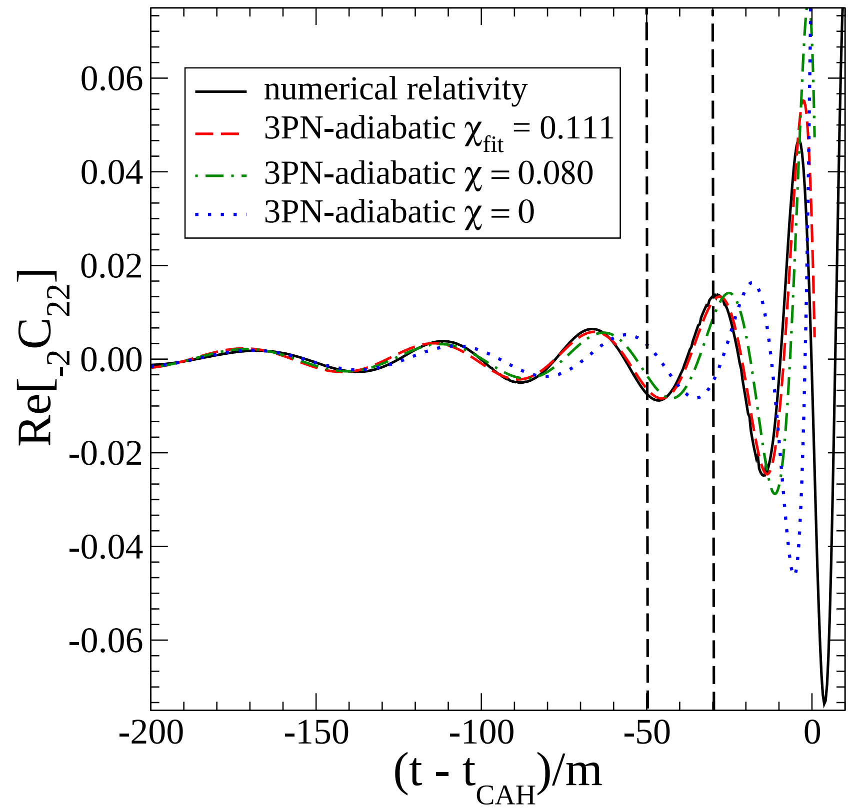

Comparison NR and PN-adiabatic model (longer run)

- The initial frequency $\omega_{\rm NR} \sim 0.0325/M$ **(e.g., for a** $(15+15)M_\odot$**,** $f_{\rm GW} \sim 70$ **Hz)**
- **The binary evolves for 4.4 orbits before a common apparent horizon forms**

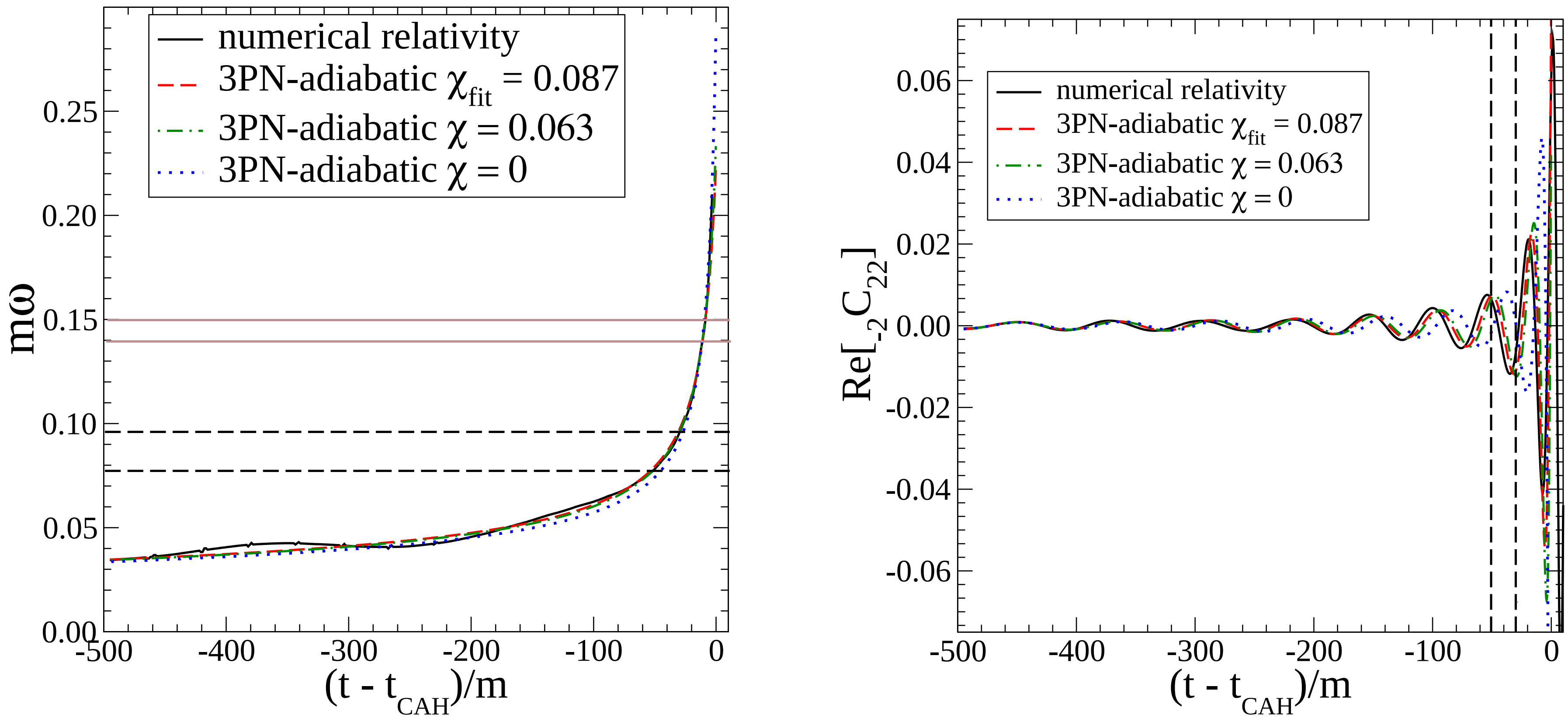

Comparison of NR and adiabatic-PN energy flux

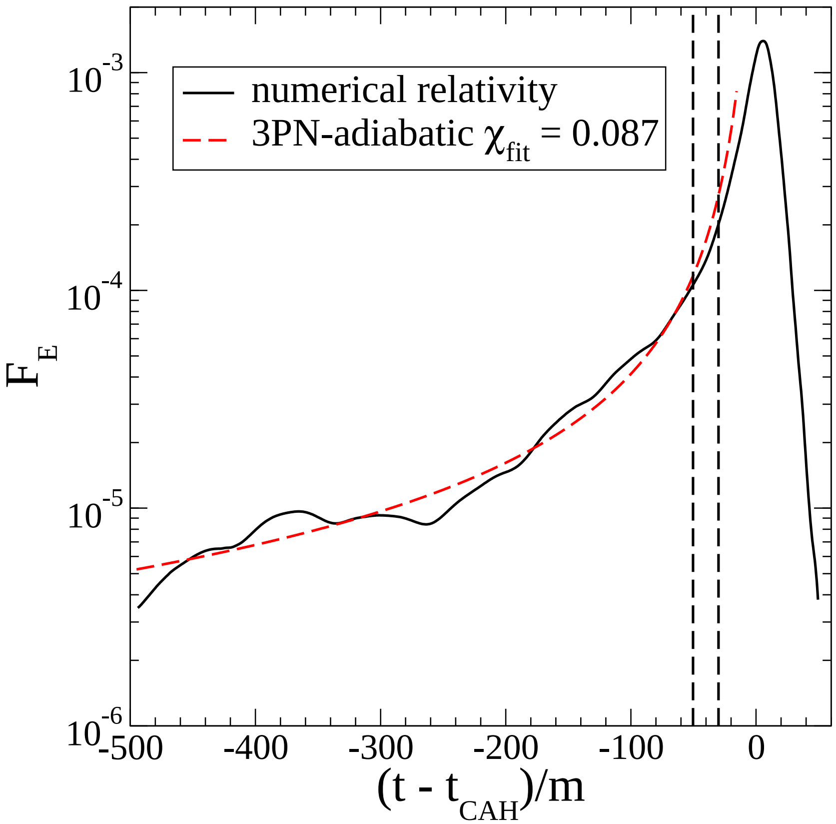

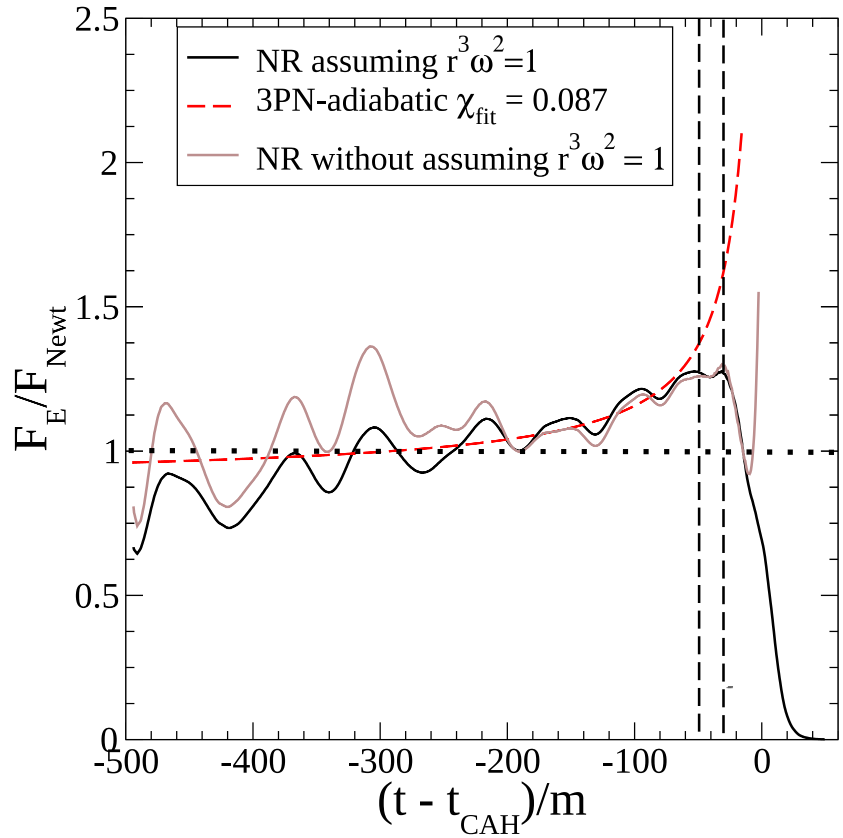

Dependence on PN order and phasing model

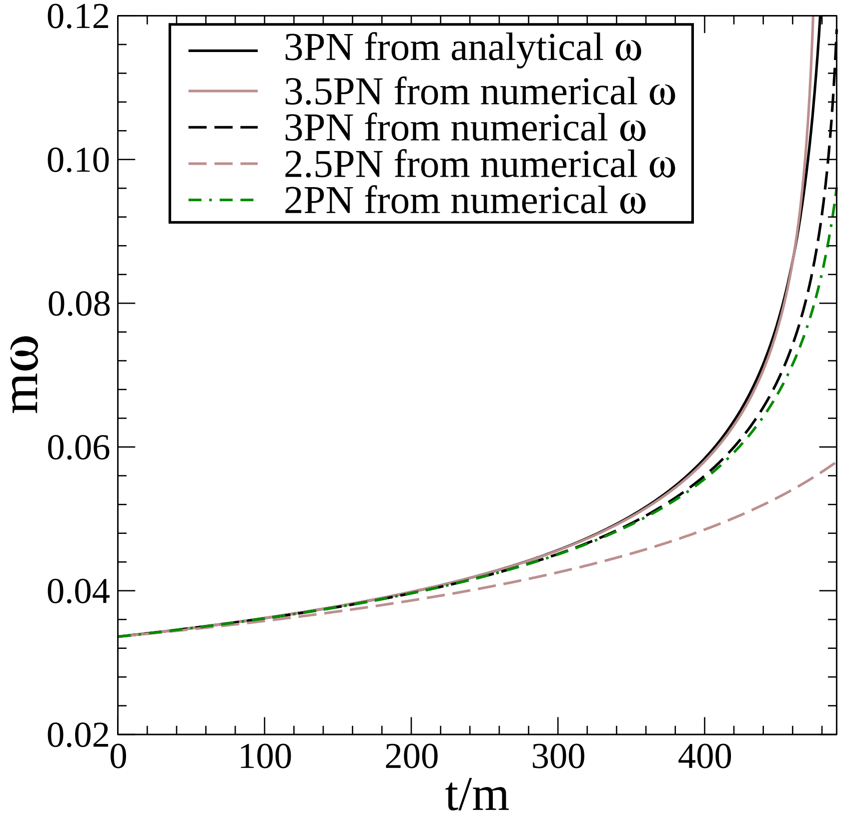

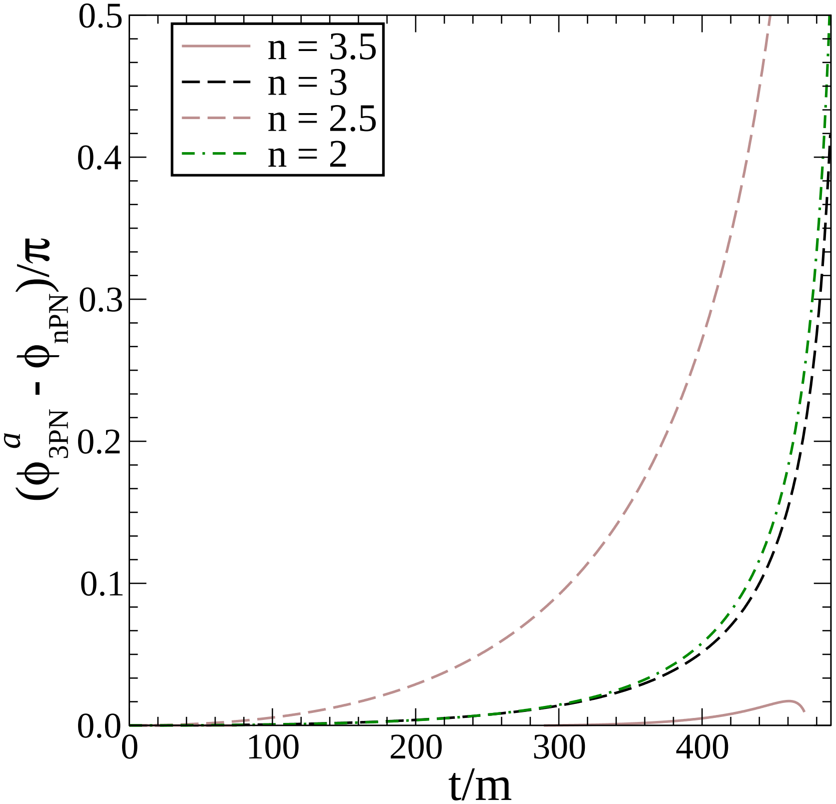

Higher-order corrections to the GW amplitude

Using amplitude corrections from Blanchet, Iyer, Wiseman & Will 96

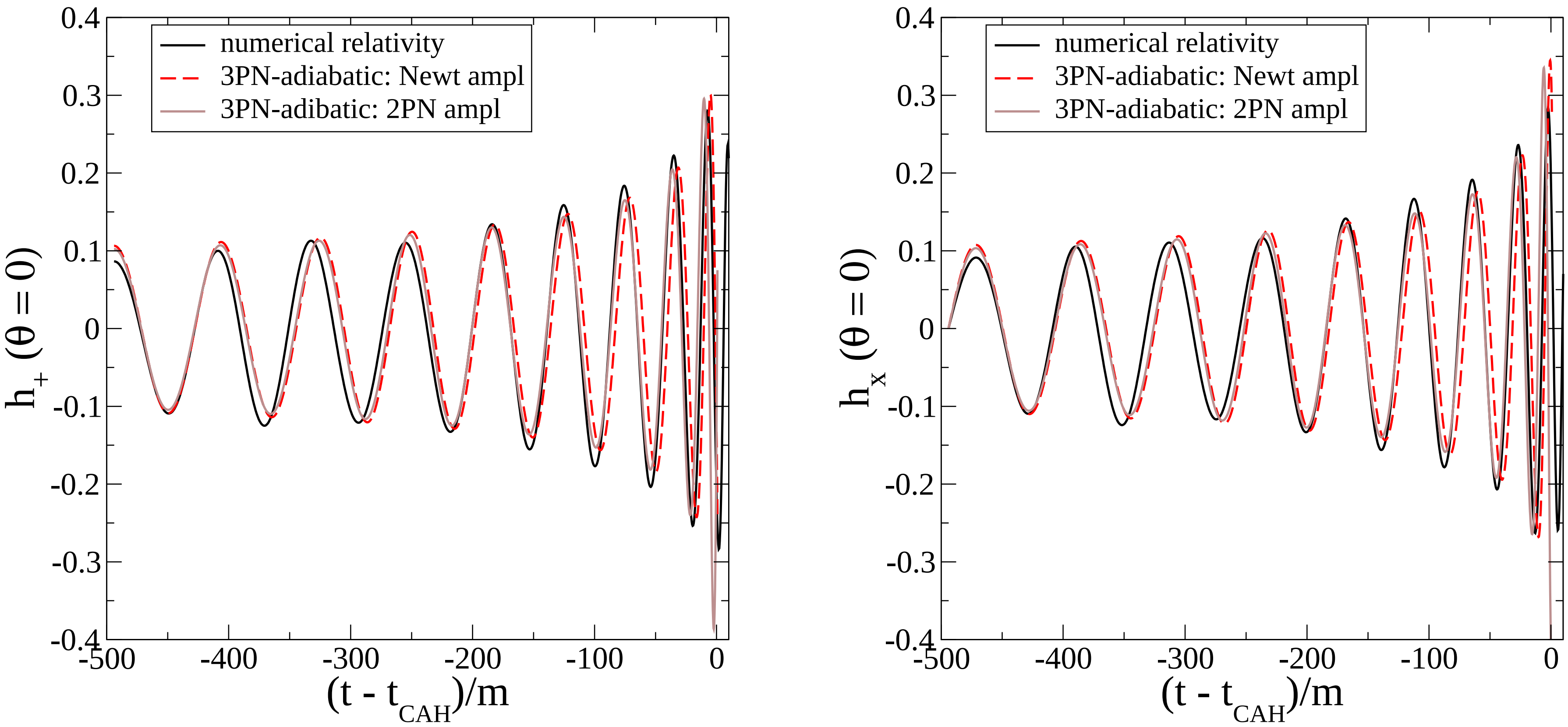

When the ring-down phase starts? Higher overtones?

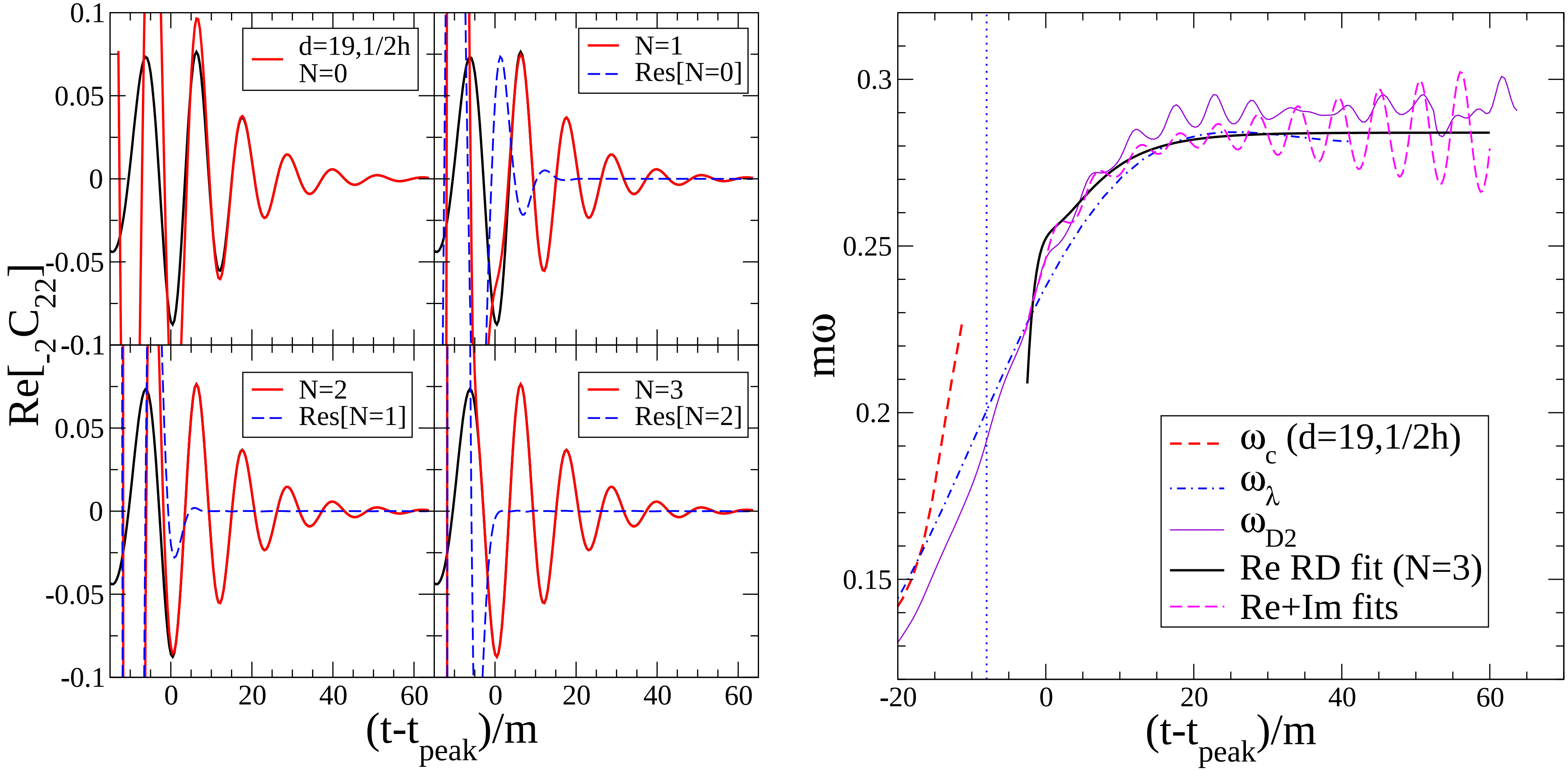

The (plunge and) merger

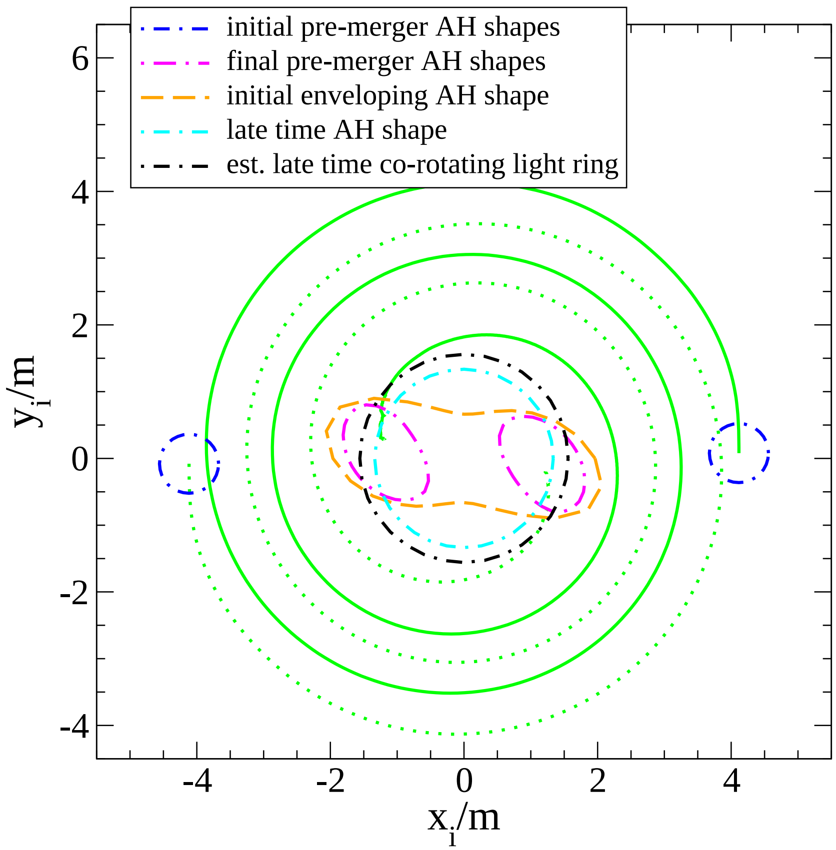

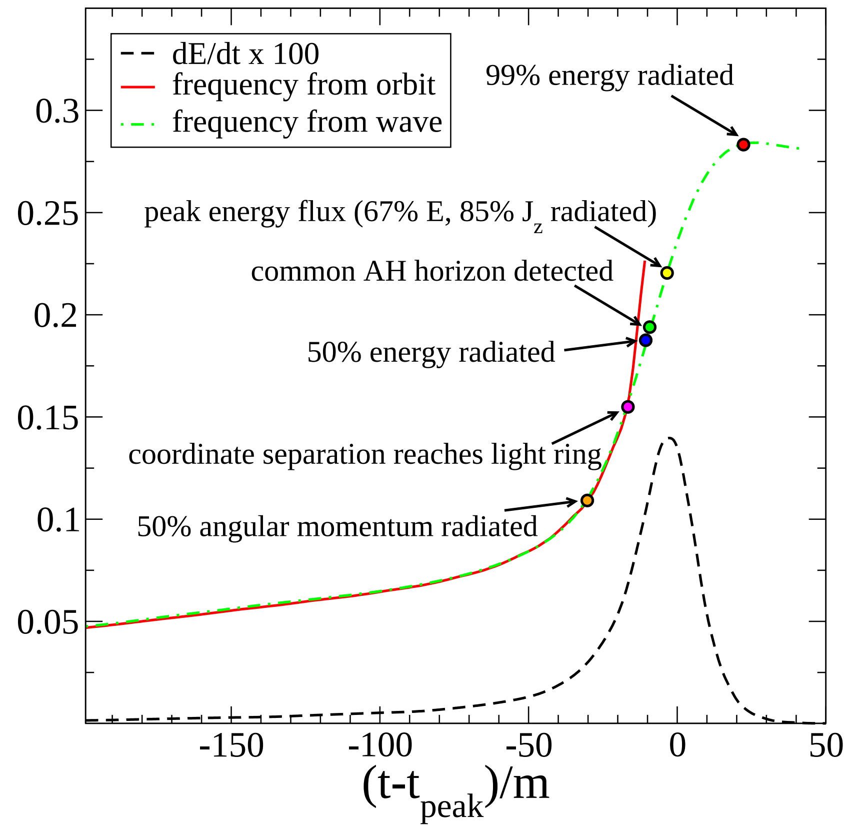

- *Short* **transition merger–ring-down**
- **Energy and angular-momentum yet to be released during merger**

Comparison NR and PN-adiabatic model (shorter run)

- The initial frequency $\omega_{\rm NR} \sim 0.0416/M$ **(e.g., for a** $(15+15)M_\odot$**,** $f_{\rm GW} \sim 89$ **Hz)**
- **The binary evolves for 2.5 orbits before a common apparent horizon forms**

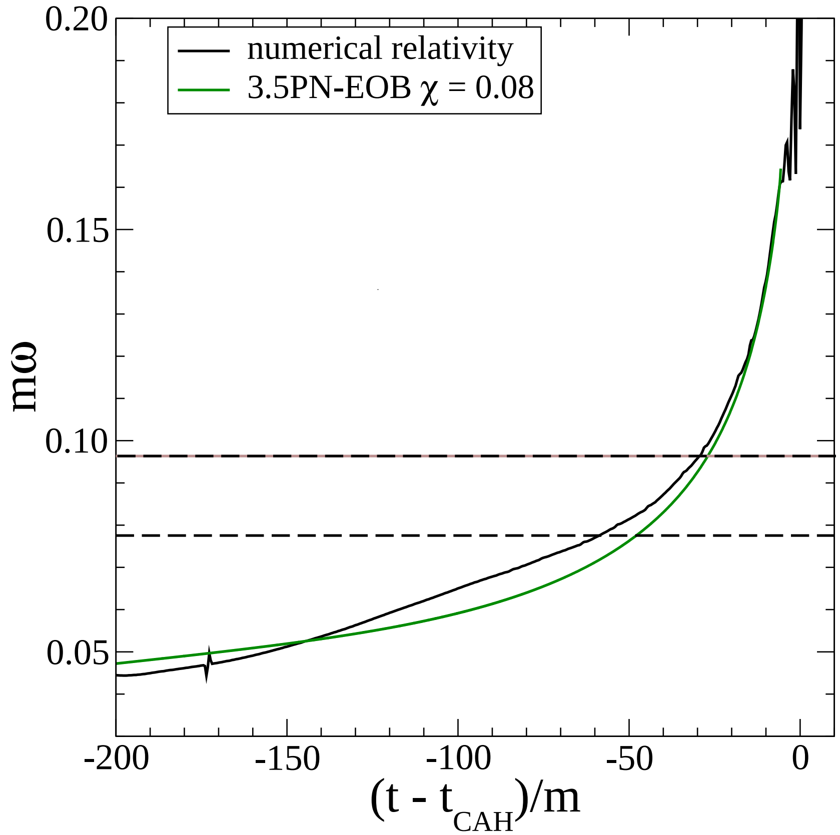

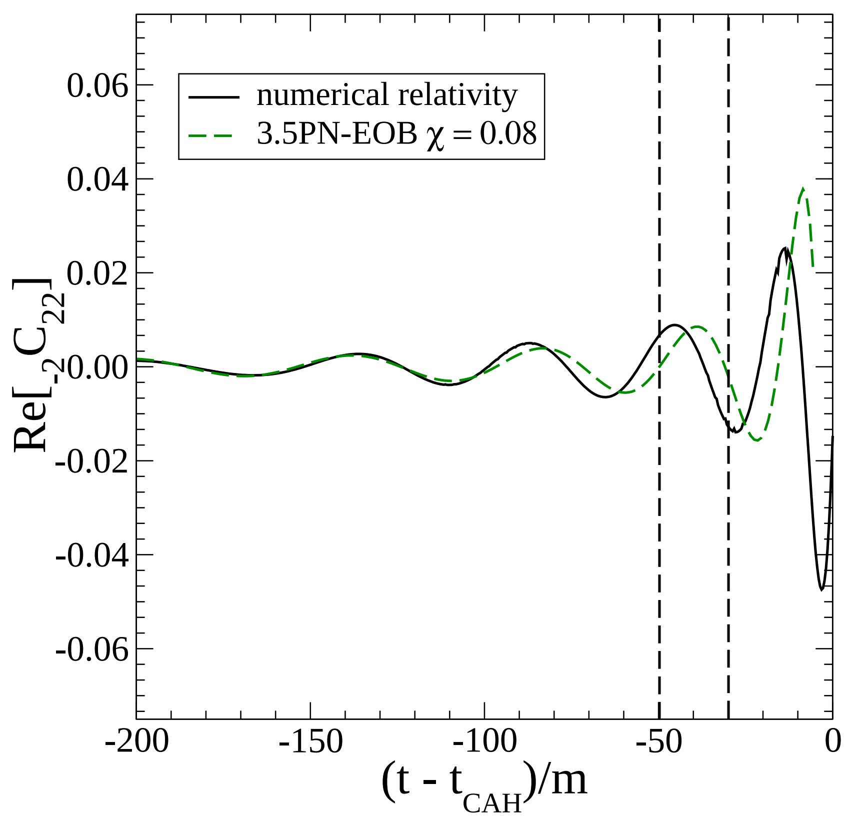

Comparison NR and EOB model (longer run)

- The initial frequency $\omega_{\rm NR} \sim 0.0325/M$ **(e.g., for a** $(15+15)M_\odot$**,** $f_{\rm GW} \sim 70$ **Hz)**
- **The binary evolves for 4.4 orbits before a common apparent horizon forms**

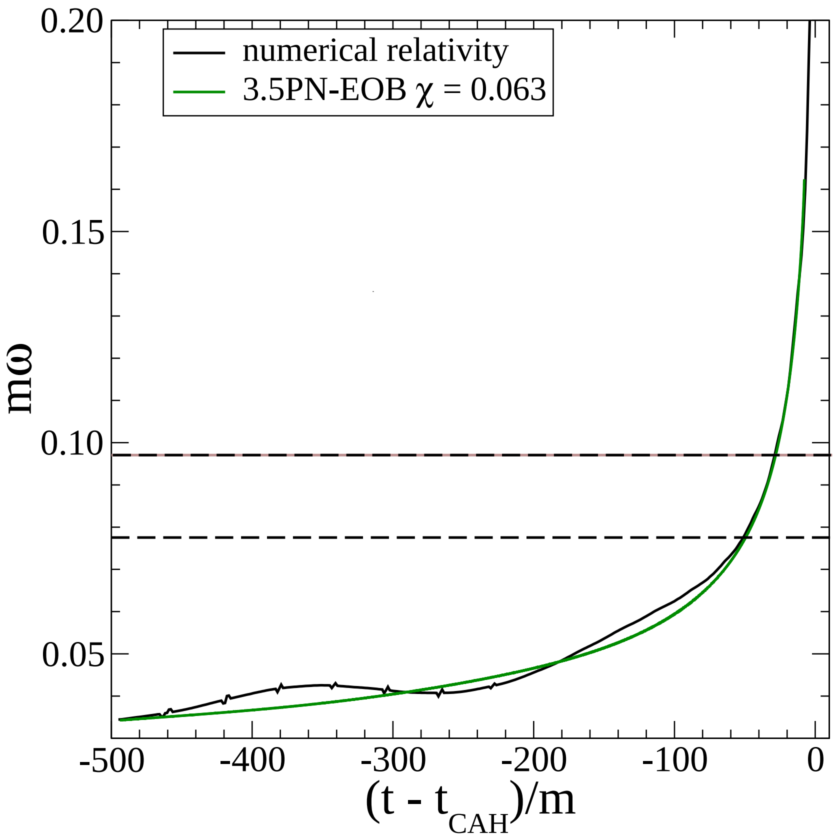

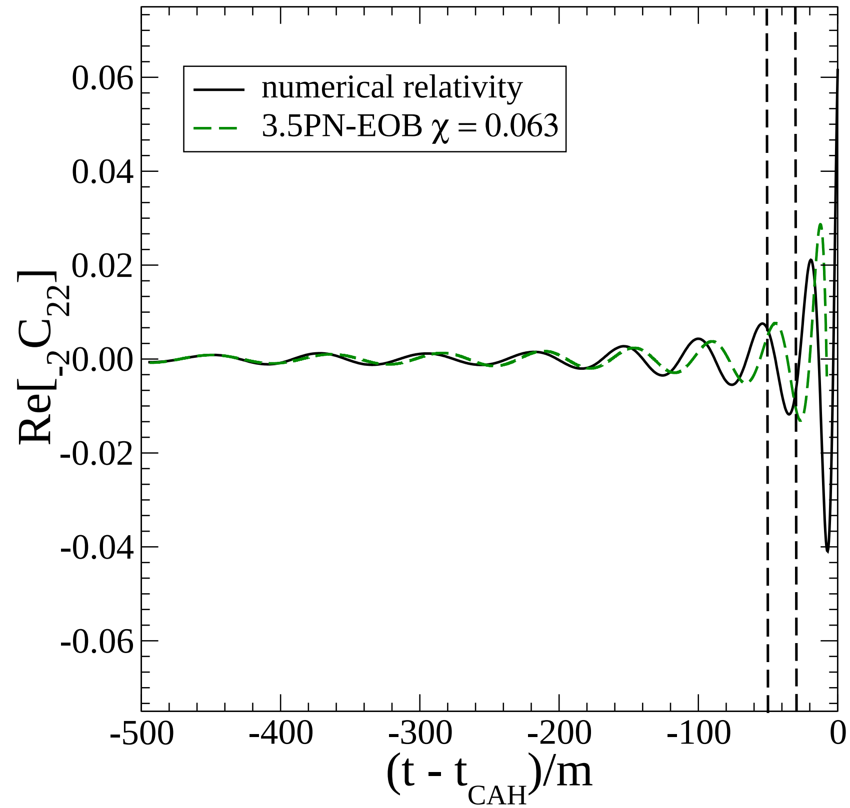

Comparison NR and EOB model including ring-down

- $M_{\rm end} = 0.971\,M$ **and** $a_{\rm end}/M_{\rm end} = 0.78$
- **Fundamental mode and two overtones included**

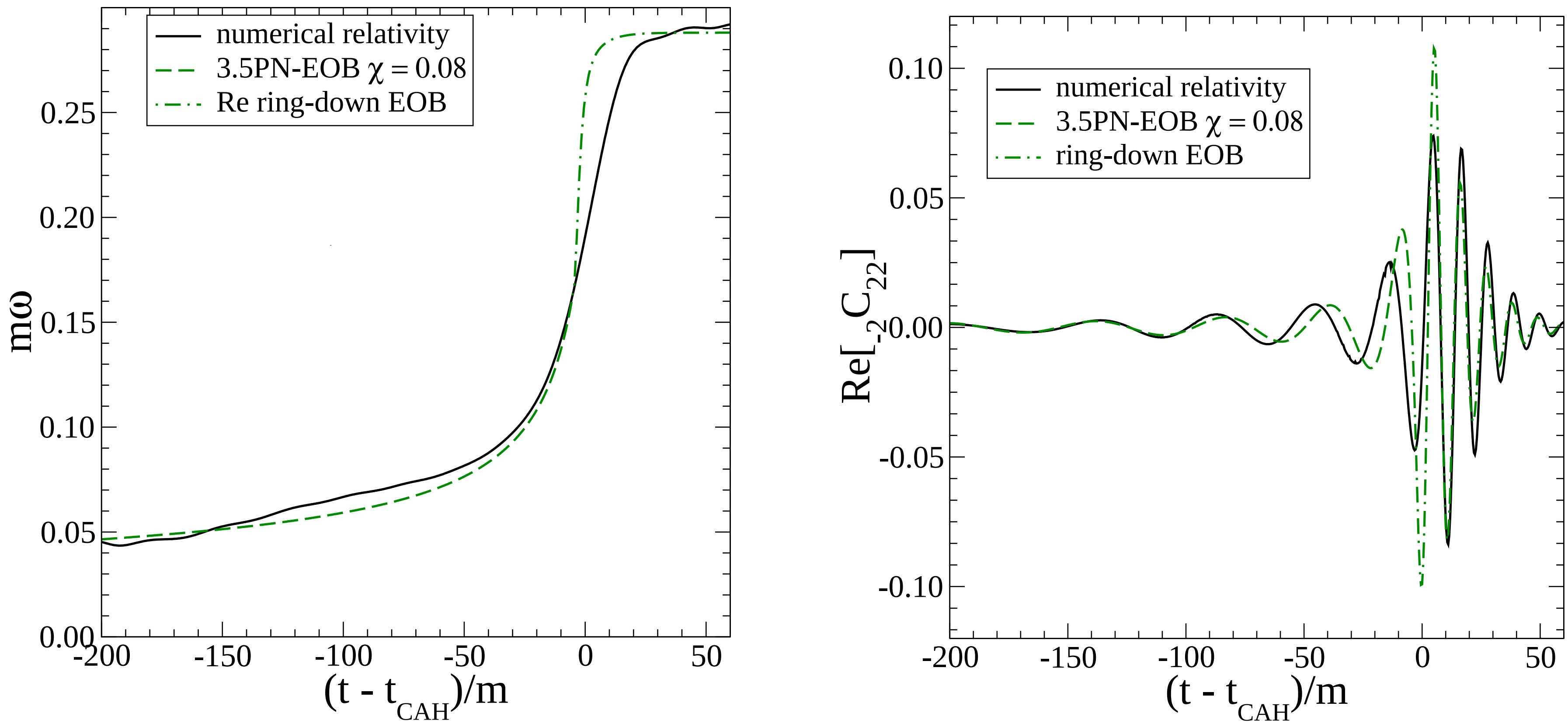

Transition inspiral to plunge in extreme mass-ratio binaries

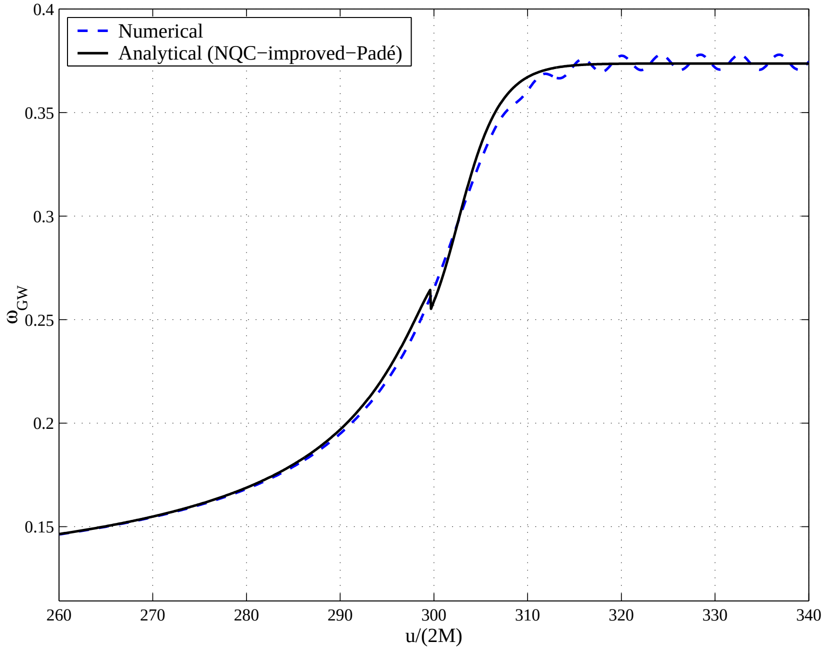

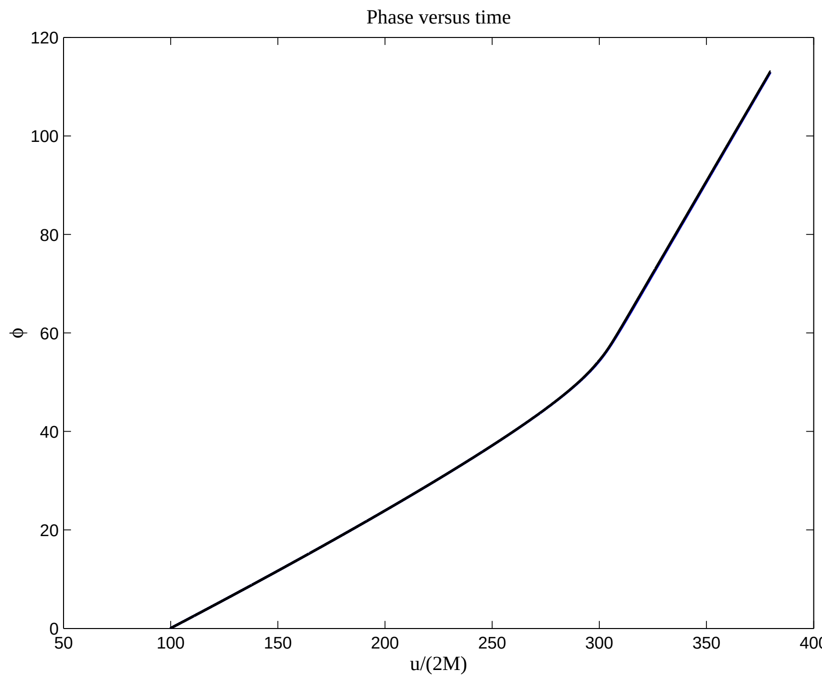

Smooth analytical transition by matching five QNMs at the BH light-ring

[Damour, Nagar & Tartaglia (in preparation)]

Some caveats of the first-order comparisons

- **Small differences in initial frequency can cause large dephasing**

- **Current NR initial-data do not** *coincide* **with PN initial data**

- **NR initial-data do not contain RR effects ⇒ eccentricity**

Those issues will be overcome as soon as simulations start at larger separations

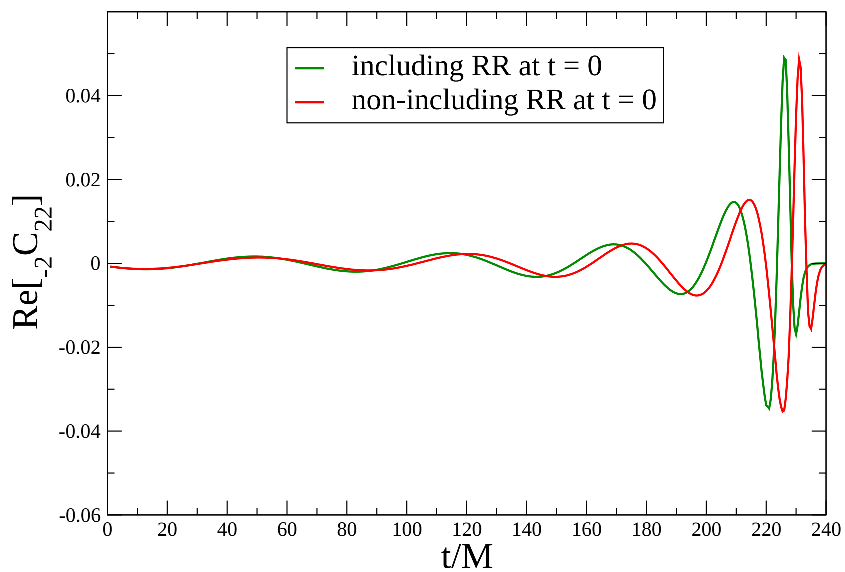

- **EOB merger–ring-down matching** *sensitive* **to matching point**
- **QNM extraction will improve with simulations lasting longer**

Detectability for ground-based detectors

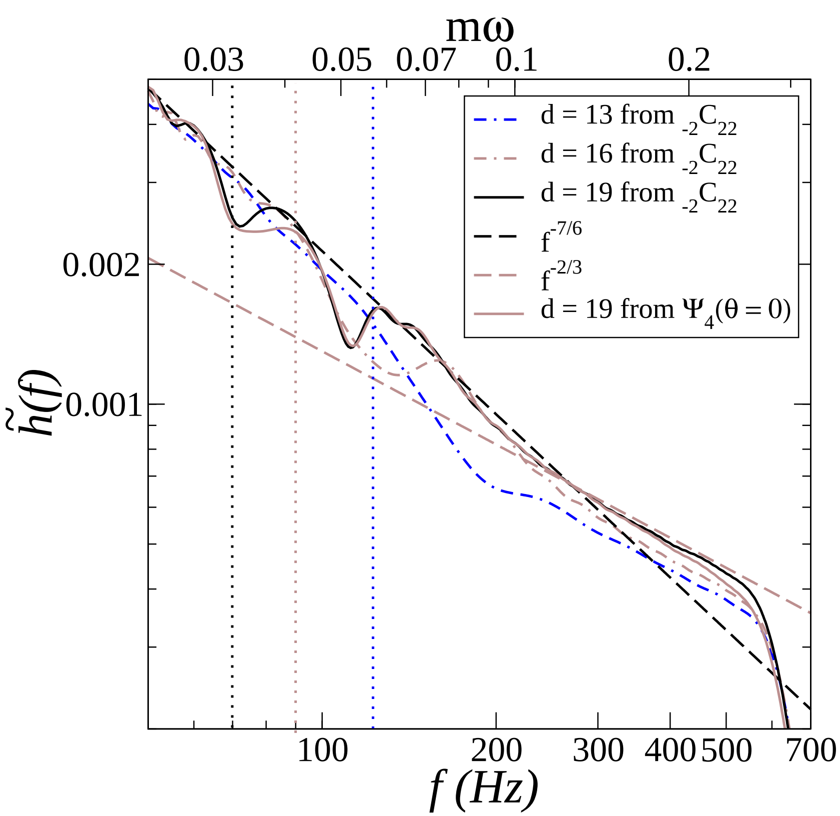

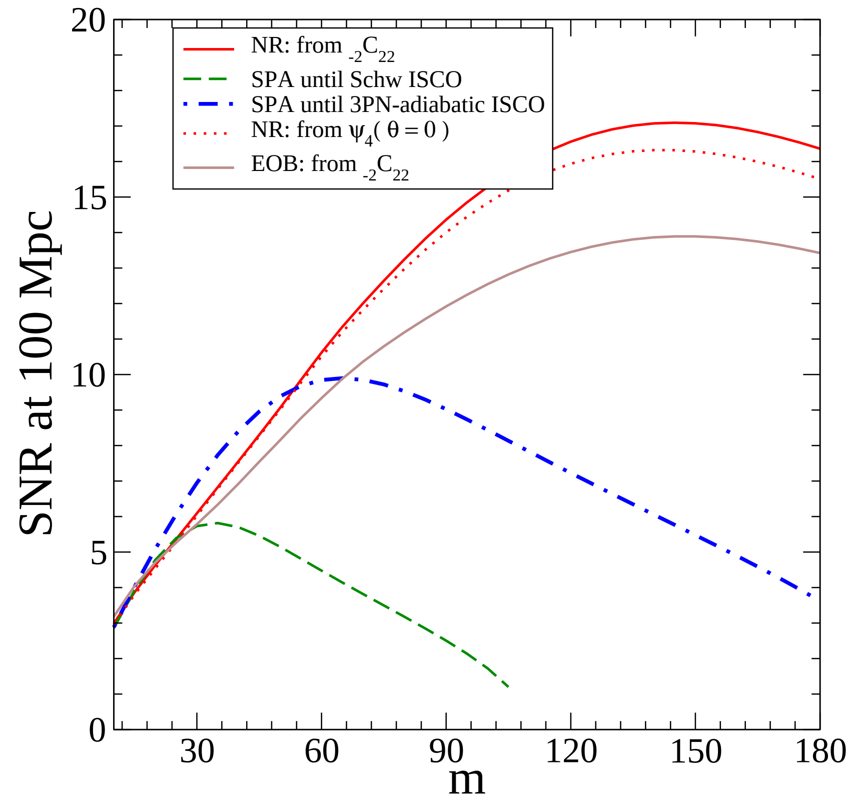

Detectability for space-based detectors

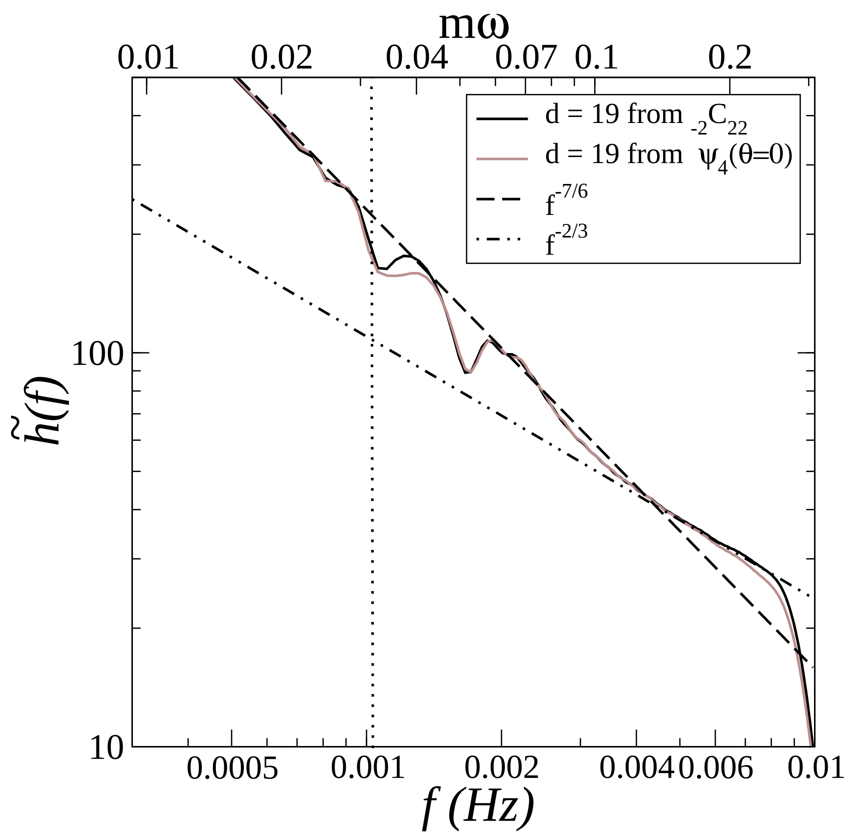

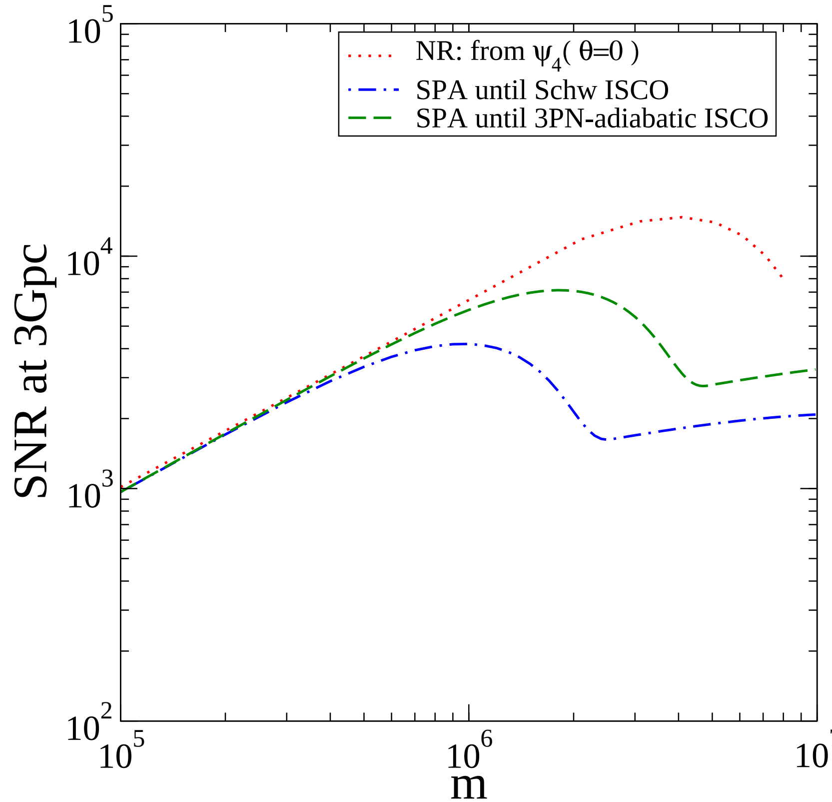

Concluding

- **The detection of GWs from compact binaries will open an exciting new era in astronomy**

- **We need to prepare the** *best tools* **to be able to extract the** *best science* **in astrophysics, general relativity or fundamental physics**